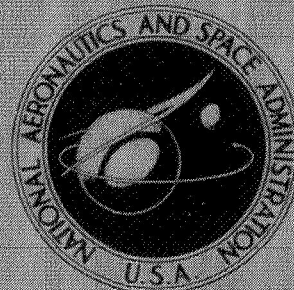


NASA TECHNICAL
MEMORANDUM



UB
NASA TM X-1348

UB
NASA TM X-1348

N70-78338

FACILITY FORM 602

(ACCESSION NUMBER)

(THRU)

(PAGES)

(CODE)

(NASA CR OR TMX OR AD NUMBER)

(CATEGORY)

ANALYTICAL STUDY OF THE
SUBSONIC DYNAMIC STABILITY
AND RESPONSE OF THE
HL-10 ENTRY VEHICLE

by Joseph L. Johnson, Jr., Joseph R. Chambers,
and Lucy C. White

Langley Research Center
Langley Station, Hampton, Va.

UNCLASSIFIED
TO: NASA
By Authority of: [Signature]
Date: 11/23/70

U. S. Government Agencies and
Contractors Only


NATIONAL AERONAUTICS AND SPACE ADMINISTRATION • WASHINGTON, D. C. • FEBRUARY 1967

Declassified by authority of NASA
Classification Change Notices No. 210
Dated **12-15-70


ANALYTICAL STUDY OF THE SUBSONIC DYNAMIC STABILITY
AND RESPONSE OF THE HL-10 ENTRY VEHICLE

By Joseph L. Johnson, Jr., Joseph R. Chambers,
and Lucy C. White

Langley Research Center
Langley Station, Hampton, Va.



NATIONAL AERONAUTICS AND SPACE ADMINISTRATION



U. S. Government Agencies and
Contractors Only



ANALYTICAL STUDY OF THE SUBSONIC DYNAMIC STABILITY
AND RESPONSE OF THE HL-10 ENTRY VEHICLE*

By Joseph L. Johnson, Jr., Joseph R. Chambers,
and Lucy C. White
Langley Research Center



SUMMARY

An analytical investigation has been made to determine the dynamic longitudinal and lateral stability and response of the HL-10 entry vehicle with particular reference to low-speed, high-angle-of-attack conditions. The calculations were made for light and heavy wing loadings for both sea level and altitude flight. The results of the calculations have been analyzed in terms of existing military specifications for handling qualities of piloted airplanes, although it is realized that in some areas these criteria may not be directly applicable to piloted entry vehicles. For comparison purposes, some of the results of the investigation have also been analyzed in terms of several proposed criteria for piloted entry vehicles.

The results indicated that the HL-10 vehicle was dynamically longitudinally and laterally stable for the conditions investigated, but that artificial damping in pitch and roll was required for some conditions in order to achieve a satisfactory degree of stability based on military handling qualities specifications for piloted airplanes. The lateral control provided by the ailerons gave satisfactory roll response in terms of a proposed criterion for piloted entry vehicles which requires that the ailerons produce a bank angle of at least 30° in 1 second; but an evaluation of the response of the roll control in terms of the sideslip induced, as well as the roll rate, indicates that the lateral control characteristics of the vehicle may be marginal.

INTRODUCTION

The National Aeronautics and Space Administration is conducting a number of experimental and analytical investigations to provide some fundamental information on the HL-10 manned lifting entry vehicle at speeds from low subsonic to hypersonic (for example, see ref. 1). These studies are aimed at developing a lifting-body configuration which



will have a hypersonic lift-drag ratio of about 1.0, a subsonic lift-drag ratio sufficiently high to allow a conventional glide landing, and adequate stability and control and handling qualities characteristics over the entire design operational range.

The present analytical investigation was conducted to provide some basic information on the low-speed dynamic longitudinal and lateral stability and control and handling qualities characteristics of the HL-10 vehicle. Calculations were made to determine the period and damping of the longitudinal and lateral modes of motion and also time histories of the vehicle dynamic response following elevator, aileron, and rudder inputs. These calculations were made over an angle-of-attack range from 14° to 45° for sea level and altitude conditions and for light and heavy wing loadings.

The results of the investigation are presented in the form of time histories, periods, and time to damp to one-half amplitude of the longitudinal and lateral oscillations. Where possible, the results are discussed in terms of handling qualities parameters which are in current usage for entry vehicle configurations.

SYMBOLS

The longitudinal data are referred to the stability-axes system and the lateral data are referred to the body-axes system. The origin of the axes is located at the reference center[†] of gravity shown in figures 1 and 2. Dimensional values are given both in U.S. Customary Units and in the International System of Units (SI). Conversion factors relating the two systems are given in reference 2.

b	reference span, feet (meters)
C_A	axial-force coefficient ($-C_X$), Axial force/ $q_\infty S$
C_D	drag coefficient, Drag/ $q_\infty S$
C_L	lift coefficient, Lift/ $q_\infty S$
C_l	rolling-moment coefficient, $M_X/q_\infty S b$
C_m	pitching-moment coefficient, $M_Y/q_\infty S l$
C_N	normal-force coefficient ($-C_Z$), Normal force/ $q_\infty S$
C_n	yawing-moment coefficient, $M_Z/q_\infty S b$



C_Y	lateral-force coefficient, Lateral force/ $q_\infty S$
$C_{1/2}$	cycles to damp to one-half amplitude
D	drag, pounds (newtons)
F_Y	side force, pounds (newtons)
f_n	longitudinal short-period undamped natural frequency, cycles/second
g	acceleration due to gravity, feet/second ² (meters/second ²)
I_X, I_Y, I_Z	moments of inertia about body axes, slug-feet ² (kilogram-meters ²)
I_{XZ}	product of inertia in XZ-plane (positive when principal axis is inclined below X-axis), slug-feet ² (kilogram-meters ²)
L	lift, pounds (newtons)
L/D	lift-drag ratio
l	body length, feet (meters)
M	Mach number
M_X	rolling moment, foot-pounds (meter-newtons)
M_Y	pitching moment, foot-pounds (meter-newtons)
M_Z	yawing moment, foot-pounds (meter-newtons)
m	vehicle mass, slugs (kilograms)
P	period, seconds
p	rolling angular velocity, radians/second
q	pitching angular velocity, radians/second
q_∞	dynamic pressure, $\rho V^2/2$, pounds/foot ² (newtons/meter ²)



r	yawing angular velocity, radians/second
S	wing area, feet ² (meters ²)
$t_{1/2}$	time to damp to one-half amplitude, seconds
V	velocity, feet/second (meters/second)
W	weight, pounds (newtons)
W/S	wing loading, pounds/foot ²
X,Y,Z	body reference axes
α	angle of attack, degrees
β	angle of sideslip, degrees
γ	flight-path angle, positive when flight path is above horizon, degrees
δ_a	aileron deflection $\delta_{eR} - \delta_{eL}$, degrees or radians
δ_e	elevator deflection $(\delta_{eR} + \delta_{eL})/2$, degrees or radians
δ_{eR}	deflection of right aileron, positive with trailing edge down, degrees
δ_{eL}	deflection of left aileron, positive with trailing edge down, degrees
δ_r	rudder deflection, positive when rudder trailing edge is deflected to left, degrees
ϵ	angle between principal longitudinal axis of inertia and longitudinal body axis, positive when reference axis is above principal axis at nose, degrees
ζ	ratio of damping in system to critical damping
θ	angle of pitch, degrees
μ	relative density factor, $m/\rho S l$



ρ	air density, slugs/foot ³ (kilograms/meter ³)
ϕ	angle of roll, degrees
$\frac{ \phi }{ \beta }$	roll-sideslip ratio
$\frac{ \phi }{ v_e }$	ratio of roll angle to equivalent side velocity, degrees/feet/second
ψ	angle of yaw, degrees
ω_d	undamped natural frequency of Dutch roll mode, radians/second
ω_ϕ	undamped natural frequency of numerator quadratic in transfer function of roll to aileron input, radians/second
$\left(\frac{\omega_\phi}{\omega_d}\right)^2$	steady-state rolling effectiveness parameter
$C_{l_p} = \frac{\partial C_l}{\partial \frac{pb}{2V}}$	per radian
$C_{l_r} = \frac{\partial C_l}{\partial \frac{rb}{2V}}$	per radian
$C_{l_\beta} = \frac{\partial C_l}{\partial \beta}$	per degree
$C_{l_{\delta_a}} = \frac{\partial C_l}{\partial \delta_a}$	per degree
$C_{l_{\delta_r}} = \frac{\partial C_l}{\partial \delta_r}$	per degree
$C_{m_q} = \frac{\partial C_m}{\partial \frac{ql}{2V}}$	per radian



$$C_{m\alpha} = \frac{\partial C_m}{\partial \alpha}, \text{ per degree}$$

$$C_{m\delta_e} = \frac{\partial C_m}{\partial \delta_e}, \text{ per degree}$$

$$C_{Nq} = \frac{\partial C_N}{\partial \frac{ql}{2V}}, \text{ per radian}$$

$$C_{np} = \frac{\partial C_n}{\partial \frac{pb}{2V}}, \text{ per radian}$$

$$C_{nr} = \frac{\partial C_n}{\partial \frac{rb}{2V}}, \text{ per radian}$$

$$C_{n\beta} = \frac{\partial C_n}{\partial \beta}, \text{ per degree}$$

$$C_{n\delta_a} = \frac{\partial C_n}{\partial \delta_a}, \text{ per degree}$$

$$C_{n\delta_r} = \frac{\partial C_n}{\partial \delta_r}, \text{ per degree}$$

$$C_{X\delta_e} = \frac{\partial C_X}{\partial \delta_e}, \text{ per degree}$$

$$C_{Yp} = \frac{\partial C_Y}{\partial \frac{pb}{2V}}, \text{ per radian}$$

$$C_{Yr} = \frac{\partial C_Y}{\partial \frac{rb}{2V}}, \text{ per radian}$$

$$C_{Y\beta} = \frac{\partial C_Y}{\partial \beta}, \text{ per degree}$$

$$C_{Y\delta_a} = \frac{\partial C_Y}{\partial \delta_a}, \text{ per degree}$$

$$C_{Y\delta_r} = \frac{\partial C_Y}{\partial \delta_r}, \text{ per degree}$$

$$C_{Z\delta_e} = \frac{\partial C_Z}{\partial \delta_e}, \text{ per degree}$$

$$C_{Y\dot{\beta}} = \frac{\partial C_Y}{\partial \frac{\dot{\beta} b}{2V}}, \text{ per radian}$$

$$C_{N\dot{\beta}} = \frac{\partial C_N}{\partial \frac{\dot{\beta} b}{2V}}, \text{ per radian}$$

$$C_{N\dot{\alpha}} = \frac{\partial C_N}{\partial \frac{\dot{\alpha} l}{2V}}, \text{ per radian}$$

$$C_{A\dot{\alpha}} = \frac{\partial C_A}{\partial \frac{\dot{\alpha} l}{2V}}, \text{ per radian}$$

$$C_{m\dot{\alpha}} = \frac{\partial C_m}{\partial \frac{\dot{\alpha} l}{2V}}, \text{ per radian}$$

$$C_{Aq} = \frac{\partial C_A}{\partial \frac{ql}{2V}}, \text{ per radian}$$

$$\left. \begin{array}{l} C_{Nq} + C_{N\dot{\alpha}}, \text{ per radian} \\ C_{Aq} + C_{A\dot{\alpha}}, \text{ per radian} \\ C_{mq} + C_{m\dot{\alpha}}, \text{ per radian} \end{array} \right\} \text{pitching oscillatory stability derivatives}$$

$$\begin{array}{l}
 \left. \begin{array}{l}
 C_{Y_p} + C_{Y_{\dot{\beta}}} \sin \alpha, \text{ per radian} \\
 C_{n_p} + C_{n_{\dot{\beta}}} \sin \alpha, \text{ per radian} \\
 C_{l_p} + C_{l_{\dot{\beta}}} \sin \alpha, \text{ per radian}
 \end{array} \right\} \text{rolling oscillatory stability derivatives} \\
 \\
 \left. \begin{array}{l}
 C_{Y_r} - C_{Y_{\dot{\beta}}} \cos \alpha, \text{ per radian} \\
 C_{n_r} - C_{n_{\dot{\beta}}} \cos \alpha, \text{ per radian} \\
 C_{l_r} - C_{l_{\dot{\beta}}} \cos \alpha, \text{ per radian}
 \end{array} \right\} \text{yawing oscillatory stability derivatives}
 \end{array}$$

VEHICLE DESCRIPTION

A three-view drawing of the HL-10 vehicle is shown in figure 2. The vehicle has a 74° delta planform with a thick, negatively cambered airfoil section and has tip fins and a center fin. The negative camber provides the desired hypersonic trim conditions with 0° elevator deflection. The present three-fin arrangement has evolved as a result of many tests over a speed range from subsonic to hypersonic, and it provides positive directional stability throughout this speed range. For low-speed flights, the base area of the vehicle is reduced by boattailing to provide increased performance. For Mach numbers from about 0.5 to 1.0, the base area is increased to provide improved longitudinal stability characteristics in this speed range. The change in base area is accomplished by moving flaps located on the inner and outer surfaces of the tip fins and on the upper surface of the elevon. (See refs. 3 and 4.) The vehicle with the base area reduced is referred to as the subsonic configuration and that with the base area increased is referred to as the transonic configuration.

CALCULATIONS AND METHODS OF ANALYSIS

Calculations were made to determine the longitudinal and lateral dynamic stability and response of the HL-10 manned lifting entry vehicle. The dimensions and mass characteristics of the test vehicle are given in table I.

Longitudinal Calculations

An analysis of the longitudinal dynamic stability of the vehicle was made to determine the period and damping of the longitudinal short-period mode. The calculations were made by using the method of reference 5, which employs linear equations with two

degrees of freedom. The results are expressed in terms of the inverse cyclic damping $1/C_{1/2}$, the natural frequency f_n , and the damping ratio ζ . The predicted short-period characteristics are compared with the military handling qualities requirements of reference 6, which are the present-day criteria for military aircraft. The results are also compared with the proposed criteria of reference 7 for piloted reentry vehicles. In addition, time histories of vehicle motions are calculated by using the nonlinear equations of motion given in the appendix in a digital computer program to determine the longitudinal motion subsequent to elevator step inputs.

Lateral Calculations

Linear three-degree-of-freedom lateral equations of motion similar to those of reference 8 were used to calculate the damping and period of the lateral modes of motion. The sensitivities of the damping and period to changes in the various aerodynamic stability derivatives were also determined. In conjunction with the linear analysis, calculations were made of the roll - side-velocity parameter $\frac{|\phi|}{|v_e|}$ and the inverse cyclic damping of the lateral oscillation. The results are compared with the handling qualities requirements of reference 6. The aileron rolling effectiveness parameter $\left(\frac{\omega_\phi}{\omega_d}\right)^2$ of reference 9 was evaluated, and in addition, the six-degree-of-freedom nonlinear equations of the appendix were used to obtain time histories of the lateral motion subsequent to both step and pulse inputs of the ailerons and rudder.

Stability Derivatives and Control Characteristics

Longitudinal.- The static longitudinal aerodynamic characteristics of the configuration are presented in figure 3. The data were obtained from the results reported in reference 3. These data were extrapolated to an angle of attack of 45° on the basis of the smaller scale data of reference 10 in order that dynamic longitudinal stability calculations could be made for this angle of attack. The dynamic longitudinal stability derivatives used in the investigation, taken from reference 10, are presented in figure 4.

Lateral.- The static and dynamic lateral stability derivatives used in the calculations are presented in figures 5 and 6, respectively. The incremental lateral force and moment coefficients produced by aileron and rudder deflections are presented in figure 7. All these lateral data are obtained from the results of the investigation of reference 10.

It should be noted that the stability derivatives used in the calculations are those measured in low-subsonic tests. At the time the calculations were made, no other derivatives were available and it was assumed that the low-subsonic data generally applied

[REDACTED]

throughout the speed range under investigation (Mach numbers up to 0.8). However, high-subsonic wind-tunnel data which were obtained later (ref. 4) showed that the configuration experienced a loss in static longitudinal stability with increasing speed (see fig. 8). This undesirable characteristic at Mach numbers above about 0.5 could be eliminated by employing the transonic configuration, for which the static longitudinal stability at the higher subsonic speeds was about the same as that for the subsonic configuration at low speeds. A similar result was achieved for the lateral stability derivatives. For example, the data of figure 9 show that the lateral stability derivatives for the transonic configuration at Mach numbers above about 0.5 were very similar to those for the subsonic configuration at low speeds. The results of figures 8 and 9, therefore, indicate that the calculated results should give good representation of the dynamic behavior of the subsonic configuration at low speeds and, in addition, should give a fairly good indication of the dynamic behavior of the transonic configuration at the higher subsonic speeds.

RESULTS AND DISCUSSION

Longitudinal Stability

The results of the calculations have been analyzed in terms of existing military specifications for handling qualities of piloted airplanes, although it is realized that in some areas these criteria may not be directly applicable to piloted entry vehicles. For comparison purposes, some of the results of the investigation have also been analyzed in terms of several proposed criteria for piloted entry vehicles.

The results of the simple two-degree-of-freedom calculations to determine the period and damping of the longitudinal short-period mode of motion are presented in figure 10. These calculations were made for sea level and for an altitude of 55 000 feet (16.8 km) for light and heavy wing loadings. The damping results are presented in terms of the time factor $1/t_{1/2}$ since increasing values of $1/t_{1/2}$ correspond to increasing values of damping. The data show that the configuration was stable for the conditions investigated. At sea level, the vehicle had values of $1/t_{1/2}$ that decreased from about 1 at the lower angles of attack (oscillation damps to one-half amplitude in 1 second) to about 0.75 at an angle of attack of 33° . A further increase in angle of attack resulted in an increase in damping. As expected, increasing altitude or wing loading reduced the damping because such changes increased the relative density factor μ .

Presented in figure 11 are the damping results for the light-wing-loading, sea level condition together with the military specification of flying qualities for piloted airplanes. (See ref. 6.) The boundary shown in this figure specifies the minimum value of $1/C_{1/2}$ required for satisfactory damping of the short-period longitudinal mode of motion. The calculated data points for the basic (unaugmented) vehicle are below this boundary, an

[REDACTED]

indication that the vehicle would have unsatisfactory longitudinal handling qualities. With the addition of artificial damping in pitch (C_{mq} increased by -0.5), the damping of the vehicle is increased enough to move most of the calculated data points above the specified boundary and thereby indicate satisfactory longitudinal handling qualities characteristics. The data of figures 10 and 11 indicate that considerably higher values of artificial damping in pitch would be required to achieve satisfactory longitudinal damping at an altitude above sea level than would be required at sea level.

For the past few years, considerable effort has been directed toward more specific longitudinal handling qualities requirements than those given in reference 6. (For example, see ref. 7.) Extensive work has been done with variable stability airplanes wherein the stick force characteristics were kept unaltered and the aerodynamics were artificially varied. The studies gave qualitative information in the form of pilot opinion and quantitative information in the form of time histories. The results of this work are still in preliminary form but are of sufficient interest to warrant including some of the suggested boundary specifications in the present analysis for comparison purposes. An example of the handling qualities information derived in these studies is given in figure 12. Presented in this figure is a plot of the undamped natural frequency f_n as a function of the short-period damping ratio ζ , together with flying qualities boundaries specified by the solid lines. It is of interest to note that the results of this figure are in good agreement with those of figure 11 in that the basic vehicle is shown to have unsatisfactory or unacceptable handling qualities. Also, it is seen that the addition of artificial damping in pitch yields acceptable or satisfactory vehicle handling qualities.

Longitudinal Response

In order to provide some basic information regarding the control response behavior of the HL-10 vehicle at sea level, calculations were made for a value of W/S of 36.10 for several angles of attack to obtain time histories in pitch following a step elevator input. These results, which are presented in figure 13, show that the motion following an abrupt change in control position was quite oscillatory. This oscillatory motion is apparently related to the low damping of the short-period mode previously discussed. Results of simulator studies indicate that this type of oscillatory response to elevator control is very objectionable to the pilot and is the primary reason for the unacceptable flight behavior for these conditions. Results of figure 14 present the time histories following elevator inputs when artificial damping in pitch is added to the system. As can be seen, the dynamic overshoot in angle of attack and the oscillatory tendency following a change in elevator position were appreciably reduced from those of the basic vehicle.

Lateral Stability

Presented in figure 15 are the period and damping characteristics of the lateral modes of motion. These calculations were made for sea level and for an altitude of 55 000 feet (16.8 km) for light and heavy wing loadings. For the sea level condition the data of figure 15 show values of $1/t_{1/2}$ for the Dutch roll mode from about 1.0 to 1.2 (oscillation damps to one-half amplitude in about 1.0 to 0.8 seconds) in the low-angle-of-attack range and show an increase in damping with an increase in angle of attack. Increasing altitude decreased the Dutch roll damping by a factor of about 3.0 over the angle-of-attack range investigated. The roll subsidence mode was also stable for all cases, but increasing altitude decreased the damping of this mode in about the same proportion as that for the Dutch roll mode. The spiral mode was stable at low angles of attack but became unstable for all cases above an angle of attack of about 23° .

Presented in figure 16 are the damping characteristics of the vehicle in terms of the military specifications for flying qualities of piloted airplanes (see ref. 6). This figure shows a plot of the inverse cyclic damping $1/C_{1/2}$ as a function of the roll - side-

velocity ratio $\frac{|\phi|}{|v_e|}$. The upper boundary in this plot specifies the value of $1/C_{1/2}$

required for satisfactory Dutch roll damping. The results of this figure show that the vehicle had satisfactory damping at sea level, but at an altitude of 55 000 feet (16.8 km) the damping decreased to the extent that the Dutch roll characteristics were unacceptable for normal operation.

Past studies of dynamic stability with highly swept configurations have indicated that the use of artificial stabilization in roll was very effective for increasing the lateral damping and for providing satisfactory Dutch roll characteristics. In order to obtain some fundamental information of this type on the present vehicle, calculations were made to determine the effect of variations in several lateral stability derivatives on the Dutch roll and aperiodic lateral modes. The results are presented in figure 17 and show, as expected, that increasing C_{l_p} negatively (increasing damping in roll) gave very pronounced increases in the damping of the Dutch roll and roll subsidence modes. It can also be seen that increasing C_{n_p} positively increased the Dutch roll damping, but this increase in Dutch roll damping was obtained at the expense of reduced damping of the roll subsidence mode. Analysis indicated that increasing C_{n_p} positively did not appreciably change the total damping but rather redistributed the damping in the system. Variations in the yawing derivatives C_{n_r} and C_{l_β} are shown to have relatively small effects on the damping of the lateral modes for the particular range of derivatives investigated.

The effect of C_{l_p} on the damping characteristics of the vehicle is shown in figure 18 in terms of the military specifications for satisfactory Dutch roll damping. The results of this figure show that for an angle of attack of 21° and an altitude of 55 000 feet (16.8 km), a value of C_{l_p} of about -0.8 is required to achieve satisfactory damping.

Another point illustrated in figure 18 is the effect of C_{l_β} on the parameter $\frac{|\phi|}{|v_e|}$. In addition to having a sizable effect on $1/C_{l/2}$, changes in C_{l_β} also produced large changes in the values of $\frac{|\phi|}{|v_e|}$. It appears from this figure that for the vehicle conditions which show high values of $\frac{|\phi|}{|v_e|}$, a reduction in $-C_{l_\beta}$ may be desirable or a reduction in $-C_{l_p}$ in combination with increases in $-C_{l_\beta}$ may be the most effective means of achieving the desired results. It should be pointed out, however, that the feasibility of reducing $-C_{l_\beta}$ for this purpose may be limited because of adverse effects on the spiral mode (see fig. 17).

The results of time-history motion studies to determine the lateral damping characteristics of the vehicle are presented in figure 19. In these calculations, the ailerons were pulsed right and left and returned to neutral to start a lateral oscillation. The results of figure 19 appear to substantiate the period and damping characteristics presented earlier in that the lateral or Dutch roll oscillation at sea level is well damped, as indicated by the rapid decay in the amplitudes of the oscillations. Also, increasing wing loading did not appreciably affect the lateral damping, but increasing altitude produced a marked deterioration in the damping of the vehicle.

Lateral Response

The calculated lateral response of the HL-10 vehicle following a step aileron input is shown in figures 20 to 22 for the wing loading and altitude conditions investigated. This information is presented in the form of time histories of the roll and yaw rates and the roll, yaw, and sideslip angular displacements. Some significant points shown in figures 20 to 22 are that right-aileron deflection produces positive yaw and roll rates and positive initial roll, yaw, and sideslip angles. The positive yaw angles generated are expected because the vehicle has favorable aileron yaw characteristics (see fig. 7(a)). At first, the positive values of sideslip seem to be in disagreement with the positive values of yaw. Analysis indicates that the positive values of sideslip occur in this case because the vehicle has relatively high values of the ratio of yaw inertia to roll inertia and therefore tends to roll about its X-axis. The initial sideslip angle generated by this type of rolling motion can be expressed as $\sin \beta = \sin \alpha \sin \phi$; this angle increases with

[REDACTED]

the angles of attack and roll. Positive values of β are therefore introduced in a right roll, and these values of β are adverse in this instance since rolling moments which oppose the rolling motion are introduced through the effective dihedral parameter $-C_{l\beta}$.

Until recently the criterion for evaluating roll performance of airplanes was through the use of the nondimensional rolling parameter $pb/2V$. The roll response data of figures 20 to 22 were analyzed in terms of this parameter and the results are presented in figure 23. Also presented in this figure is the roll requirement for fighter type aircraft ($pb/2V = 0.05$) based on present military handling qualities requirements. The data of figure 23 show that the HL-10 vehicle has values of $pb/2V$ which are considerably below the required value for satisfactory roll response. Although the vehicle is deficient in roll response with regard to the parameter $pb/2V$, recent flight tests with high-speed, highly swept aircraft have brought about discrepancies between pilot ratings and military specifications based on this rolling-performance factor. Such discrepancies have led to research investigations with the objective of arriving at a more realistic rolling performance criterion for modern high-speed aircraft and reentry vehicles. At the present time there are no recognized revised military specifications for roll performance of modern aircraft, but one investigation which merits considerable attention is presented in reference 7. In this reference, revised roll performance requirements have been devised based on NASA ground simulator work as well as flight investigations. The results of this study have been used as a basis for evaluating the roll performance of the HL-10 vehicle. Briefly, the revised criterion specifies that in the landing approach condition the vehicle shall be capable of 30° of roll in 1 second after an initiation of an abrupt aileron deflection. In addition, the time required for the rolling velocity to reach 63 percent of the steady-state rolling velocity shall not be greater than 2 seconds.

An indication of the roll performance of the vehicle in terms of the revised criterion can be seen in figure 24 where the roll response information of figures 20 to 22 are summarized. The roll displacement data of figure 24 indicate that at an angle of attack of 14° the vehicle rolls about 110° in 1 second. As the angle of attack increases, however, the roll response decreases rapidly until near an angle of attack of about 25° the roll response levels off to about 45° in 1 second and then remains about constant at this value for most of the higher angles of attack. The decrease in roll response with increasing angle of attack can be attributed to reduced trim speeds at the higher angles of attack, increased adverse sideslip produced by rolling, and increased damping in roll. (See fig. 6(a).) In any event, an examination of the roll response data of figures 20 to 22 and figure 24 in terms of the proposed criterion indicates that the vehicle meets both the roll angle and roll rate requirements specified and therefore should have satisfactory roll control characteristics with respect to this criterion.

The calculated lateral response of the vehicle following a step rudder input is presented in figures 25 to 27 and summarized in figure 28 in terms of yaw and roll rates and angular displacements. One significant point illustrated in the data of figures 25 to 27 is that the initial roll rates and roll angles produced by rudder deflection are adverse. These initial adverse motions are produced by the rolling moment due to rudder deflection $C_{l\delta_r}$ in combination with high values of the parameter I_Z/I_X . Rolling motions such as these result in a time lag between the pilot control input and the desired rolling motion which, under some conditions, might lead to pilot-induced oscillations. The results of figure 28 show that rudder deflection produced favorable yaw and roll angles after a 1-second interval for angles of attack up to about 30° .

At the lower angles of attack, the rudder deflection used ($\delta_r = 7^\circ$) was in about the right proportion to the aileron deflection used ($\delta_a = 20^\circ$) to keep the initial sideslip angle relatively low in a coordinated turn. This point is illustrated in figure 29 where the sideslip angles produced by this combination of rudder and aileron deflection are plotted. This figure shows that the rudder produced a sideslip angle opposite to that produced by the ailerons and that the resulting sideslip angle was relatively small up to about 0.7 second.

Recent flight tests and simulator studies of lateral handling qualities have revealed two parameters which appear significantly to affect pilot evaluation of aircraft handling qualities. These parameters, which include the ratio of roll angle to sideslip angle $\frac{|\phi|}{|\beta|}$ and the roll effectiveness parameter $\left(\frac{\omega_\phi}{\omega_d}\right)^2$, are derived and discussed in detail in references 9 and 11. A value of $\left(\frac{\omega_\phi}{\omega_d}\right)^2$ of 1.0 corresponds to a steady-state rolling velocity equivalent to that given by a one-degree-of-freedom rolling analysis. Values of $\left(\frac{\omega_\phi}{\omega_d}\right)^2$ less than 1.0 indicate a steady-state rolling velocity less than that of the simplified analysis, and such a condition is generally associated with aileron adverse yaw.

Values of $\left(\frac{\omega_\phi}{\omega_d}\right)^2$ less than 0 indicate rolling reversal; that is, the vehicle will reach a steady-state rolling velocity opposite in direction to that desired. In the investigation of reference 11, an effort was made to evaluate a range of flight conditions sufficiently large to encompass the probable dynamic characteristics of future piloted entry vehicles. During the study, evaluations were made to correlate pilot opinion of flying qualities and

[REDACTED]

flight ratings with the parameters $\frac{|\phi|}{|\beta|}$ and $\frac{\omega\phi}{\omega_d}$. The results of the investigation indicate that the pilot, in using ailerons to control bank angle, preferred values of $\frac{\omega\phi}{\omega_d}$ near 1.0, but for high values of $\frac{|\phi|}{|\beta|}$ and low Dutch roll damping, values of $\frac{\omega\phi}{\omega_d}$ slightly less than 1.0 were preferred because the pilot could control the wing bank angle without introducing excessive sideslip.

Values of $\frac{|\phi|}{|\beta|}$ and $\left(\frac{\omega\phi}{\omega_d}\right)^2$ for the HL-10 vehicle are presented in figures 30 and

and 31, respectively. The data of figure 30 show that the ratio $\frac{|\phi|}{|\beta|}$ varies from about 3.5 at an angle of attack of 14° to values approaching 1.0 at angles of attack between 35° and 45° . For comparison purposes, the expression for the sideslip angle generated by rolling about the X-axis at an initial angle of attack has been simplified from

$\sin \beta = \sin \alpha \sin \phi$ to the term $1/\sin \alpha = \frac{\sin \phi}{\sin \beta} \approx \frac{|\phi|}{|\beta|}$ and plotted in figure 30. The

results of reference 12 indicate that this simplified expression can be used to approximate the roll-sideslip ratio of the lateral oscillation for highly swept vehicles which have large values of I_Z/I_X . The results of figure 30 show that this term is in fair agreement with the values of $\frac{|\phi|}{|\beta|}$ for the HL-10 vehicle.

The data of figure 31 show values of $\left(\frac{\omega\phi}{\omega_d}\right)^2$ varying from about 0.5 to 0.7. The

data of reference 4 indicate that, on the basis of the values of $\frac{|\phi|}{|\beta|}$ shown in figure 30,

the HL-10 vehicle should have values of $\frac{\omega\phi}{\omega_d}$ in a range from about 0.8 to 1.1 in order to

have satisfactory flight ratings (pilot ratings of 3 or less). Since the data of figure 31

show values of $\frac{\omega\phi}{\omega_d}$ generally less than those in this range, the results of reference 11

indicate that the HL-10 vehicle may have marginal lateral control characteristics.

CONCLUDING REMARKS

An analytical investigation has been made to determine the dynamic longitudinal and lateral stability and response of the HL-10 entry vehicle with particular reference

[REDACTED]

to low-speed, high-angle-of-attack conditions. The results of the calculations have been analyzed in terms of existing military specifications for handling qualities of piloted airplanes, although it is realized that in some areas these criteria may not be directly applicable to piloted entry vehicles. For comparison purposes, some of the results of the investigation have also been analyzed in terms of several proposed criteria for piloted entry vehicles. From the results of the investigation, the following conclusions are drawn:

1. The vehicle was dynamically longitudinally stable for the conditions investigated, but artificial damping in pitch was required for some conditions to achieve a satisfactory degree of longitudinal stability based on military handling qualities specifications for piloted airplanes.

2. The vehicle had satisfactory damping of the Dutch roll oscillation for sea level conditions, but at altitude required artificial damping in roll to achieve the lateral damping specified for satisfactory lateral handling qualities.

3. The lateral control provided by the ailerons gave satisfactory roll response in terms of a proposed criterion for piloted entry vehicles which requires that the ailerons produce a bank angle of at least 30° in 1 second; but an evaluation of the response to roll control in terms of the sideslip induced, as well as the roll rate, indicates that the lateral control characteristics of the vehicle may be marginal.

Langley Research Center,
National Aeronautics and Space Administration,
Langley Station, Hampton, Va., August 31, 1966,
124-07-02-36-23.

00000
00000
00000

00000
00000

00000
00000

00000
00000

00000
00000

00000
00000

00000
00000

00000
00000

00000
00000

00000
00000

00000
00000

00000
00000

[REDACTED]

APPENDIX

SIX-DEGREE-OF-FREEDOM EQUATIONS OF MOTION

The following equations represent six-degree-of-freedom equations of motion about a system of body axes. The aerodynamic coefficients used in the equations were programmed for the digital computer as functions of angle of attack. Solutions were obtained by the Runge-Kutta method of numerical integration.

Normal-force equation:

$$\dot{\alpha} - (\tan \alpha \tan \beta) \dot{\beta} + \left(\frac{\tan \alpha}{V} \right) \dot{V} = \frac{q_{\infty} S}{mV} \frac{C_Z + C_{Z\delta_e} \delta_e}{\cos \beta \cos \alpha} + \frac{g}{V} \left(\frac{\cos \theta \cos \phi}{\cos \beta \cos \alpha} \right) - \frac{p \tan \beta}{\cos \alpha} + q$$

Lateral-force equation:

$$\begin{aligned} \dot{\beta} + \left(\frac{\tan \beta}{V} \right) \dot{V} = & \frac{q_{\infty} S}{mV \cos \beta} \left[C_{Y\beta} \beta + C_{Y\delta_a} \delta_a + C_{Y\delta_r} \delta_r + \frac{b}{2V} (C_{Yp} p + C_{Yr} r) \right] \\ & + \frac{g}{V} \left(\frac{\cos \theta \sin \phi}{\cos \beta} \right) + p \sin \alpha - r \cos \alpha \end{aligned}$$

Longitudinal-force equation:

$$(V \tan \alpha) \dot{\alpha} + (V \tan \beta) \dot{\beta} - \dot{V} = - \frac{q_{\infty} S}{m} \left(\frac{C_X + C_{X\delta_e} \delta_e}{\cos \beta \cos \alpha} \right) + g \left(\frac{\sin \theta}{\cos \beta \cos \alpha} \right) + qV \tan \alpha - rV \left(\frac{\tan \beta}{\cos \alpha} \right)$$

Pitching-moment equation:

$$\dot{q} = \left(\frac{I_Z - I_X}{I_Y} \right) pr + \frac{I_{XZ}}{I_Y} (r^2 - p^2) + \frac{q_{\infty} S l}{I_Y} \left(C_{m\alpha} \alpha + C_{m\delta_e} \delta_e + \frac{l}{2V} C_{mq} q \right)$$

Rolling-moment equation:

$$\dot{p} = \left(\frac{I_{XZ}}{I_X} \right) \dot{r} + \left(\frac{I_Y - I_Z}{I_X} \right) qr + \left(\frac{I_{XZ}}{I_X} \right) pq + \frac{q_{\infty} S b}{I_X} \left[C_{l\beta} \beta + C_{l\delta_a} \delta_a + C_{l\delta_r} \delta_r + \frac{b}{2V} (C_{lp} p + C_{lr} r) \right]$$

APPENDIX

Yawing-moment equation:

$$\frac{I_{XZ}}{I_Z} \dot{p} - \dot{r} = \left(\frac{I_Y - I_X}{I_Z} \right) pq + \frac{I_{XZ}}{I_Z} qr - \frac{q_\infty S b}{I_Z} \left[C_{n_\beta} \beta + C_{n_{\delta_a}} \delta_a + C_{n_{\delta_r}} \delta_r + \frac{b}{2V} (C_{n_p} p + C_{n_r} r) \right]$$

The following auxiliary equations were also used in the calculations:

$$\dot{\theta} = q \cos \phi - r \sin \phi$$

$$\dot{\phi} = p + r \tan \theta \cos \phi + q \tan \theta \sin \phi$$

$$\dot{\psi} = \frac{r \cos \phi + q \sin \phi}{\cos \theta}$$

00000
00000
00000

00000
00000
00000

00000
00000
00000

00000
00000
00000

00000
00000
00000

00000
00000
00000

00000
00000
00000

00000
00000
00000

00000
00000
00000

00000
00000
00000

00000
00000
00000

00000
00000
00000

REFERENCES

1. Rainey, Robert W.: Summary of an Advanced Manned Lifting Entry Vehicle Study. NASA TM X-1159, 1965.
2. Mechtly, E. A.: The International System of Units -- Physical Constants and Conversion Factors. NASA SP-7012, 1964.
3. Ware, George M.: Full-Scale Wind-Tunnel Investigation of the Aerodynamic Characteristics of the HL-10 Manned Lifting Entry Vehicle. NASA TM X-1160, 1965.
4. Henderson, William P.: Static Stability Characteristics of a Manned Lifting Entry Vehicle at High Subsonic Speeds. NASA TM X-1349, 1967.
5. Etkin, Bernard: Dynamics of Flight. John Wiley & Sons, Inc., c.1959.
6. Anon.: Flying Qualities of Piloted Airplanes. Mil. Specification MIL-F-8785 (ASG), Sept. 1, 1954.
7. Breuhaus, W. O.; Reynolds, P. A.; and Kidd, F. A.: Handling Qualities Requirements for Hyper-Velocity Aircraft. Rept. No. TC-1332-F-1 (Contract No. AF33(616)-6240), Cornell Aeron. Lab., Inc., Sept. 30, 1959 (Rev. Jan. 28, 1960). (Available from ASTIA as AD 323 250.)
8. Johnson, Joseph L.; and Sternfield, Leonard: A Theoretical Investigation of the Effect of Yawing Moment Due to Rolling on Lateral Oscillatory Stability. NACA TN 1723, 1948.
9. Ashkenas, Irving L.; and McRuer, Duane T.: The Determination of Lateral Handling Quality Requirements From Airframe-Human Pilot System Studies. WADC Tech. Rept. 59-135, ASTIA Doc. No. AD 212 152, U.S. Air Force, June 1959.
10. Ware, George M.: Investigation of the Flight Characteristics of a Model of the HL-10 Manned Lifting Entry Vehicle. NASA TM X-1307, 1967.
11. Harper, Robert P., Jr.: In-Flight Simulation of the Lateral-Directional Handling Qualities of Entry Vehicles. WADD Tech. Rept. 61-147, U.S. Air Force, Nov. 1961.
12. Pinsker, W. J. G.: The Lateral Motion of Aircraft, and In Particular of Inertially Slender Configurations. R. & M. No. 3334, Brit. A.R.C., 1963.

TABLE I.- HL-10 DIMENSIONAL AND MASS CHARACTERISTICS
USED IN INVESTIGATION

b	13.7 ft	(4.18 m)
S	160 ft ²	(14.86 m ²)
l	21.17 ft	(6.45 m)
Weight,		
Light	5776 lbf	(25 692 N)
Heavy	9350 lbf	(41 589 N)
W/S,		
Light	36.10 lbf/ft ²	(1728.47 N/m ²)
Heavy	58.44 lbf/ft ²	(2109.68 N/m ²)
I _X ,		
Light	1112.0 slug-ft ²	(1507.2 kg-m ²)
Heavy	1334.5 slug-ft ²	(1808.8 kg-m ²)
I _Y ,		
Light	5818.6 slug-ft ²	(7886.5 kg-m ²)
Heavy	6379.7 slug-ft ²	(8647.0 kg-m ²)
I _Z ,		
Light	6293.8 slug-ft ²	(8530.6 kg-m ²)
Heavy	6652.4 slug-ft ²	(9016.7 kg-m ²)
ε,		
Light		6.98°
Heavy		7.17°

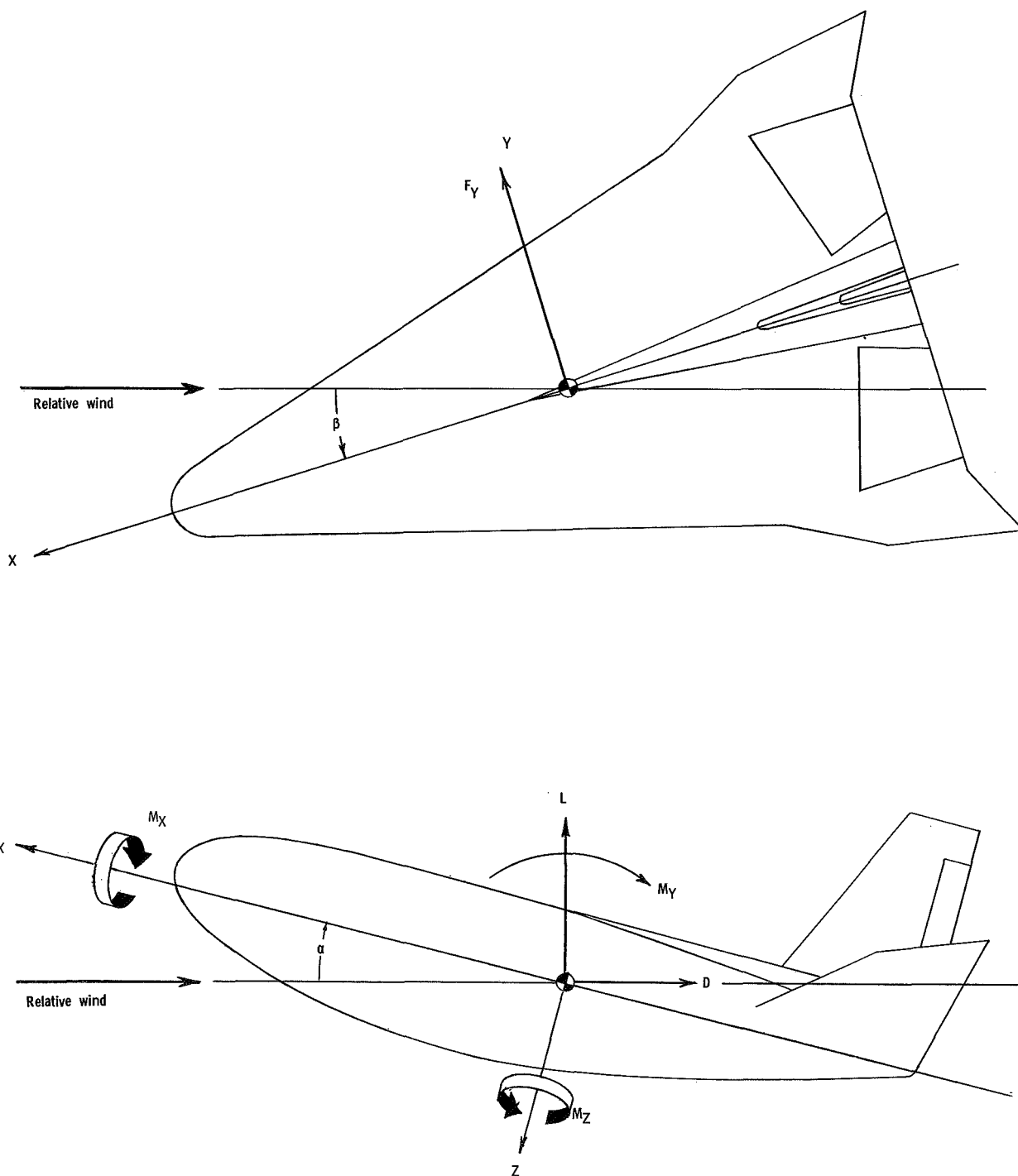


Figure 1:- System of axes used in investigation. All data are referred to body axes except lift and drag, which are referred to wind axes. Arrows indicate positive direction of forces, moments, and angles.

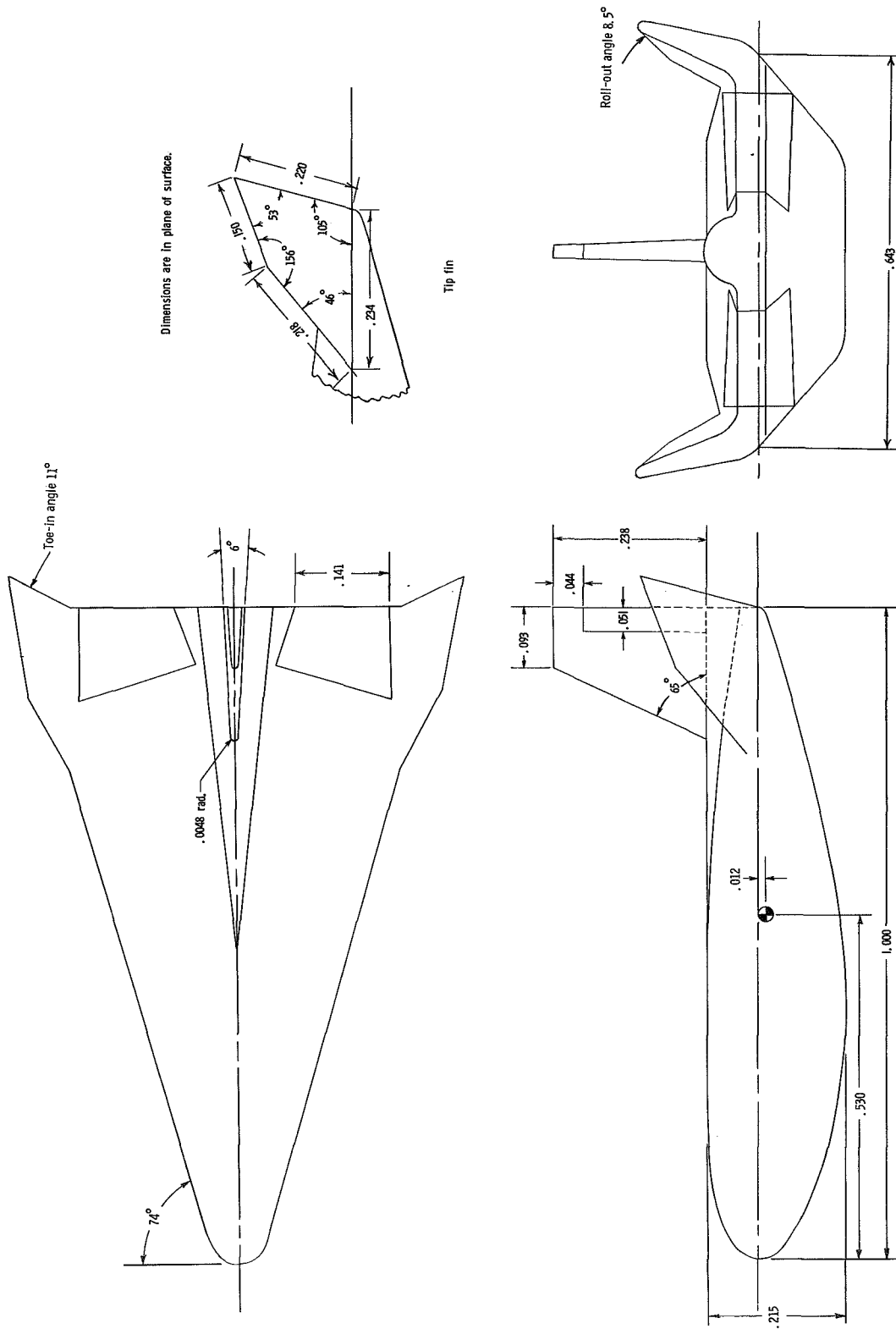


Figure 2.- Three-view drawing of HL-10 entry vehicle used in investigation. Dimensions are nondimensionalized with respect to body length.

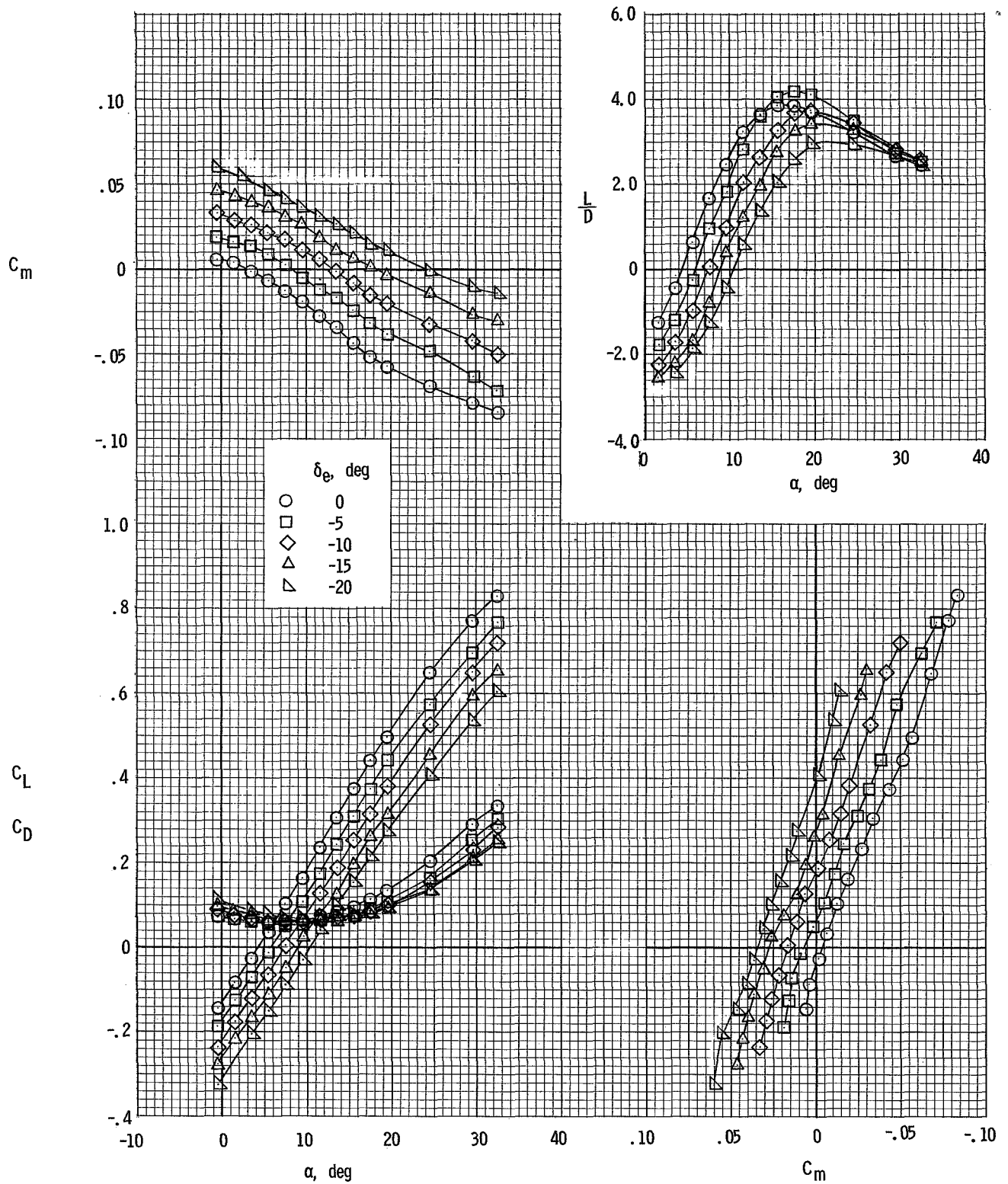


Figure 3.- Static longitudinal aerodynamic characteristics of HL-10 entry vehicle. Mach number = 0.05. Data from reference 3.

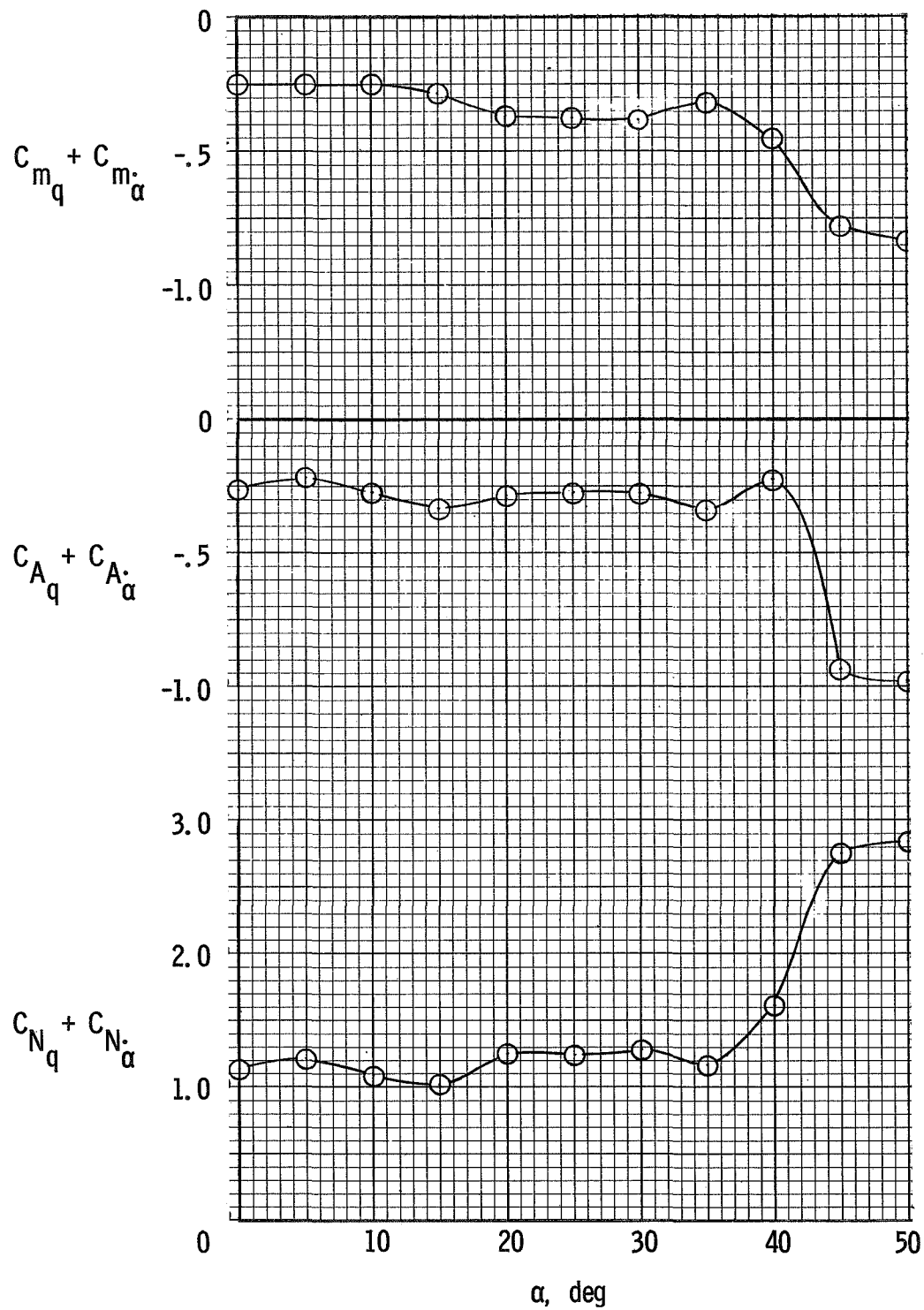


Figure 4.- Dynamic longitudinal stability derivatives of HL-10 entry vehicle. Mach number = 0.05. Data from reference 10.

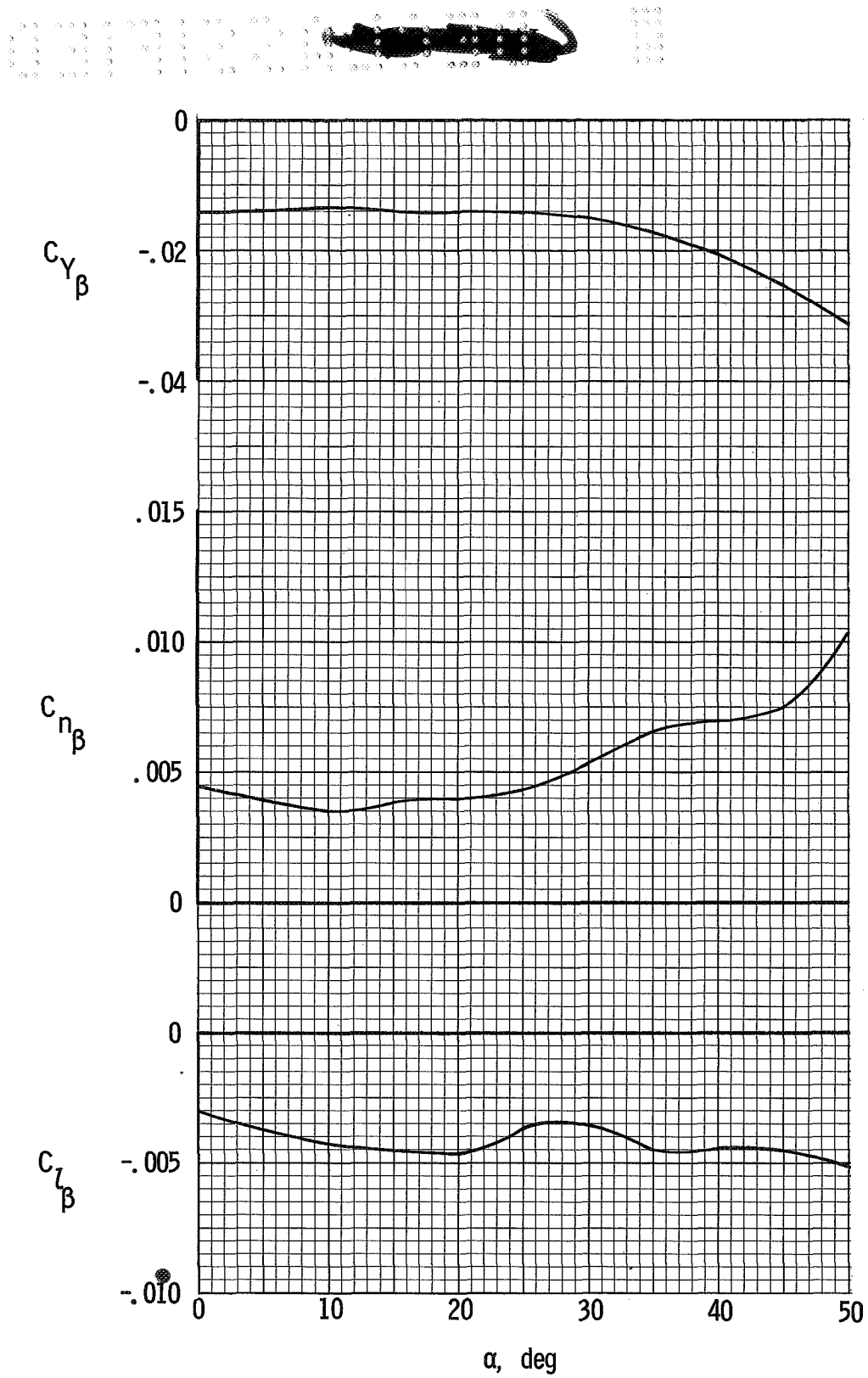
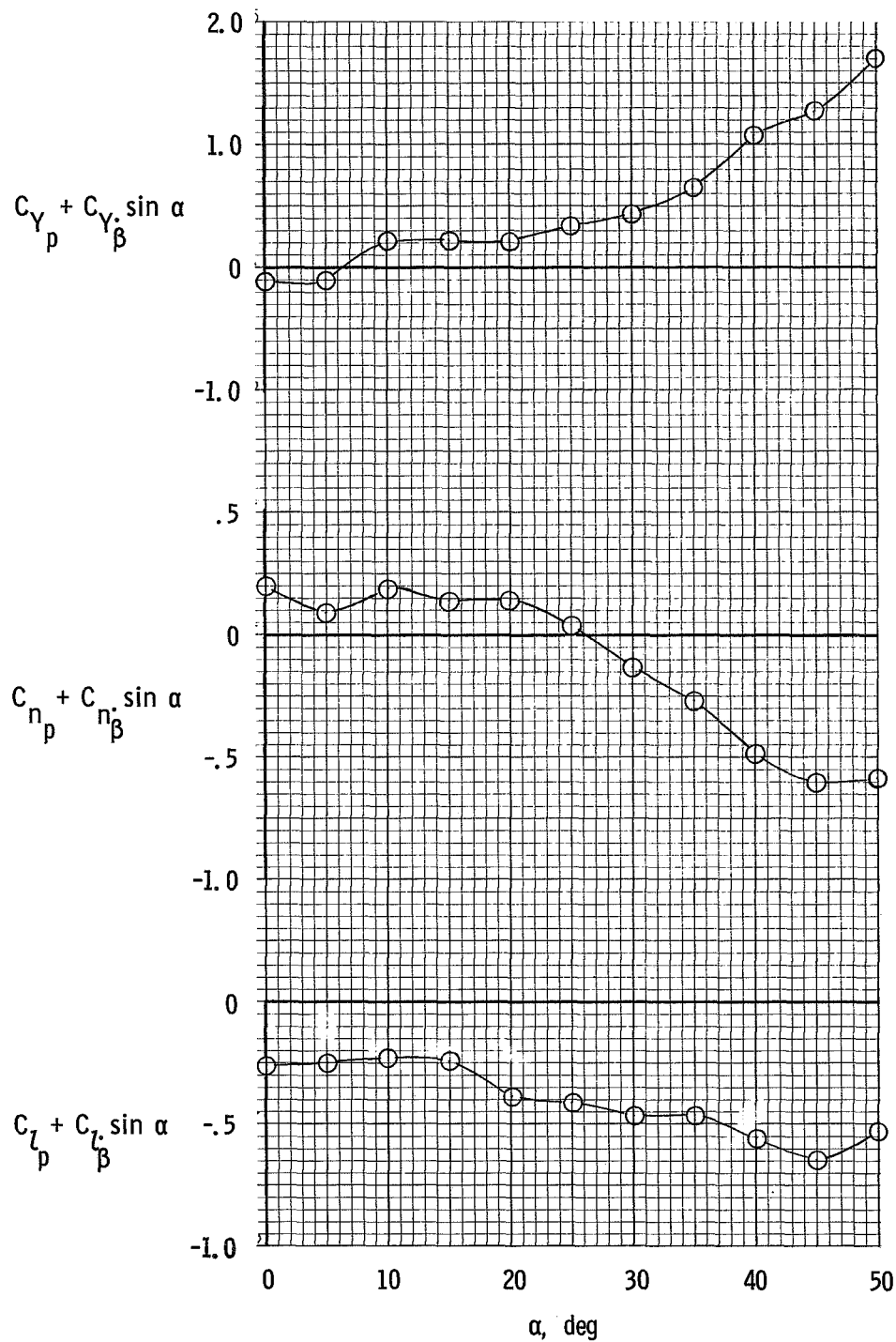


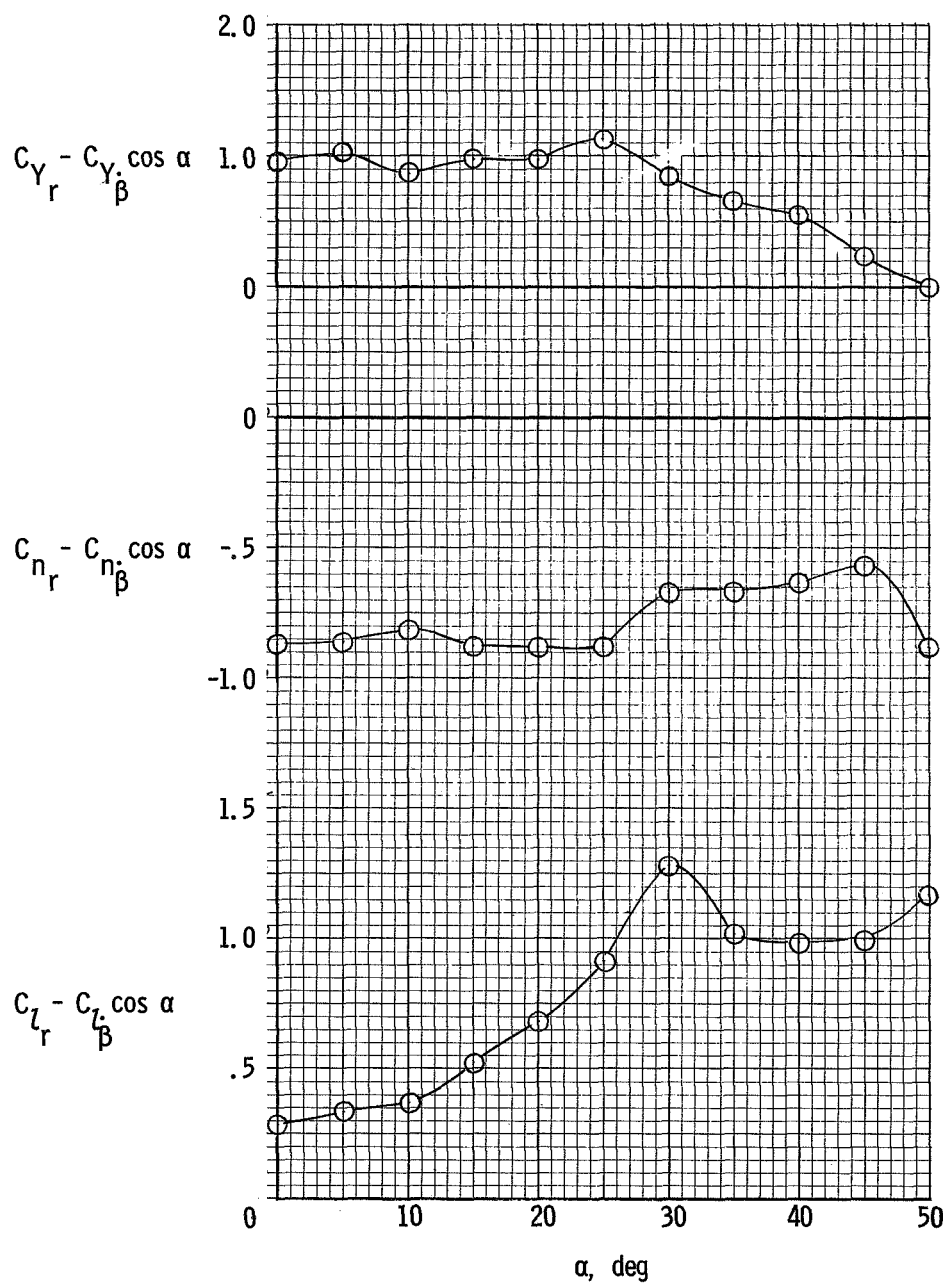
Figure 5.- Static lateral stability derivatives of HL-10 entry vehicle. Mach number = 0.05. Data from reference 10.



(a) Dynamic stability derivatives in roll.

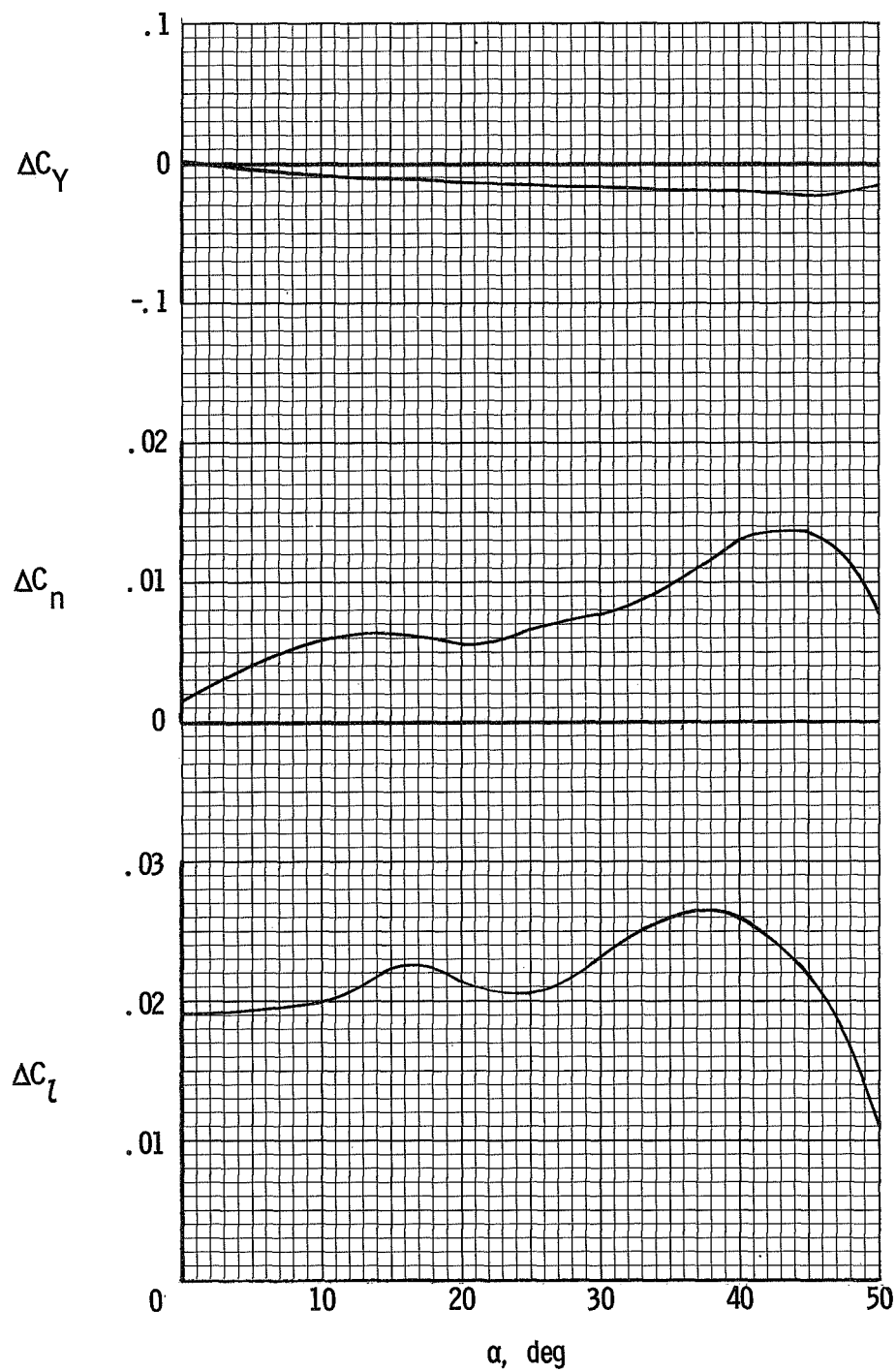
Figure 6.- Dynamic lateral stability derivatives of HL-10 entry vehicle. Mach number = 0.05. Data from reference 10.

13 12 11 10 9 8 7 6 5 4 3 2 1 0 1 2 3 4 5 6 7 8 9 10 11 12 13 14 15 16 17 18 19 20 21 22 23 24 25 26 27 28 29 30 31 32 33 34 35 36 37 38 39 40 41 42 43 44 45 46 47 48 49 50 51 52 53 54 55 56 57 58 59 60 61 62 63 64 65 66 67 68 69 70 71 72 73 74 75 76 77 78 79 80 81 82 83 84 85 86 87 88 89 90 91 92 93 94 95 96 97 98 99 100



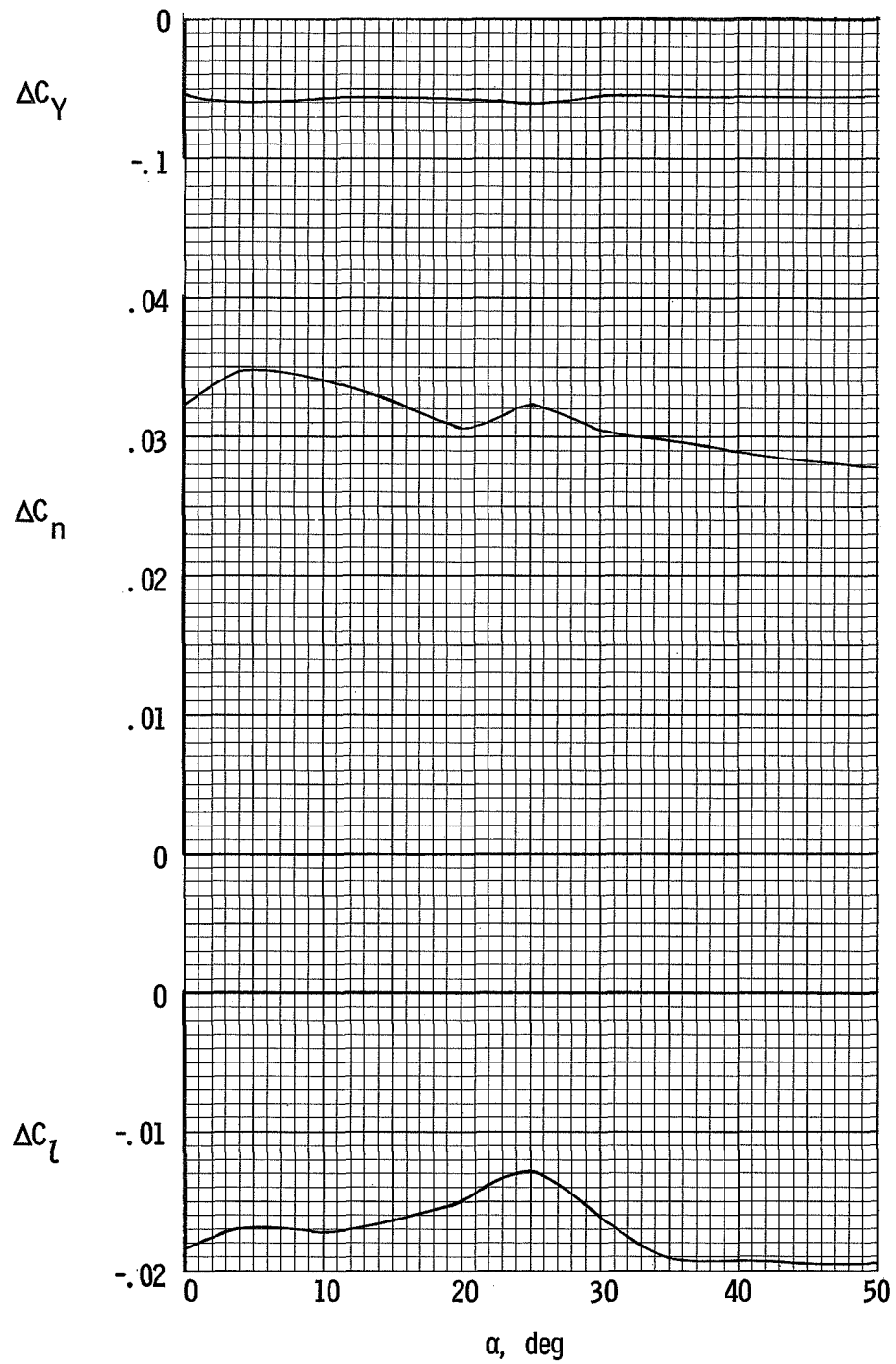
(b) Dynamic stability derivatives in yaw.

Figure 6.- Concluded.



(a) Aileron control; $\delta_{eL} = 10^\circ$; $\delta_{eR} = -10^\circ$.

Figure 7.- Incremental lateral force and moment coefficients of HL-10 entry vehicle produced by aileron and rudder deflections. Mach number = 0.05. Data from reference 10.



(b) Rudder control; $\delta_r = 20^\circ$.

Figure 7.- Concluded.



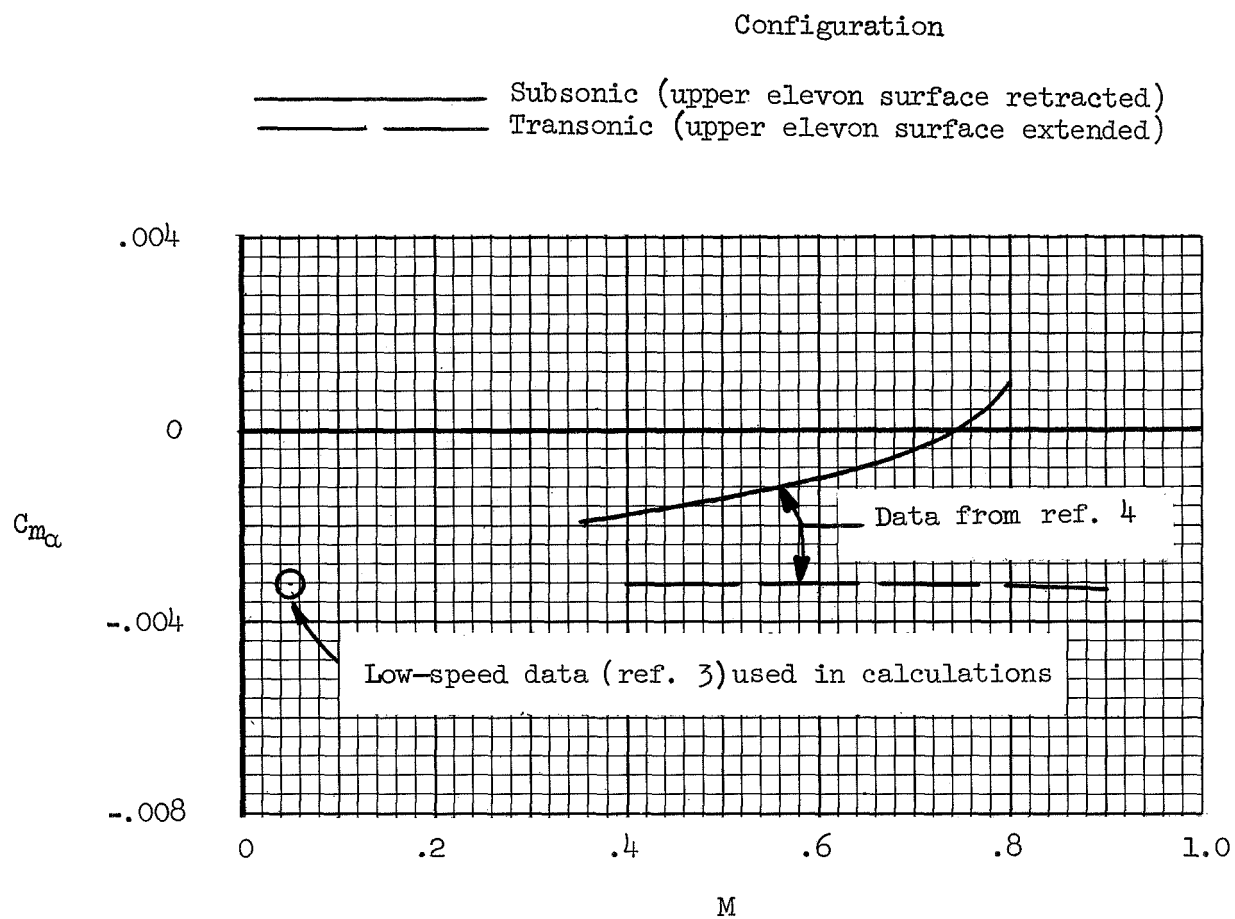
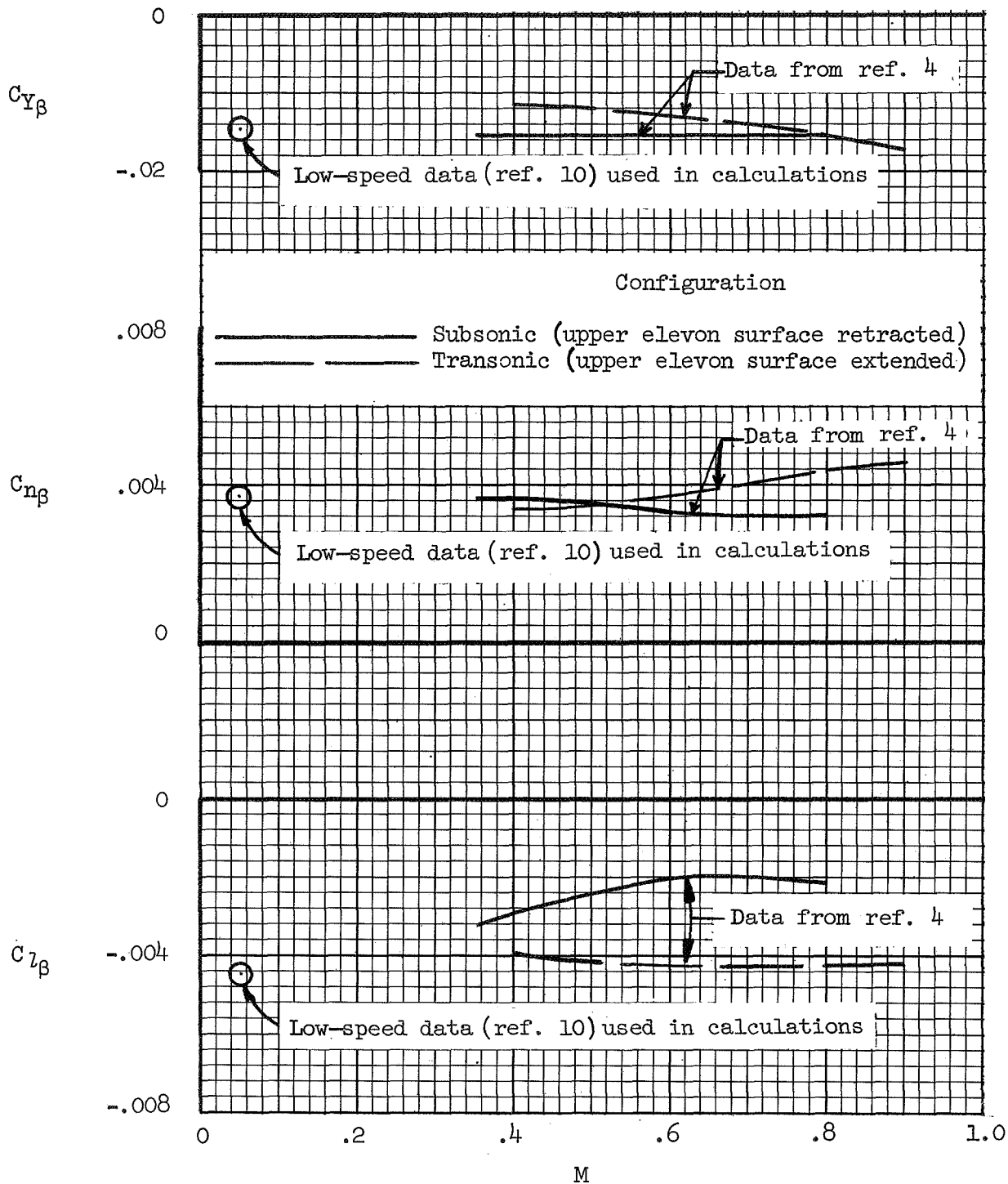
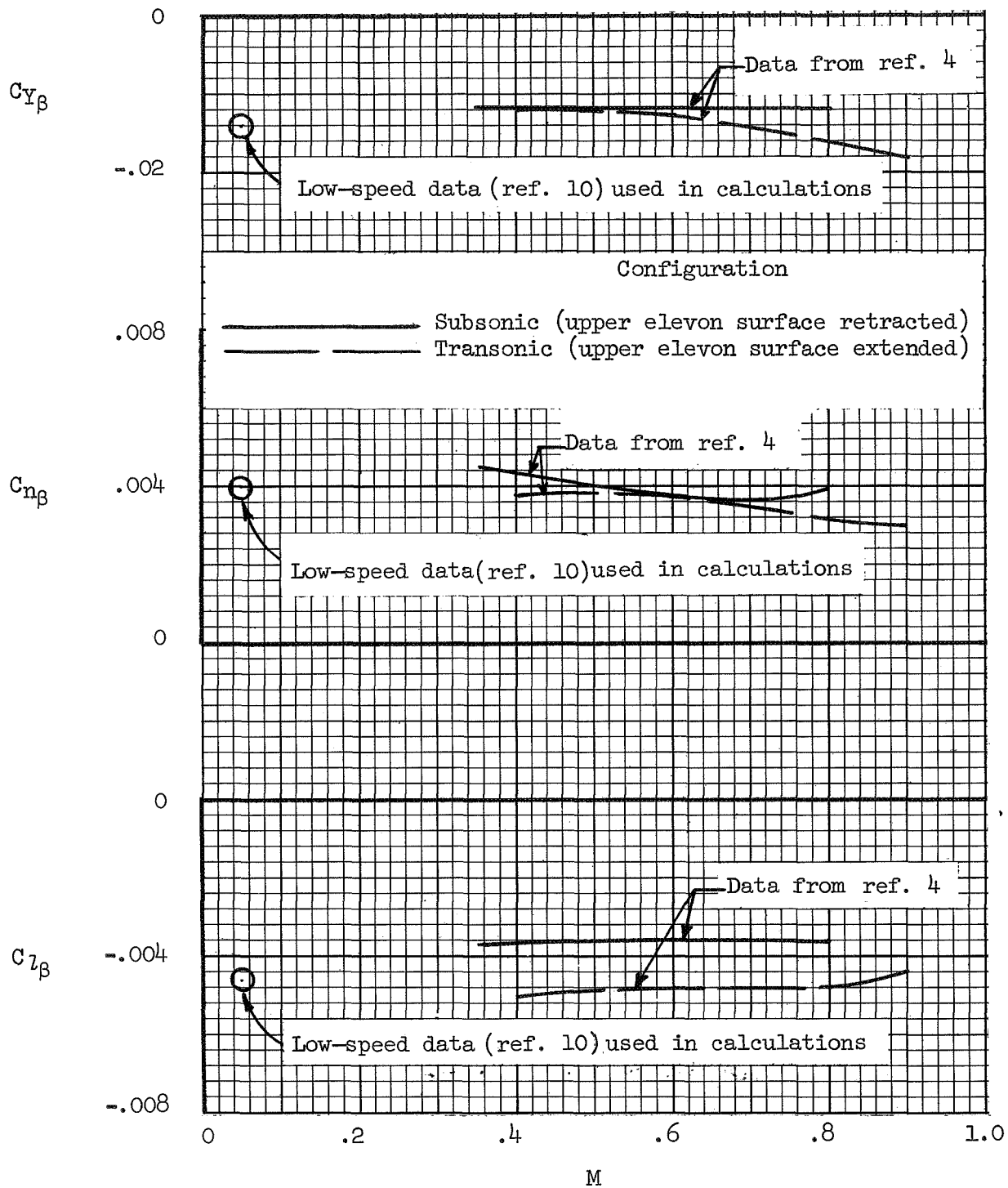


Figure 8.- Variation of static longitudinal stability parameter with Mach number for HL-10 entry vehicle.



(a) $\alpha = 14^\circ$.

Figure 9.- Variation of static lateral stability parameters with Mach number for HL-10 entry vehicle.



(b) $\alpha = 21^\circ$.

Figure 9.- Concluded.

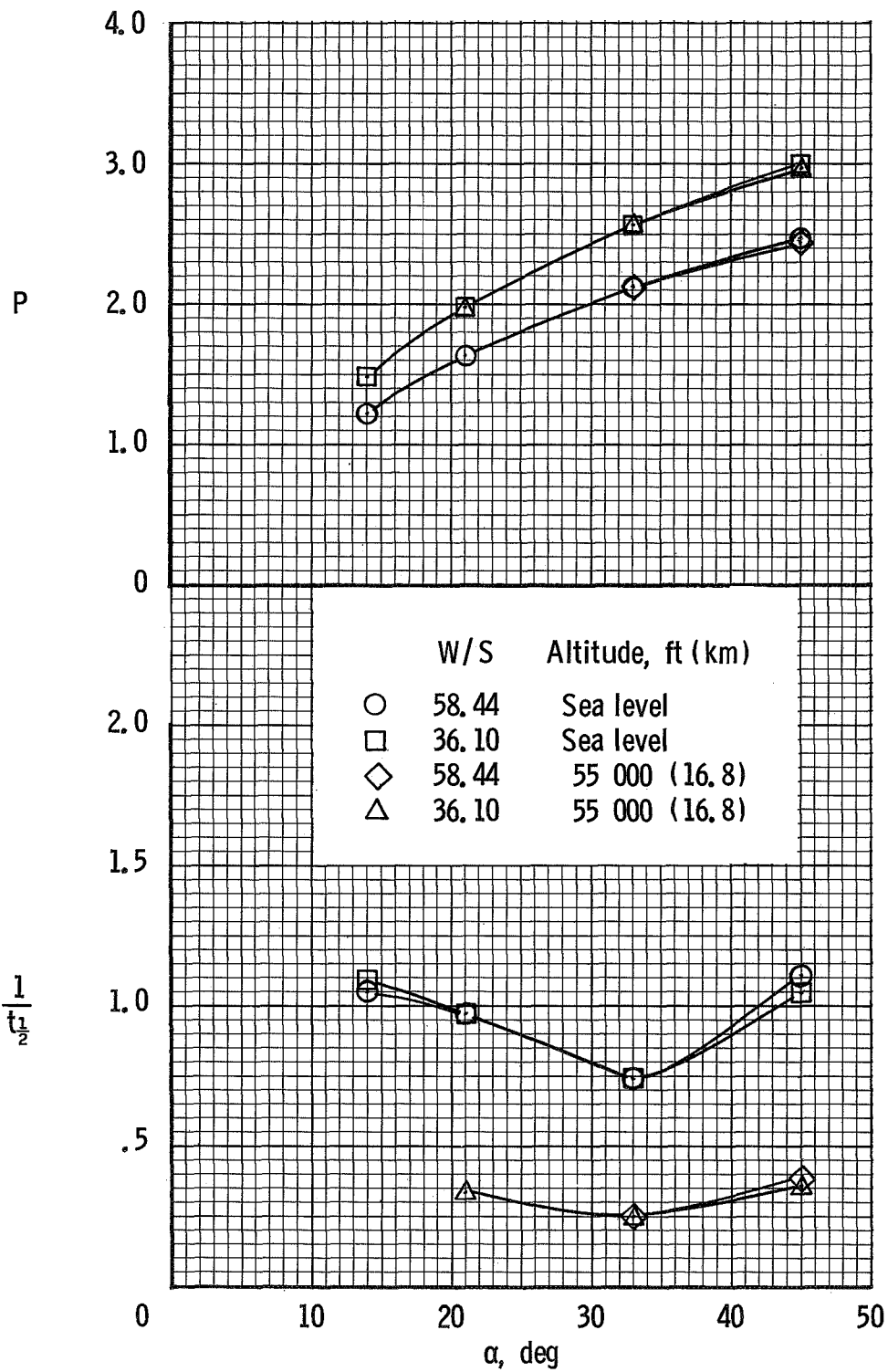


Figure 10.- Variation of period and damping characteristics of short-period longitudinal mode with angle of attack for HL-10 entry vehicle.

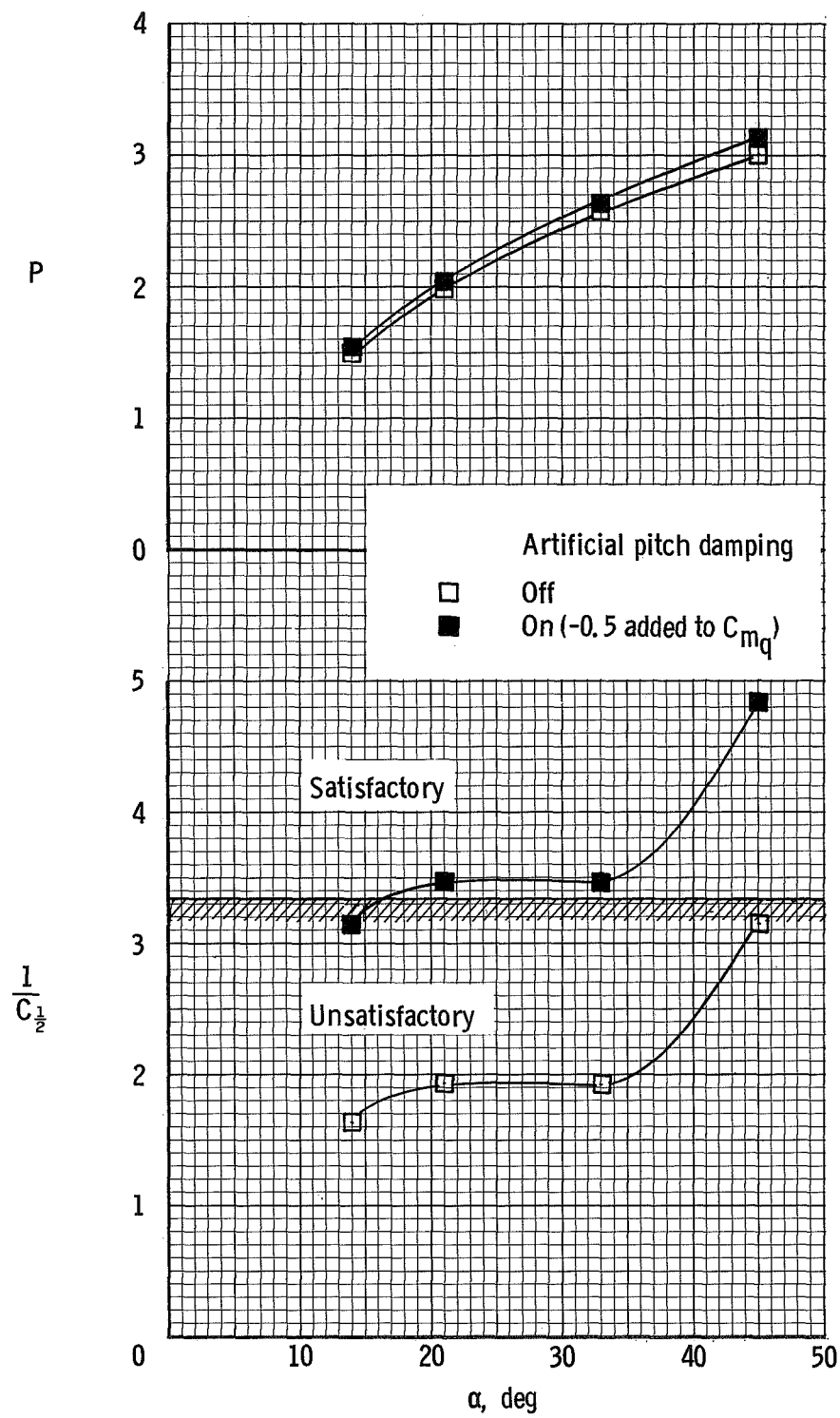


Figure 11.- Effect of damping in pitch on period and damping characteristics of short-period longitudinal mode for HL-10 entry vehicle.
W/S = 36.10; sea level.

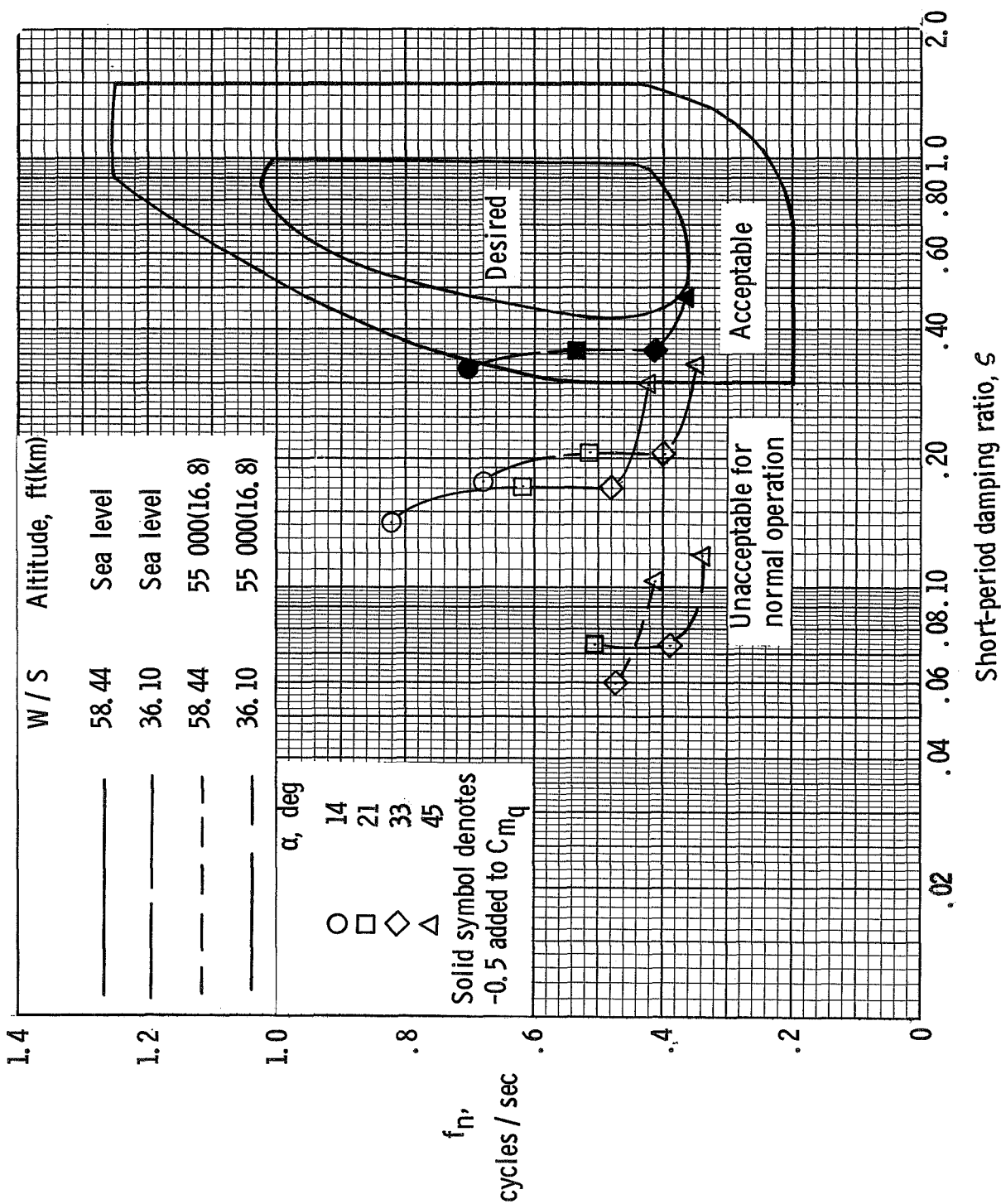
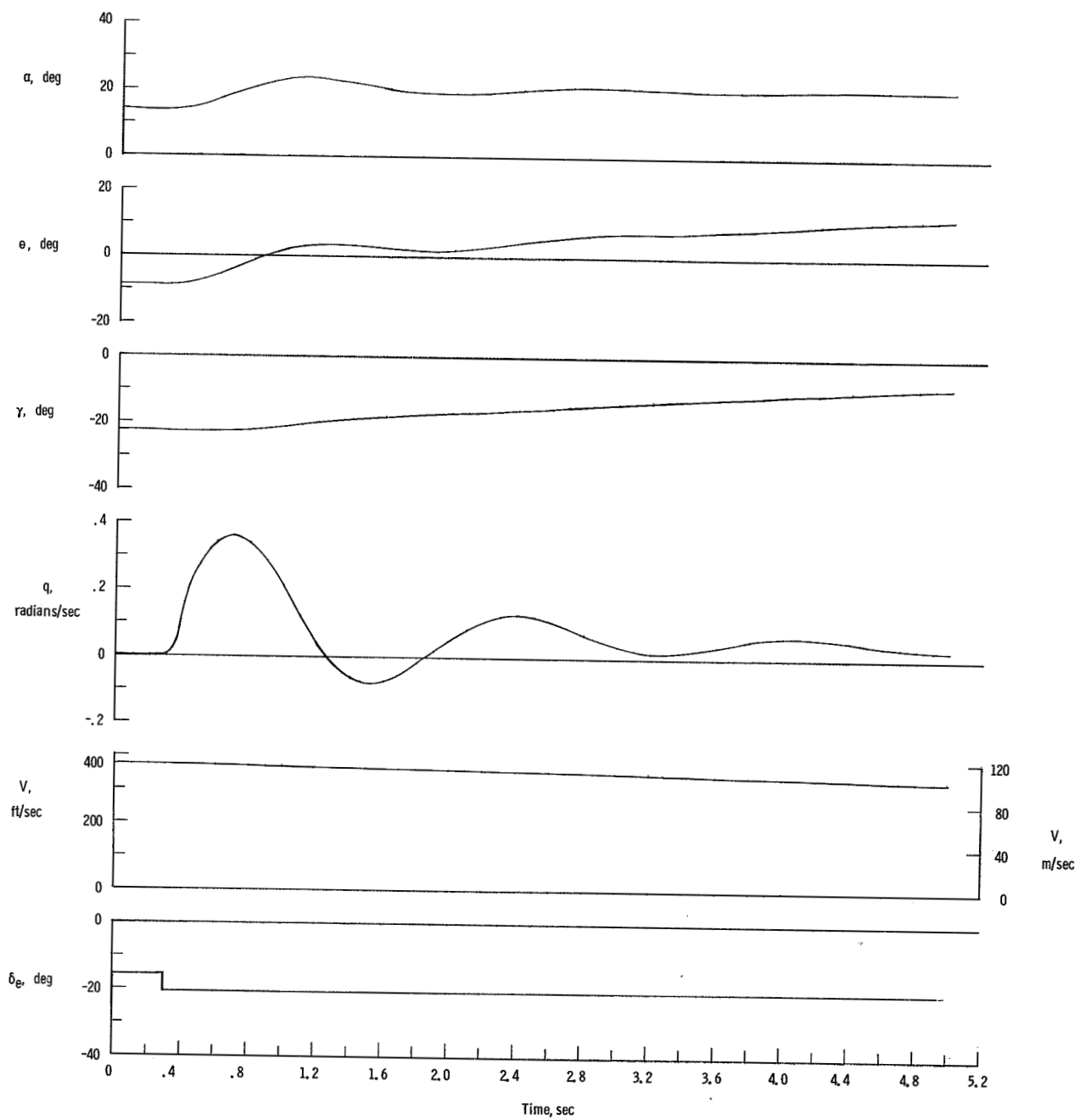
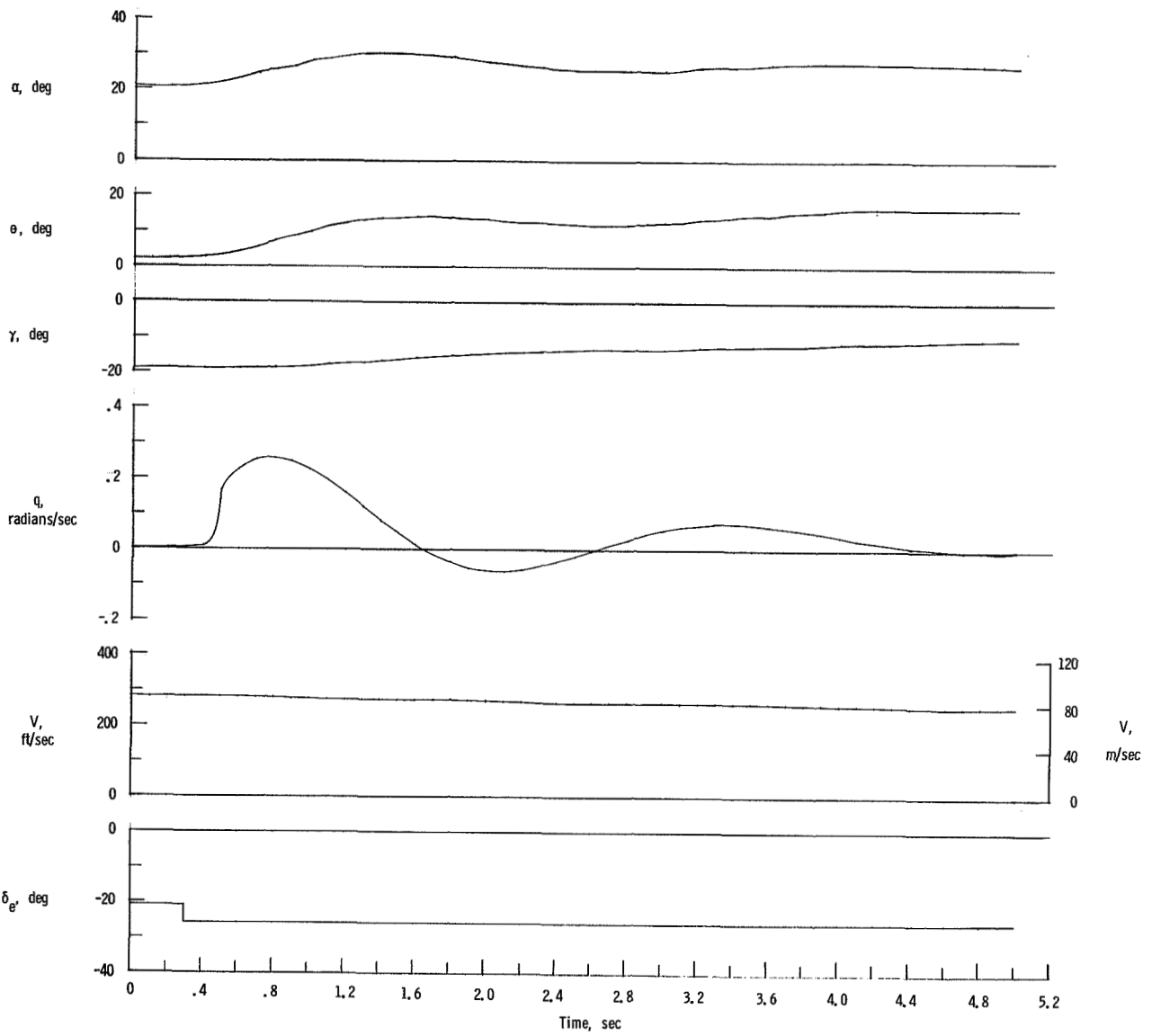


Figure 12.- Comparison of HL-10 entry vehicle longitudinal damping characteristics with handling qualities requirements from reference 7.



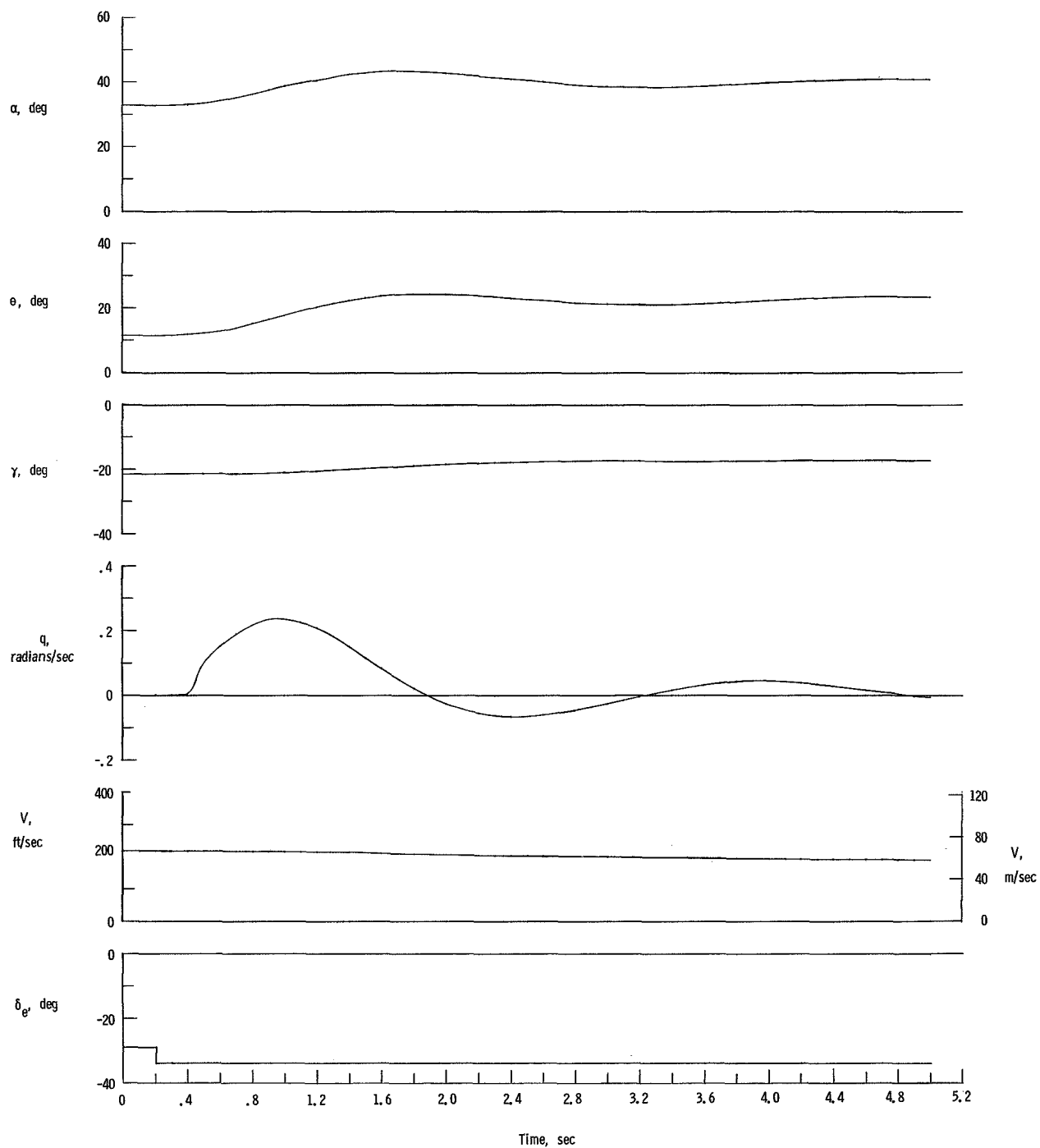
(a) $\alpha = 14^\circ$.

Figure 13.- Time histories of longitudinal motions following a step elevator input for HL-10 entry vehicle. W/S = 36.10; sea level.



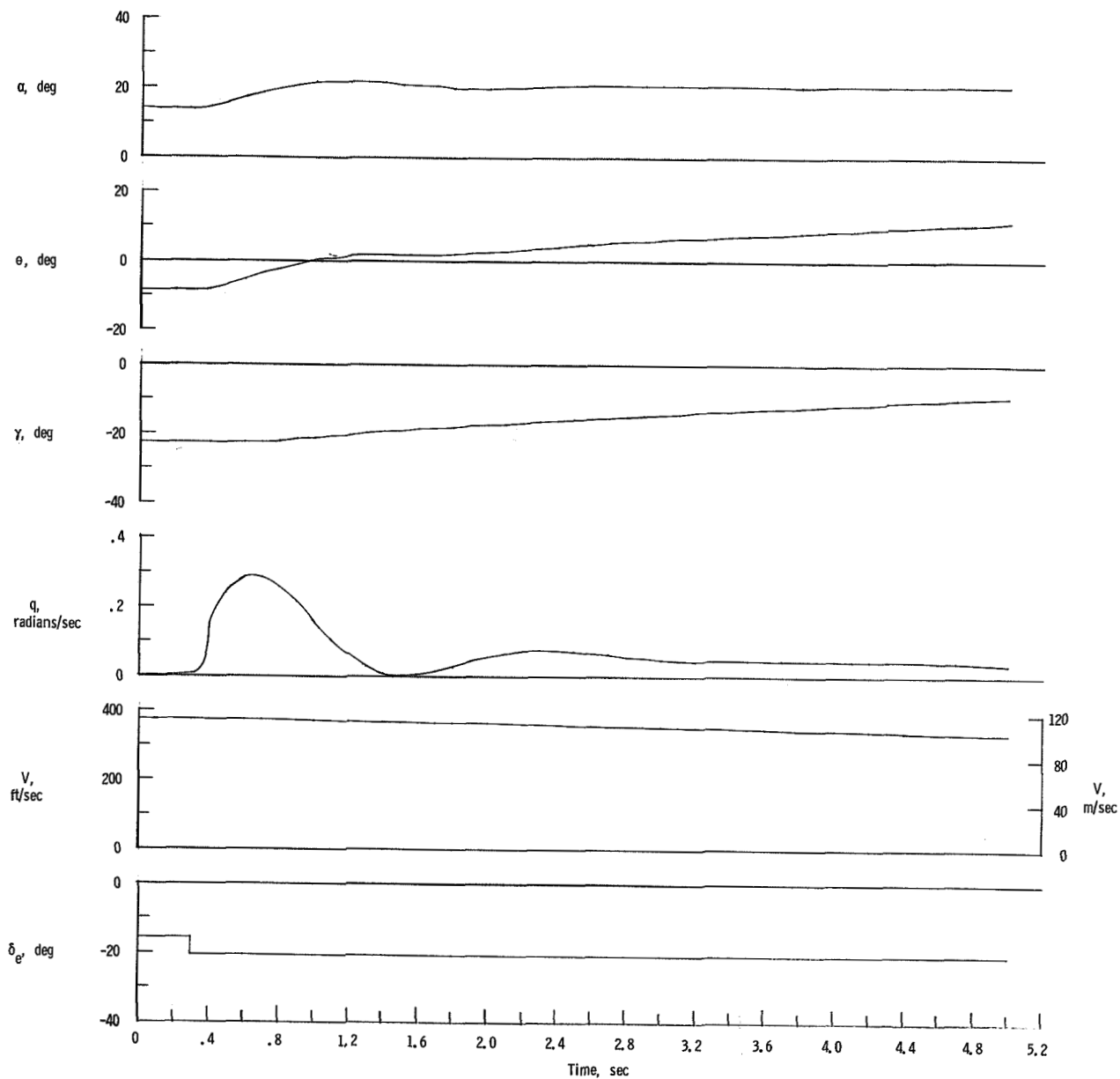
(b) $\alpha = 21^\circ$.

Figure 13.- Continued.



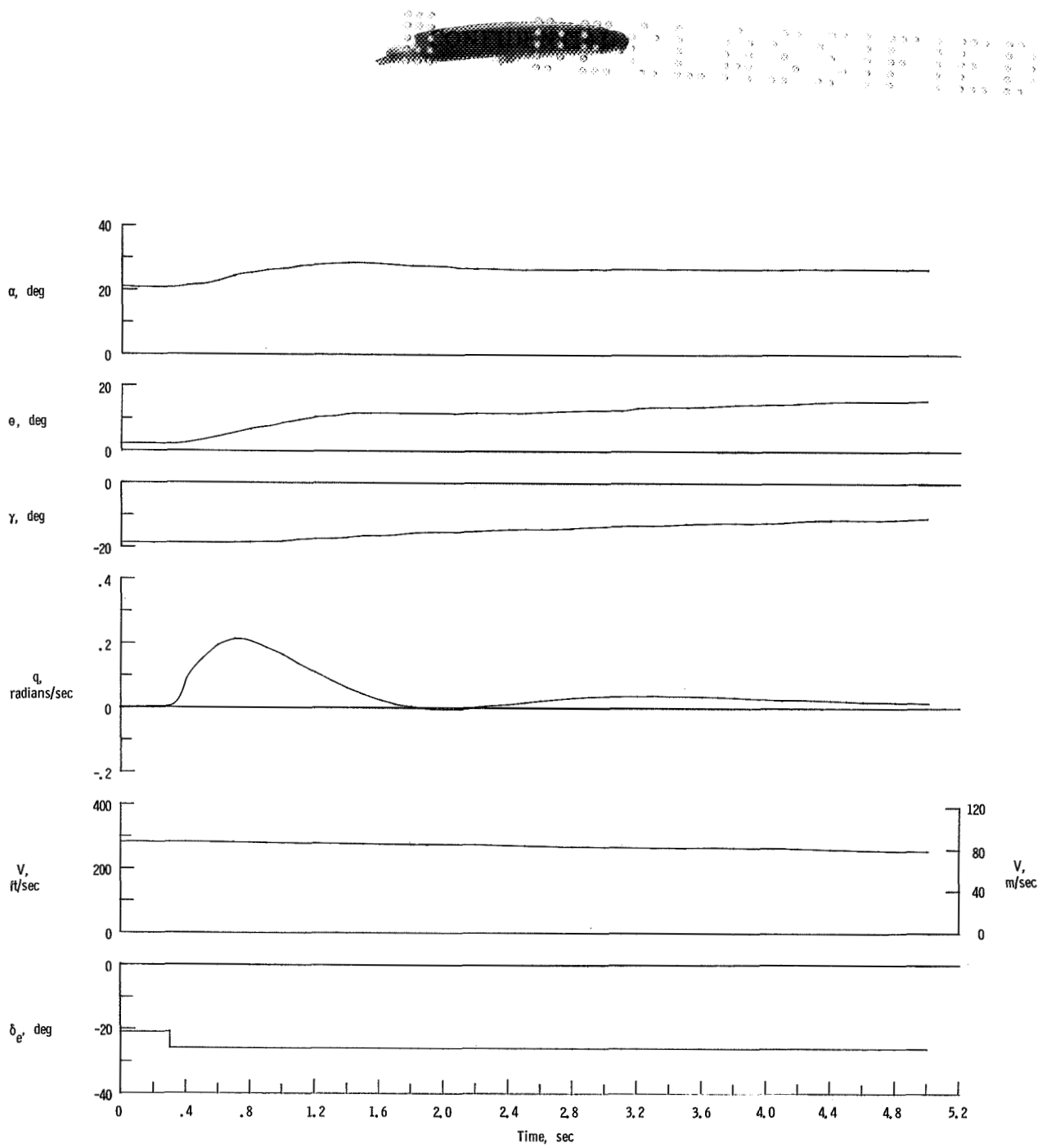
(c) $\alpha = 33^\circ$.

Figure 13.- Concluded.



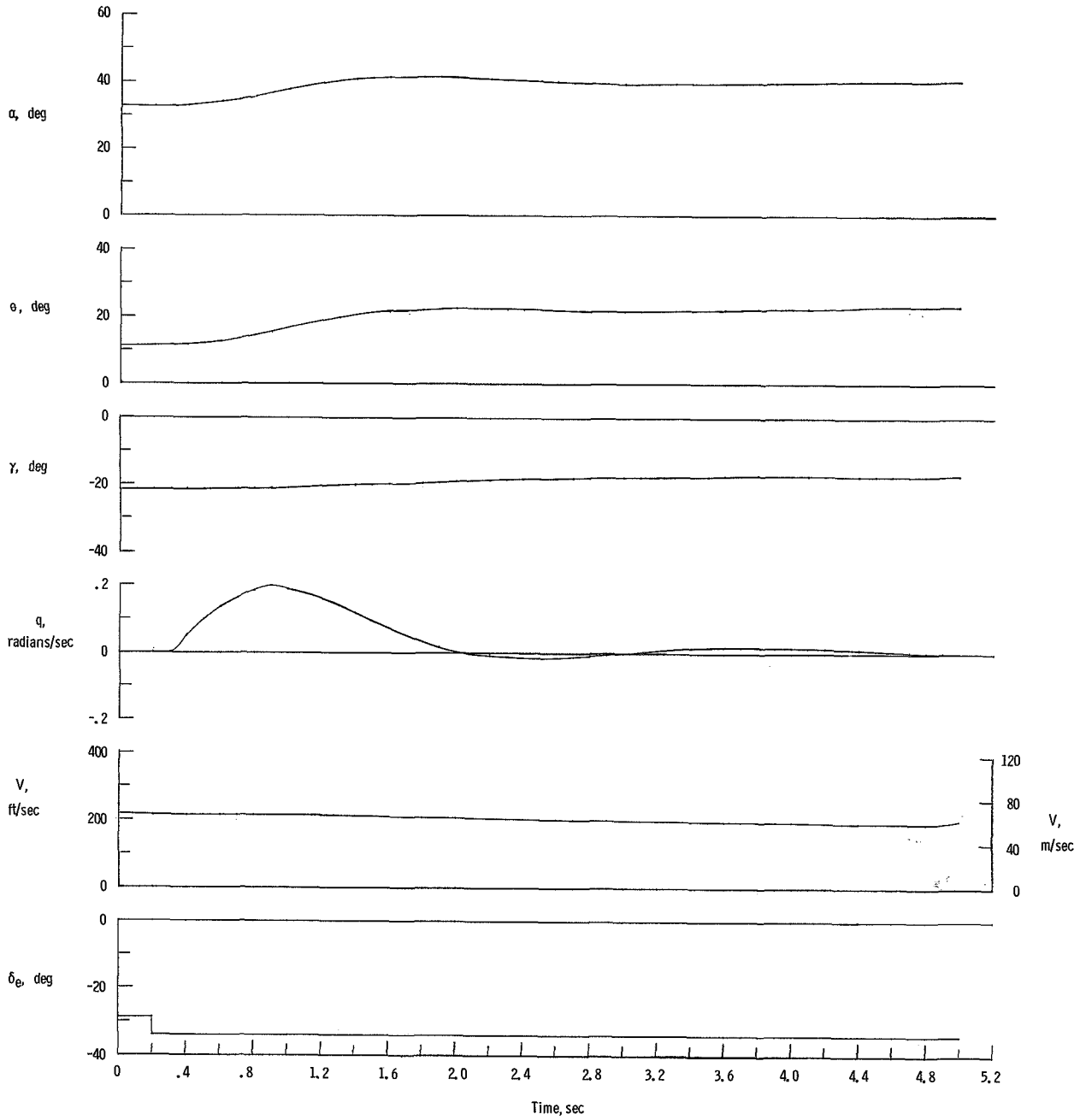
(a) $\alpha = 14^\circ$.

Figure 14.- Effect of damping in pitch on longitudinal motions following a step elevator input for HL-10 entry vehicle. $W/S = 36.10$; sea level; -0.5 added to C_{mq} .



(b) $\alpha = 21^\circ$.

Figure 14.- Continued.



(c) $\alpha = 33^\circ$.

Figure 14.- Concluded.

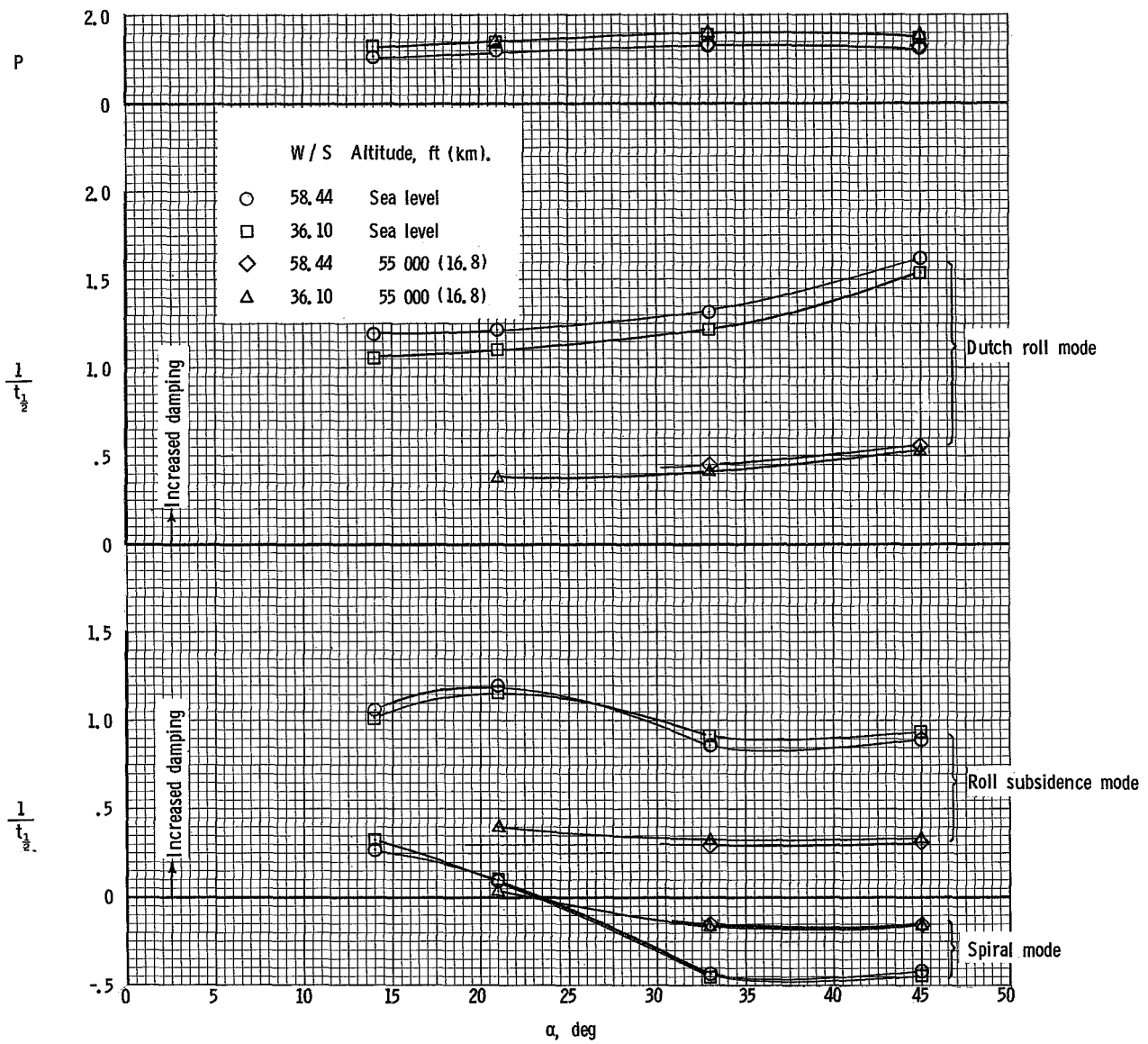


Figure 15.- Variation of period and damping of lateral modes of motion with angle of attack for HL-10 entry vehicle.



	W/S	Altitude, ft (km)
————	58.44	Sea level
————	36.10	Sea level
----	58.44	55 000 (16.8)
----	36.10	55 000 (16.8)

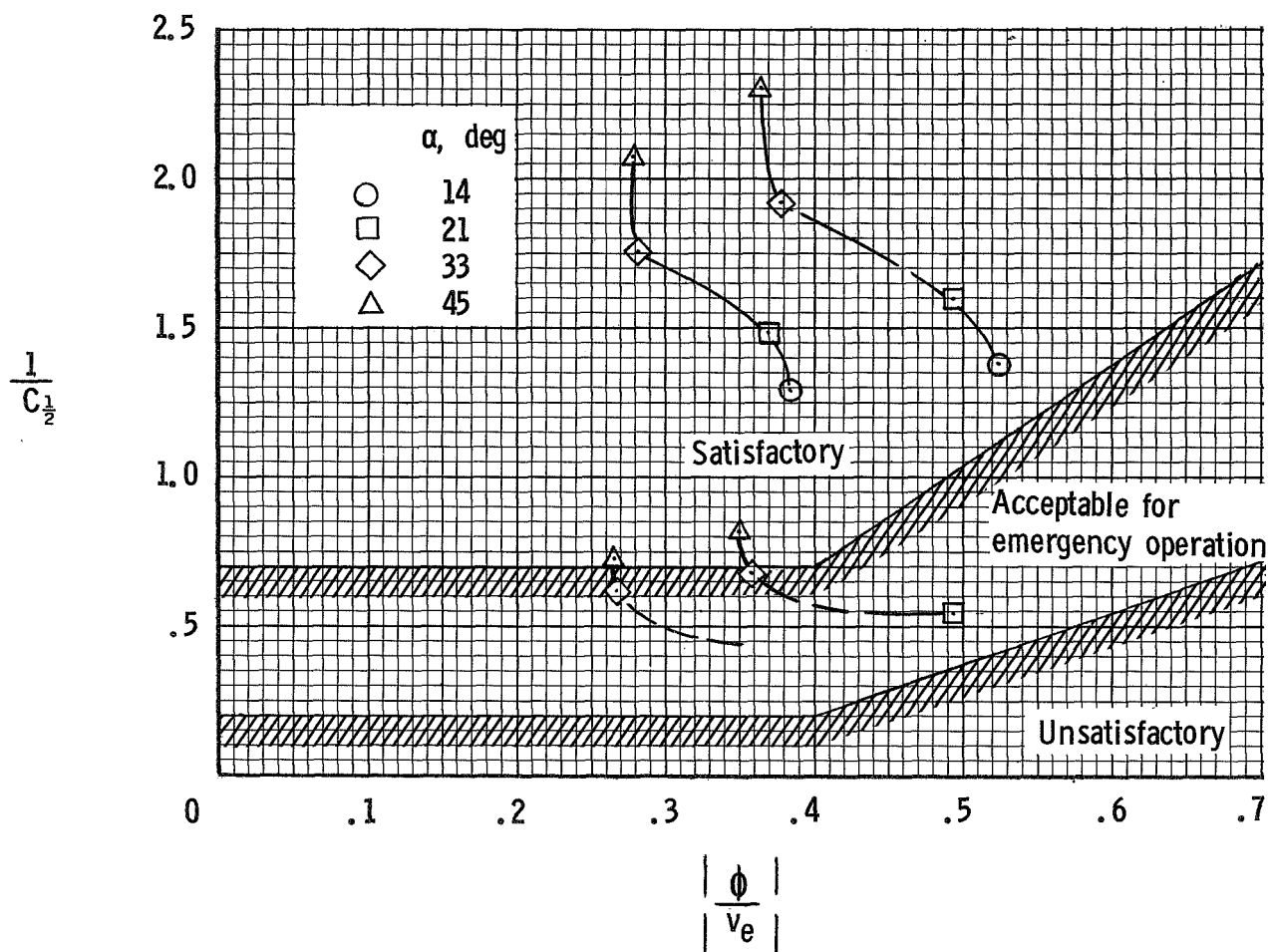


Figure 16.- Comparison of lateral damping characteristics of HL-10 entry vehicle in terms of military specifications for flying qualities of piloted airplanes.



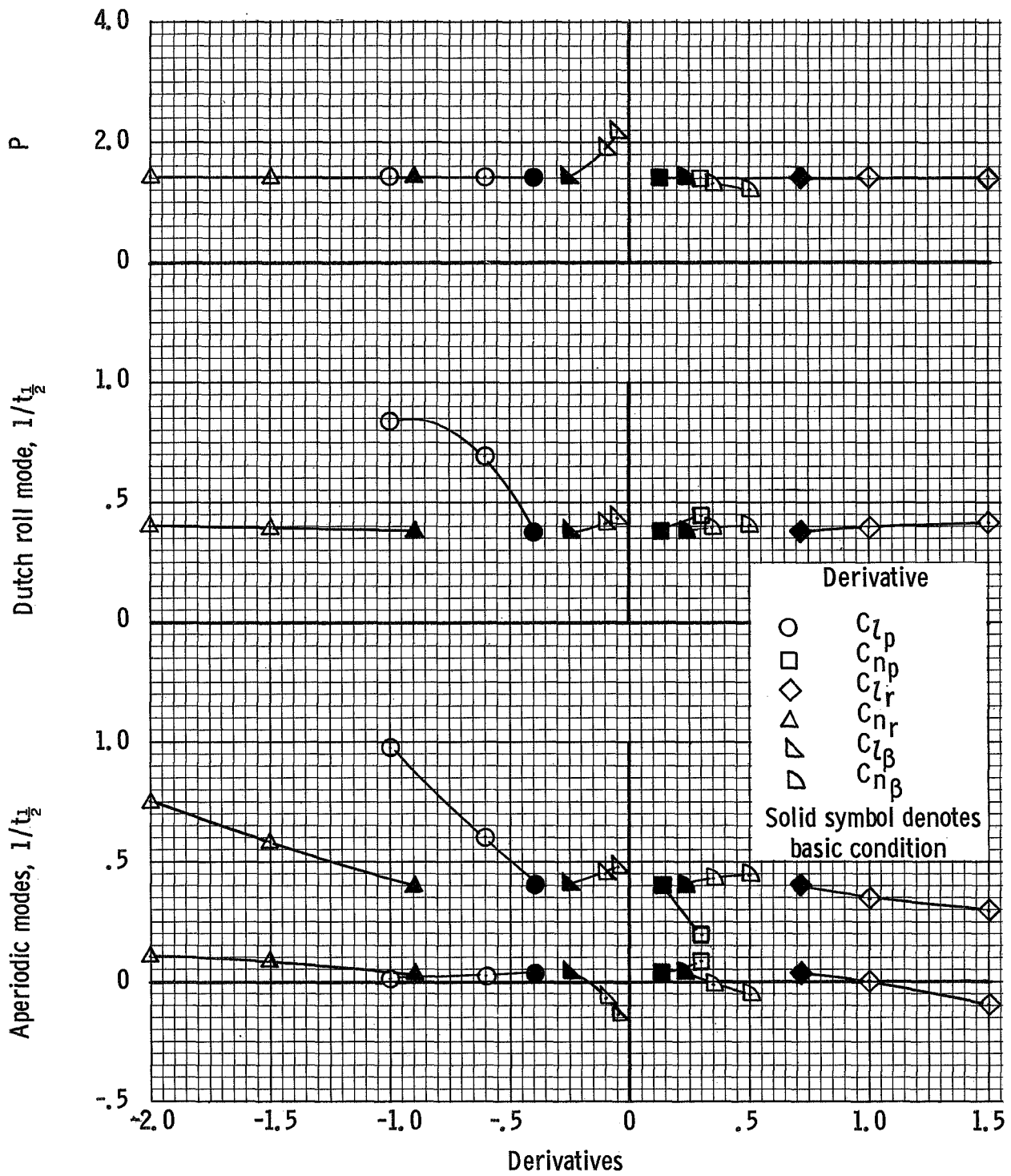


Figure 17.- Effect of derivative variation on lateral period and damping characteristics of HL-10 entry vehicle. W/S = 36.10; Altitude = 55 000 ft (16.8 km); $\alpha = 21^\circ$.

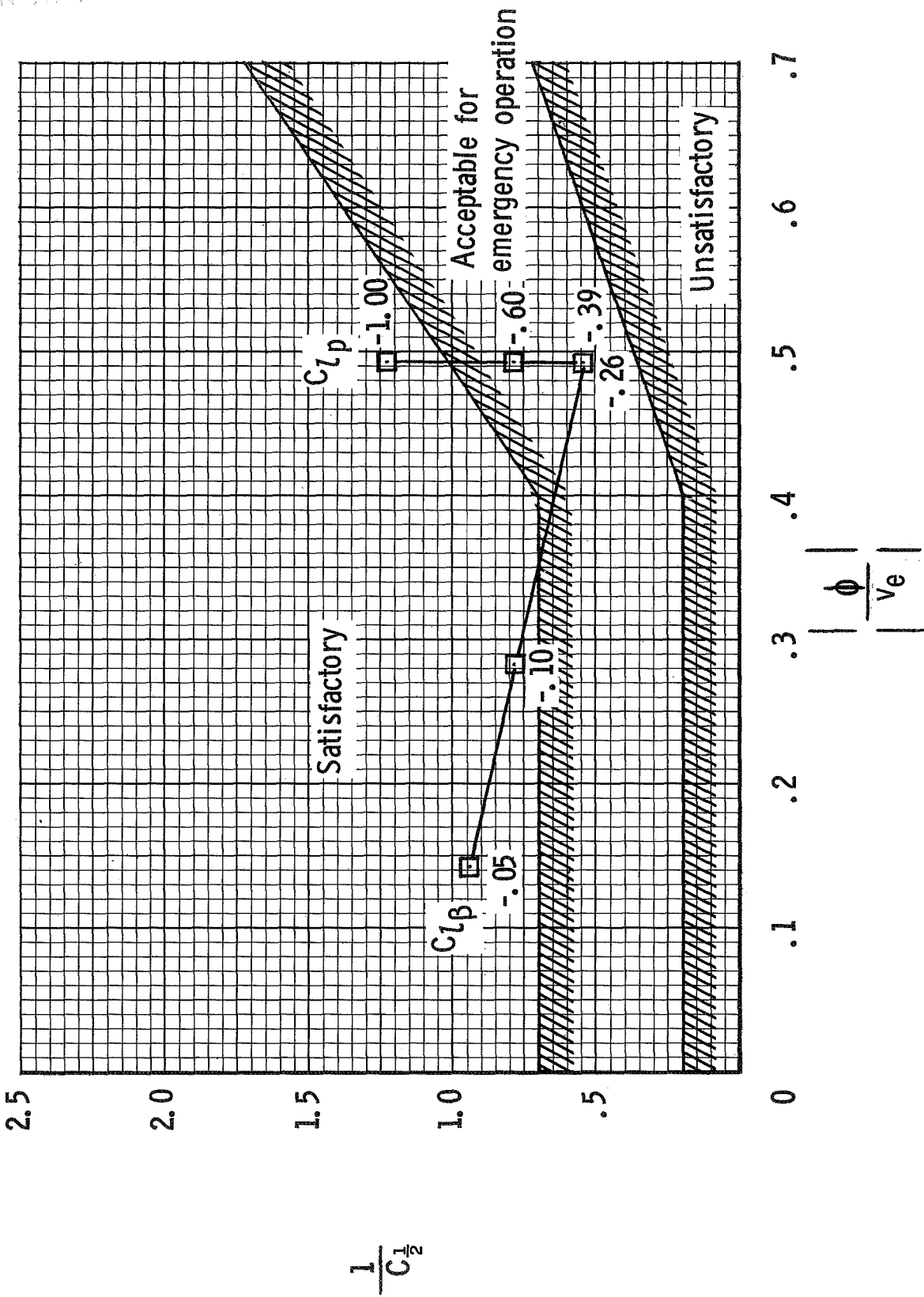
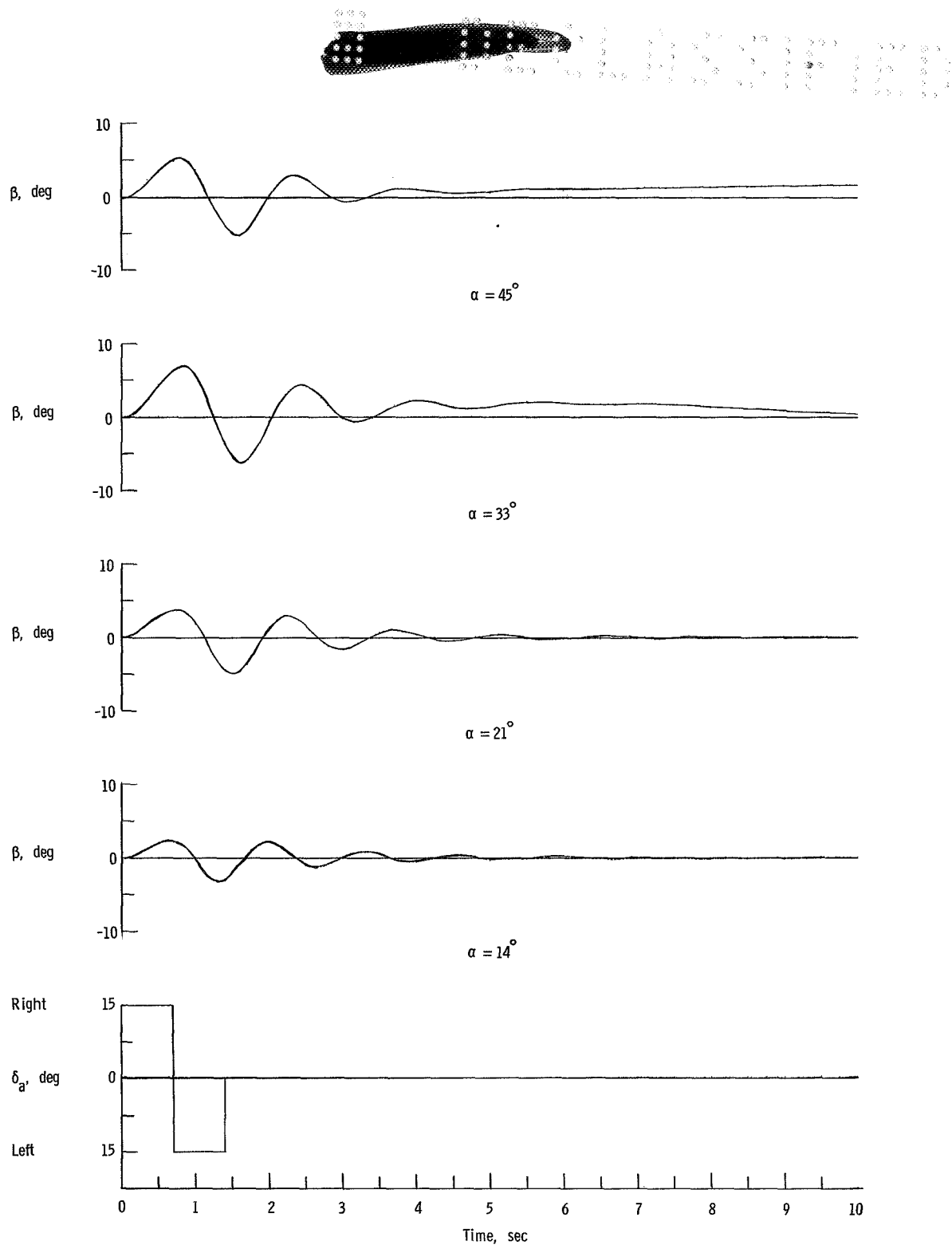
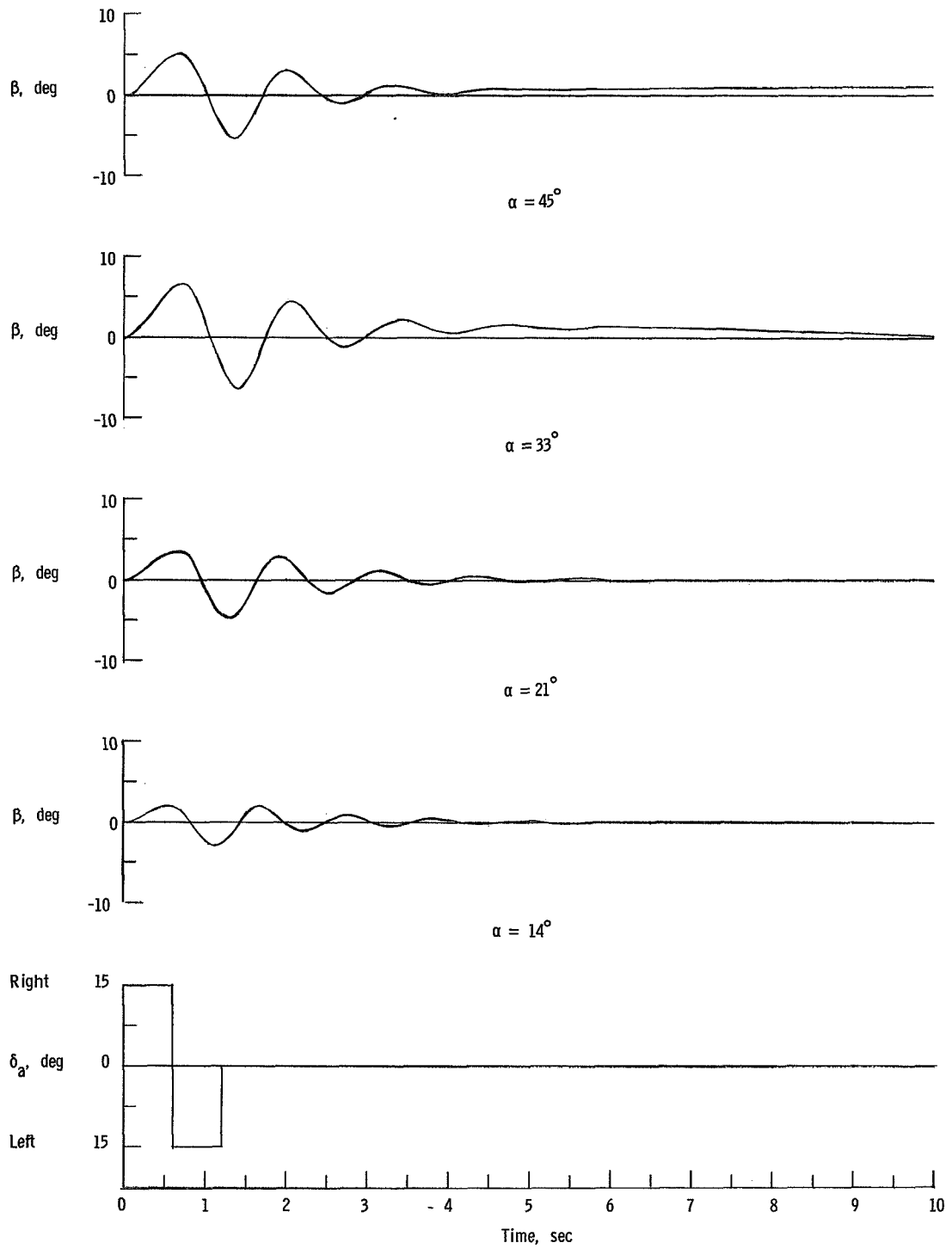


Figure 18.- Evaluation of effect of C_{Lp} and C_{Lb} on lateral damping characteristics of HL-10 entry vehicle in terms of handling qualities requirements. $W/S = 36.10$; Altitude $\approx 55\ 000$ ft (16.8 km); $\alpha = 21^\circ$.



(a) $W/S = 36.10$; sea level.

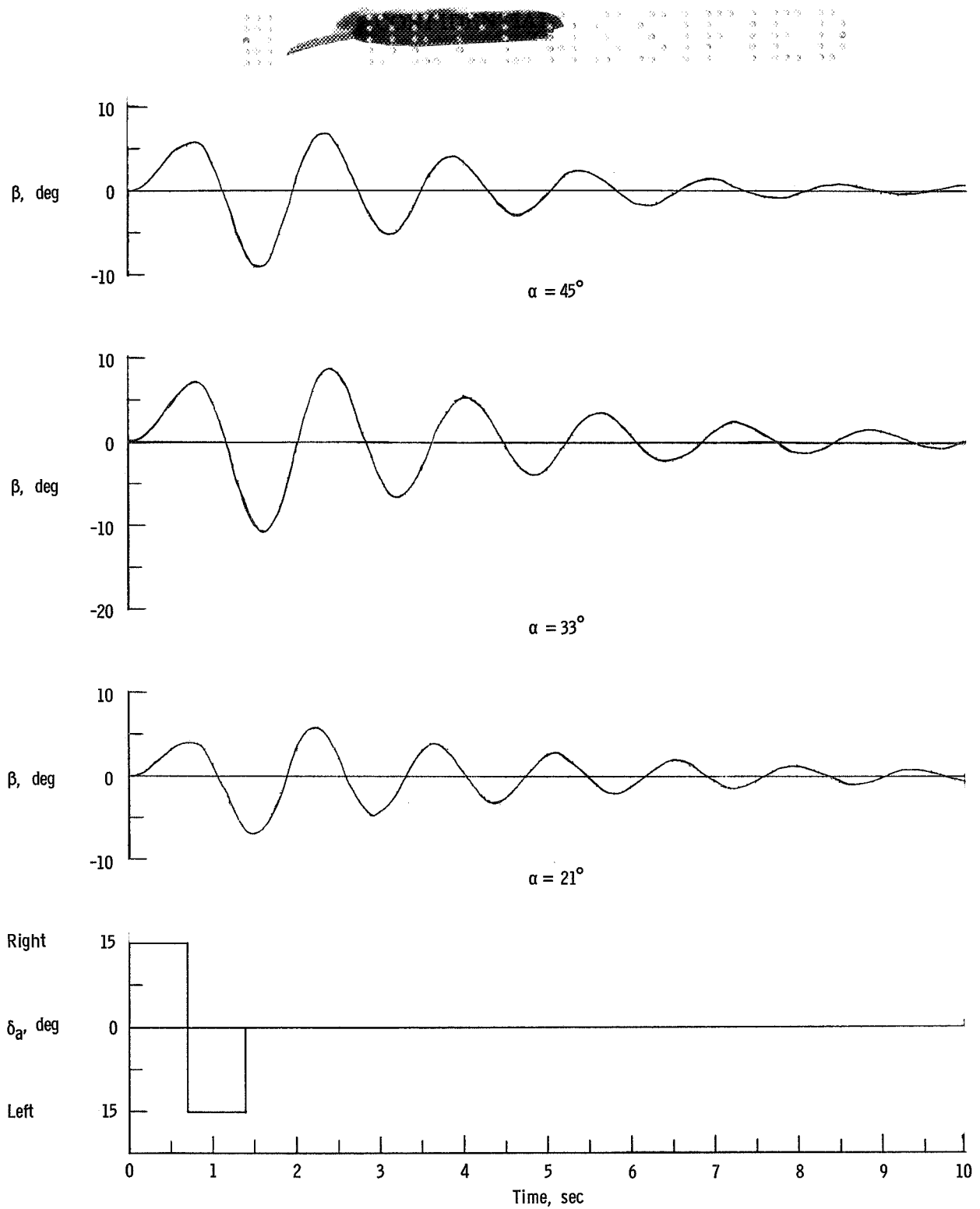
Figure 19.- Time histories of lateral motions following aileron pulse input for HL-10 entry vehicle.



(b) $W/S = 58.44$; sea level.

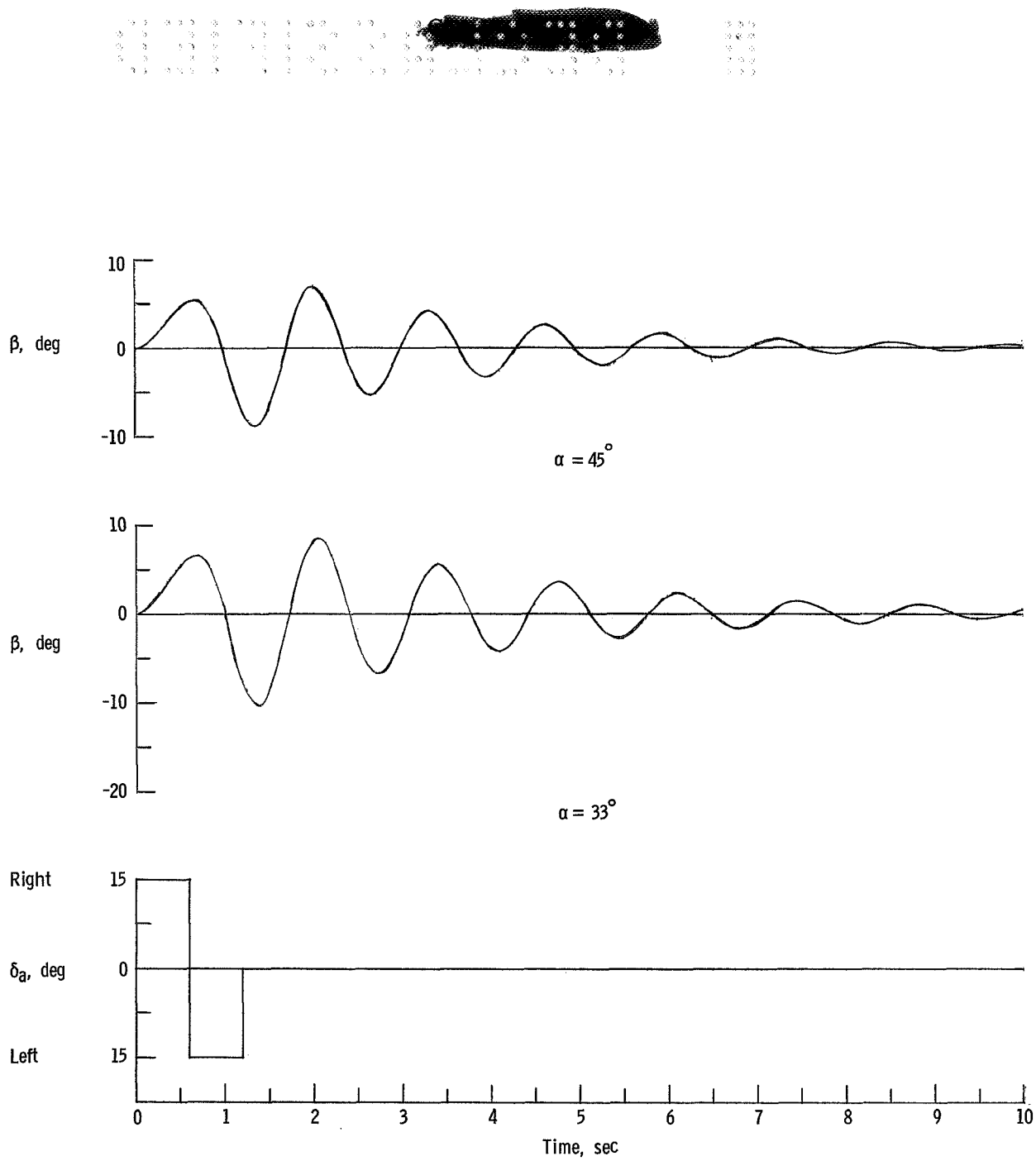
Figure 19.- Continued.





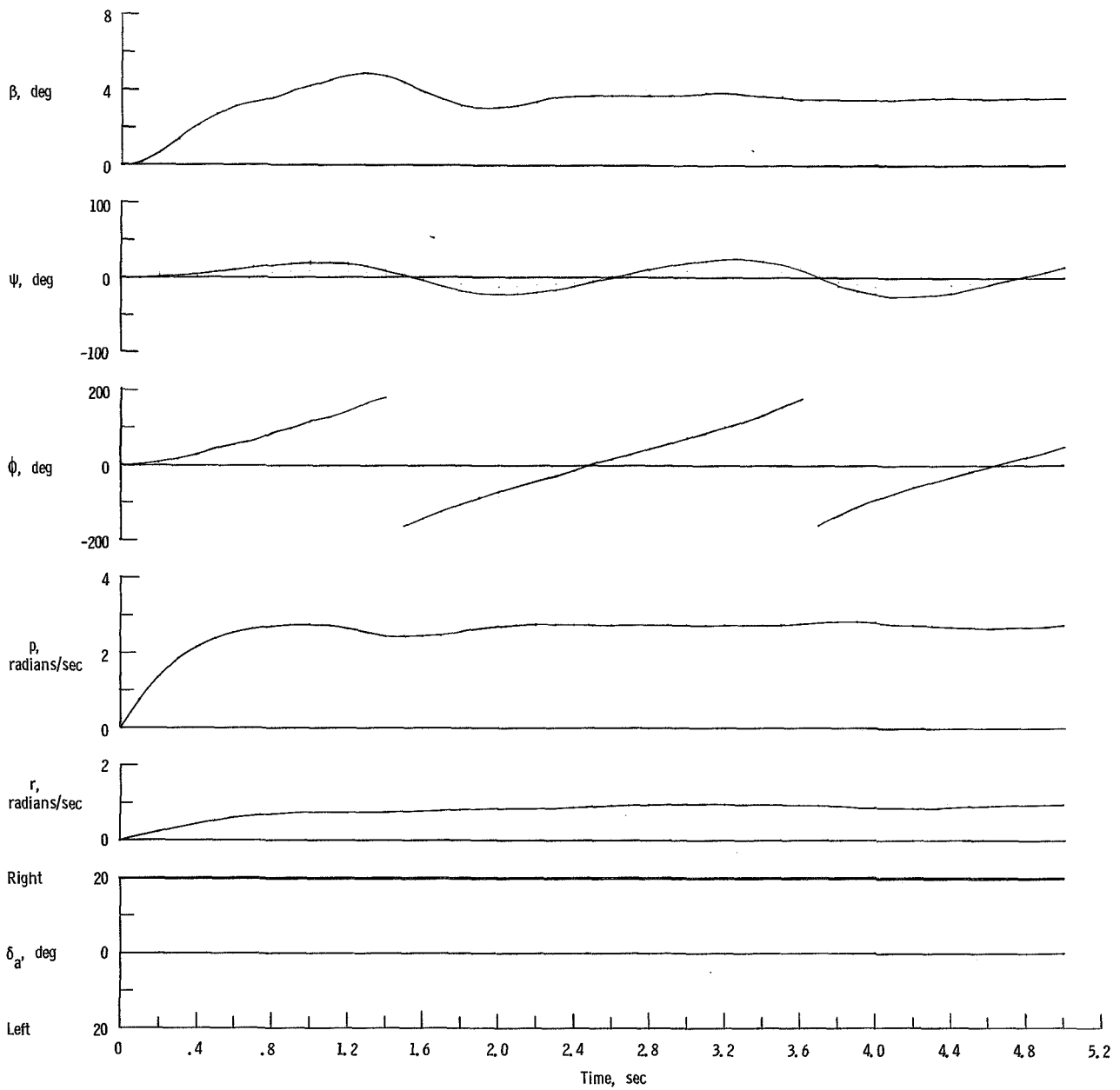
(c) $W/S = 36.10$; Altitude = 55 000 ft (16.8 km).

Figure 19.- Continued.



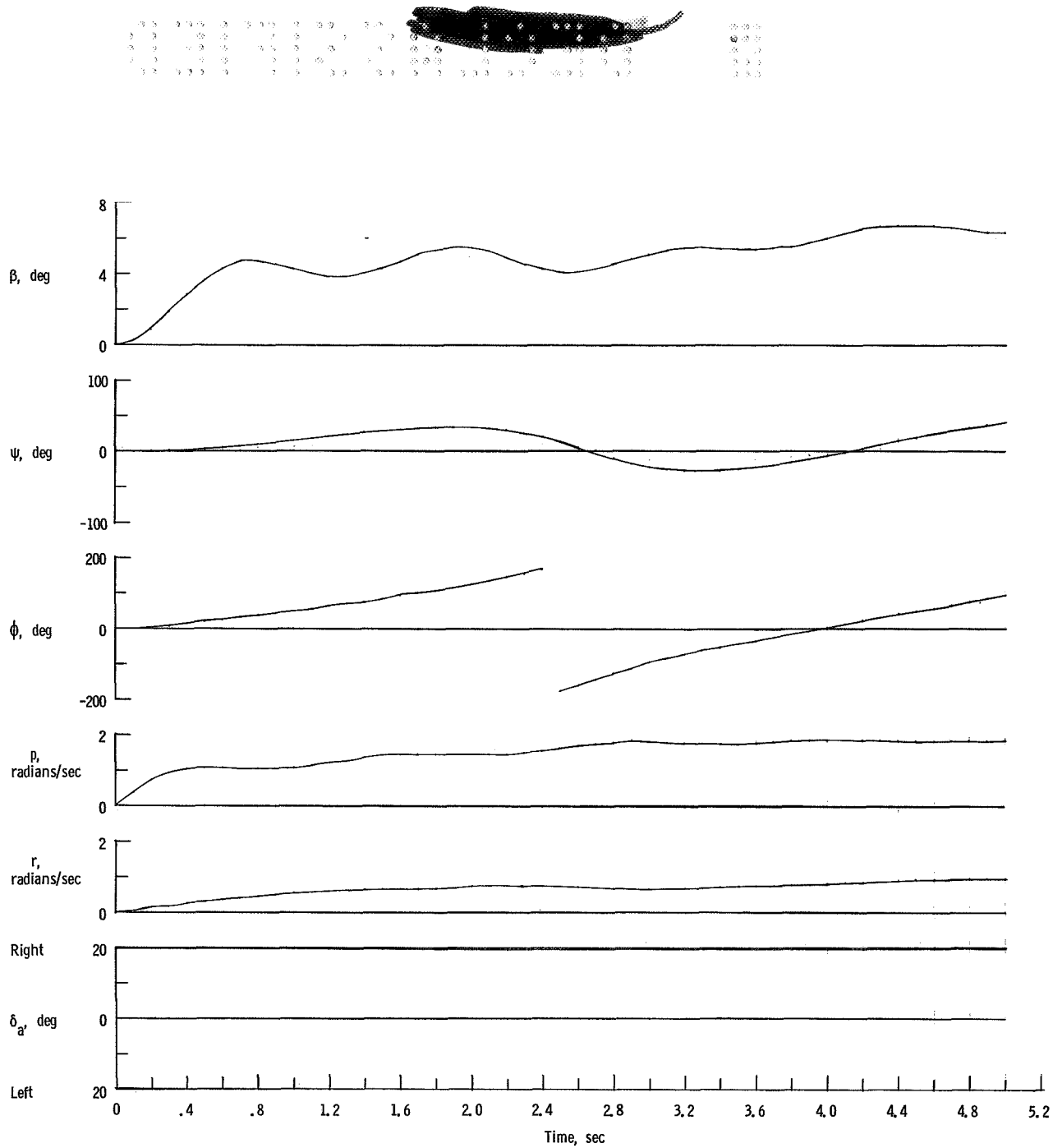
(d) $W/S = 58.44$; Altitude = 55 000 ft (16.8 km).

Figure 19.- Concluded.



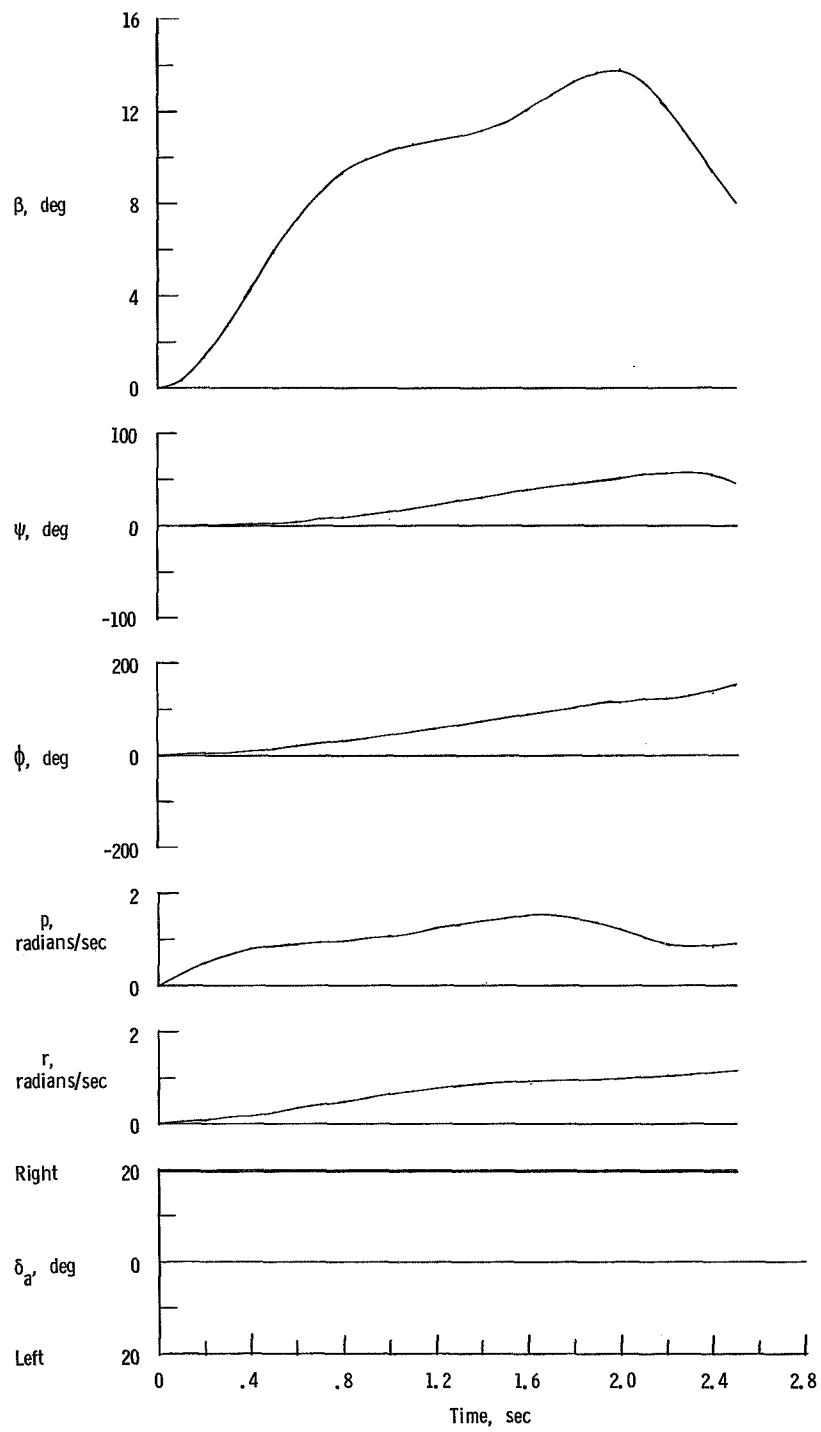
(a) $\alpha = 14^\circ$.

Figure 20.- Time histories of lateral motions following a step aileron input for HL-10 entry vehicle. $W/S = 36.10$; sea level.



(b) $\alpha = 21^\circ$.

Figure 20.- Continued.



(c) $\alpha = 33^\circ$.

Figure 20.- Concluded.

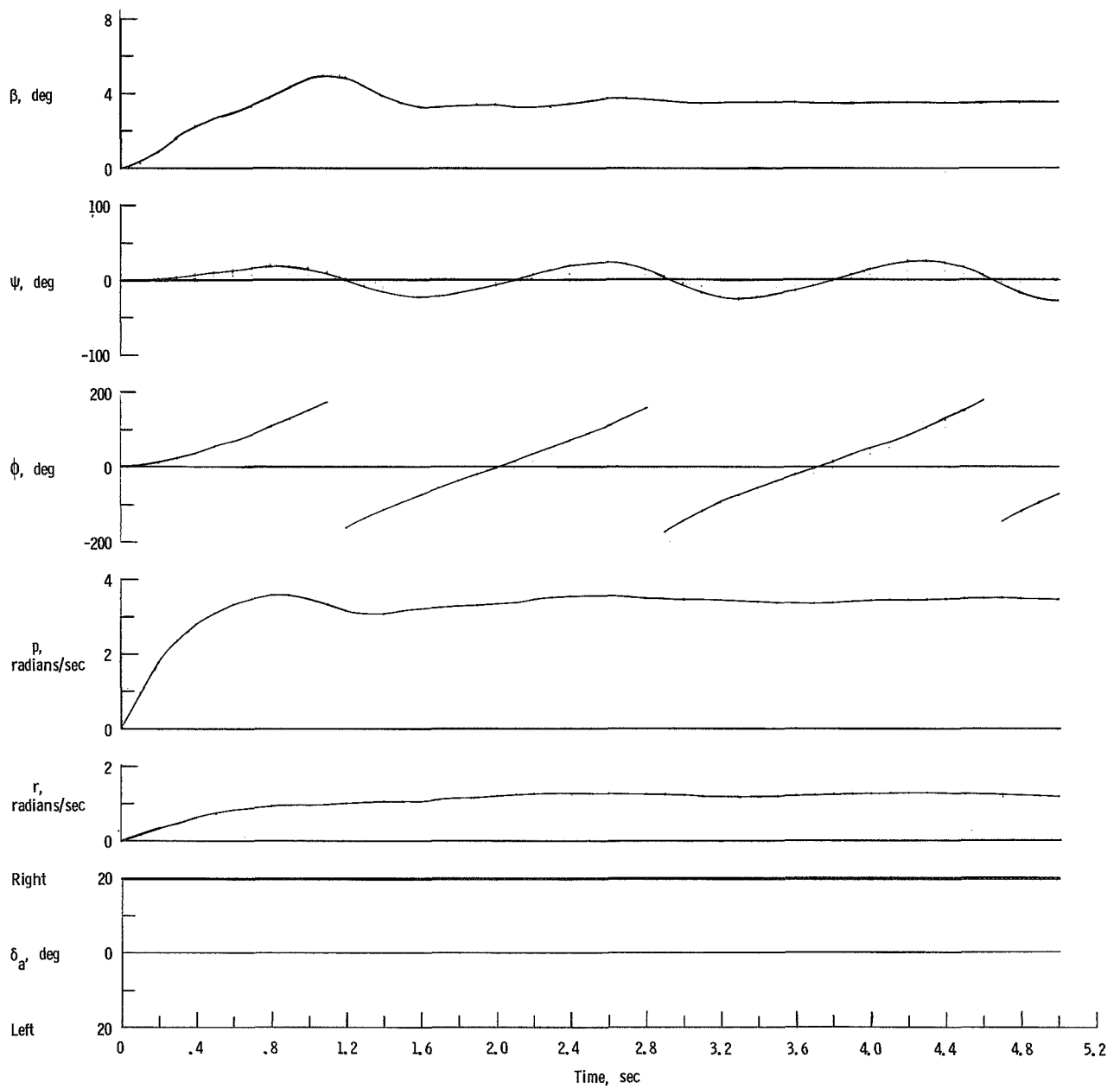
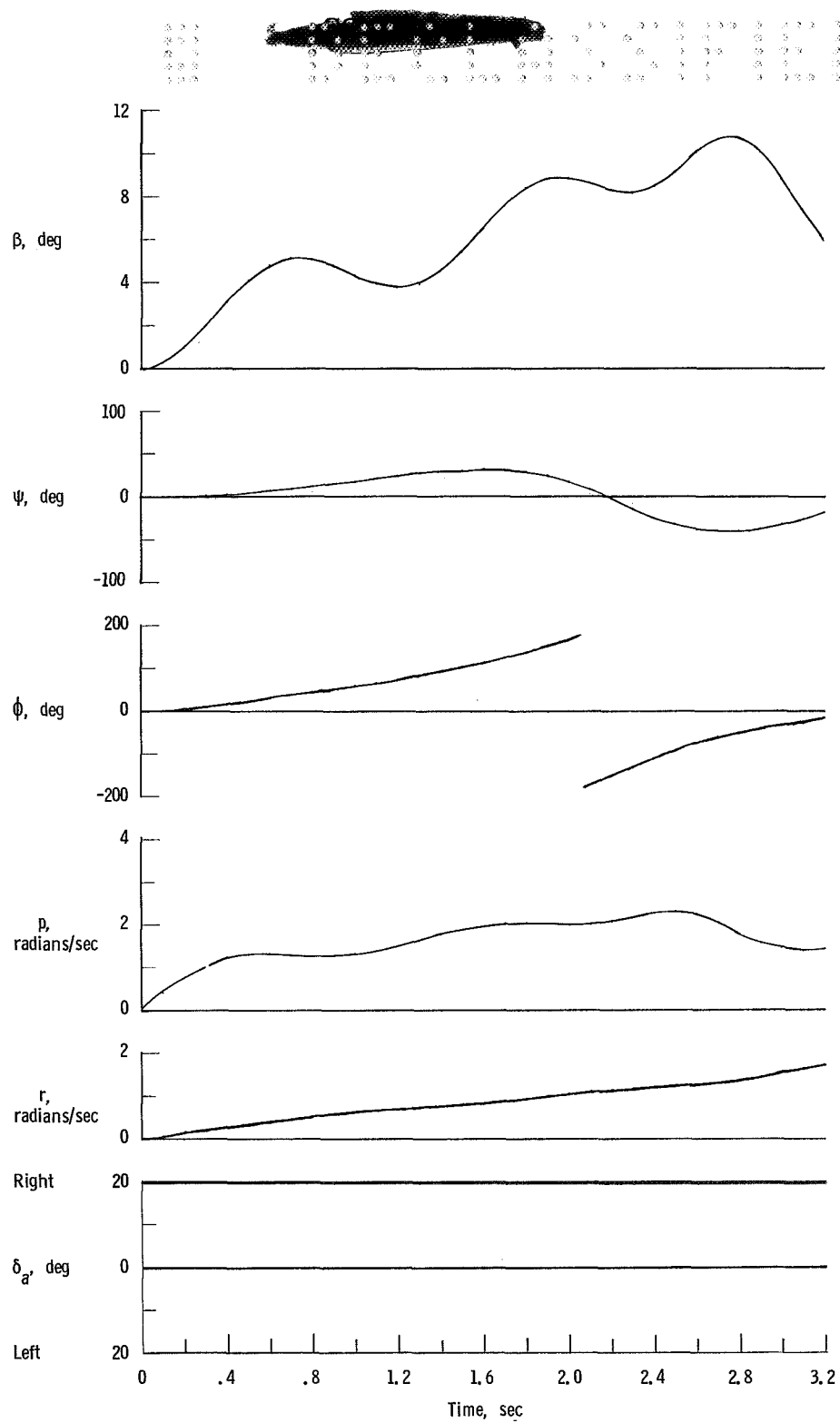


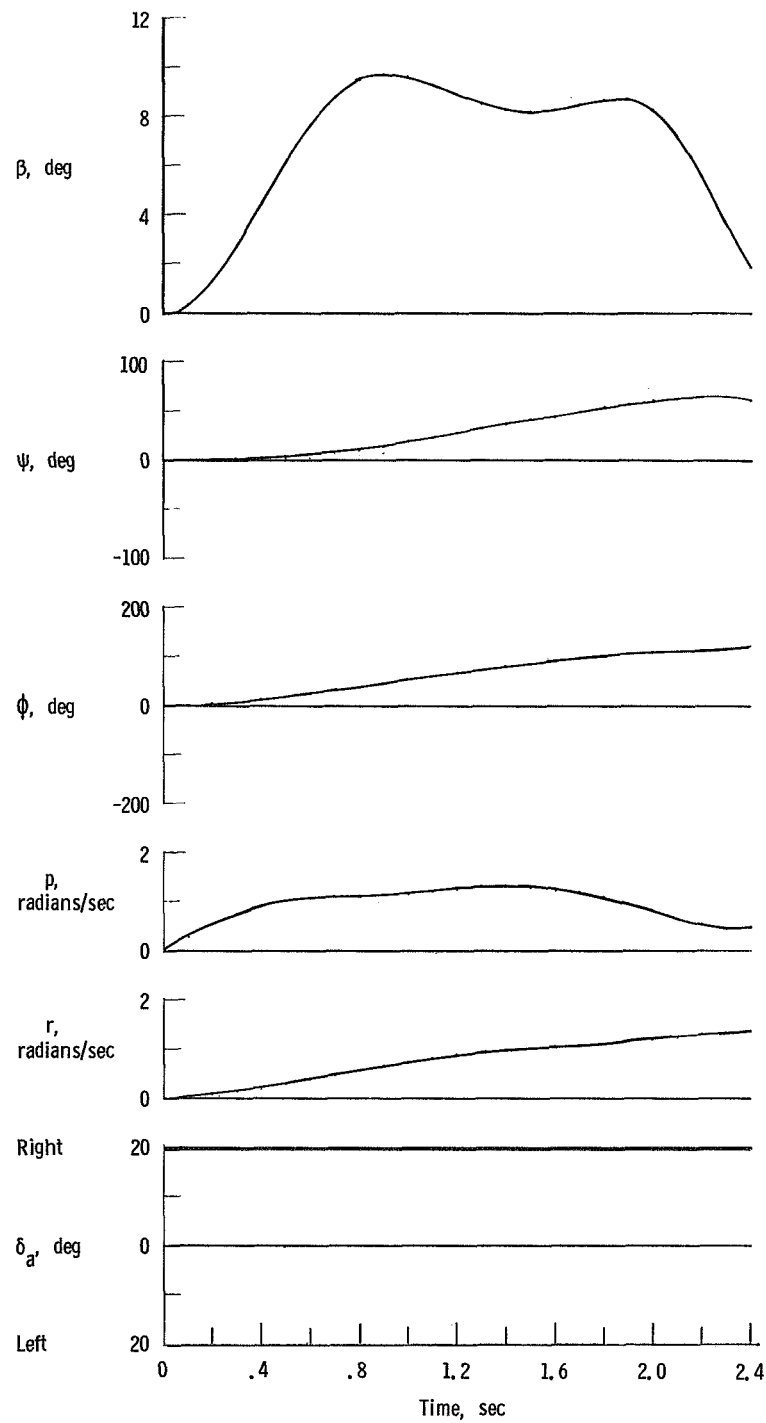
Figure 21.- Time histories of lateral motion following a step aileron input for HL-10 entry vehicle. $W/S = 58.44$; sea level; $\alpha = -14^\circ$.



(a) $\alpha = 21^\circ$.

Figure 22.- Time histories of lateral motions following a step aileron input for HL-10 entry vehicle. $W/S = 36.10$; Altitude = 55 000 ft (16.8 km).

1.0 2.0 3.0 4.0 5.0 6.0 7.0 8.0 9.0 10.0 11.0 12.0 13.0 14.0 15.0 16.0 17.0 18.0 19.0 20.0 21.0 22.0 23.0 24.0 25.0 26.0 27.0 28.0 29.0 30.0 31.0 32.0 33.0 34.0 35.0 36.0 37.0 38.0 39.0 40.0 41.0 42.0 43.0 44.0 45.0 46.0 47.0 48.0 49.0 50.0 51.0 52.0 53.0 54.0 55.0 56.0 57.0 58.0 59.0 60.0 61.0 62.0 63.0 64.0 65.0 66.0 67.0 68.0 69.0 70.0 71.0 72.0 73.0 74.0 75.0 76.0 77.0 78.0 79.0 80.0 81.0 82.0 83.0 84.0 85.0 86.0 87.0 88.0 89.0 90.0 91.0 92.0 93.0 94.0 95.0 96.0 97.0 98.0 99.0 100.0



(b) $\alpha = 33^\circ$.

Figure 22.- Concluded.

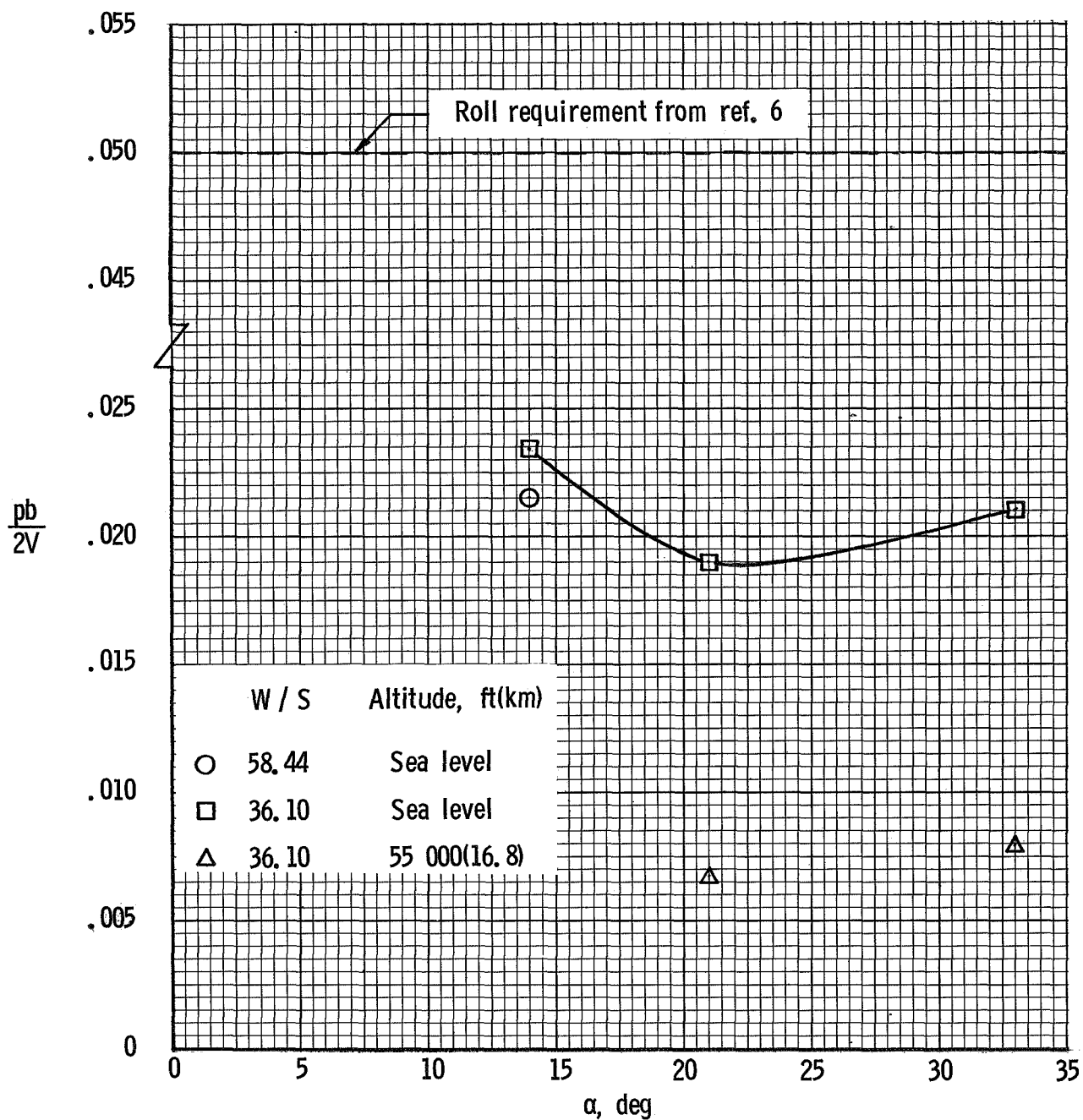


Figure 23.- Calculated roll effectiveness parameter $pb/2V$ for HL-10 entry vehicle based on present military handling qualities requirements for piloted airplanes.

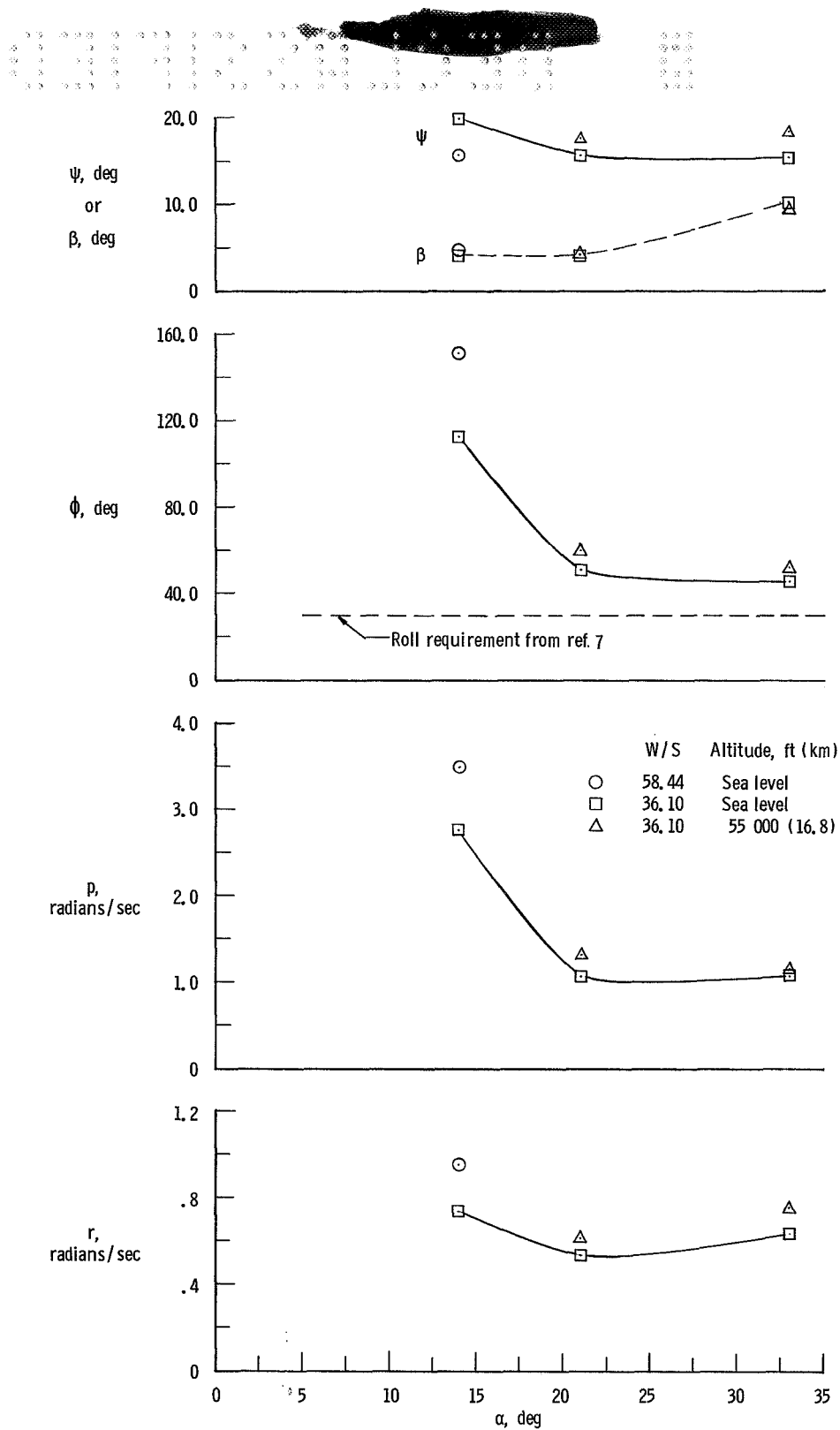
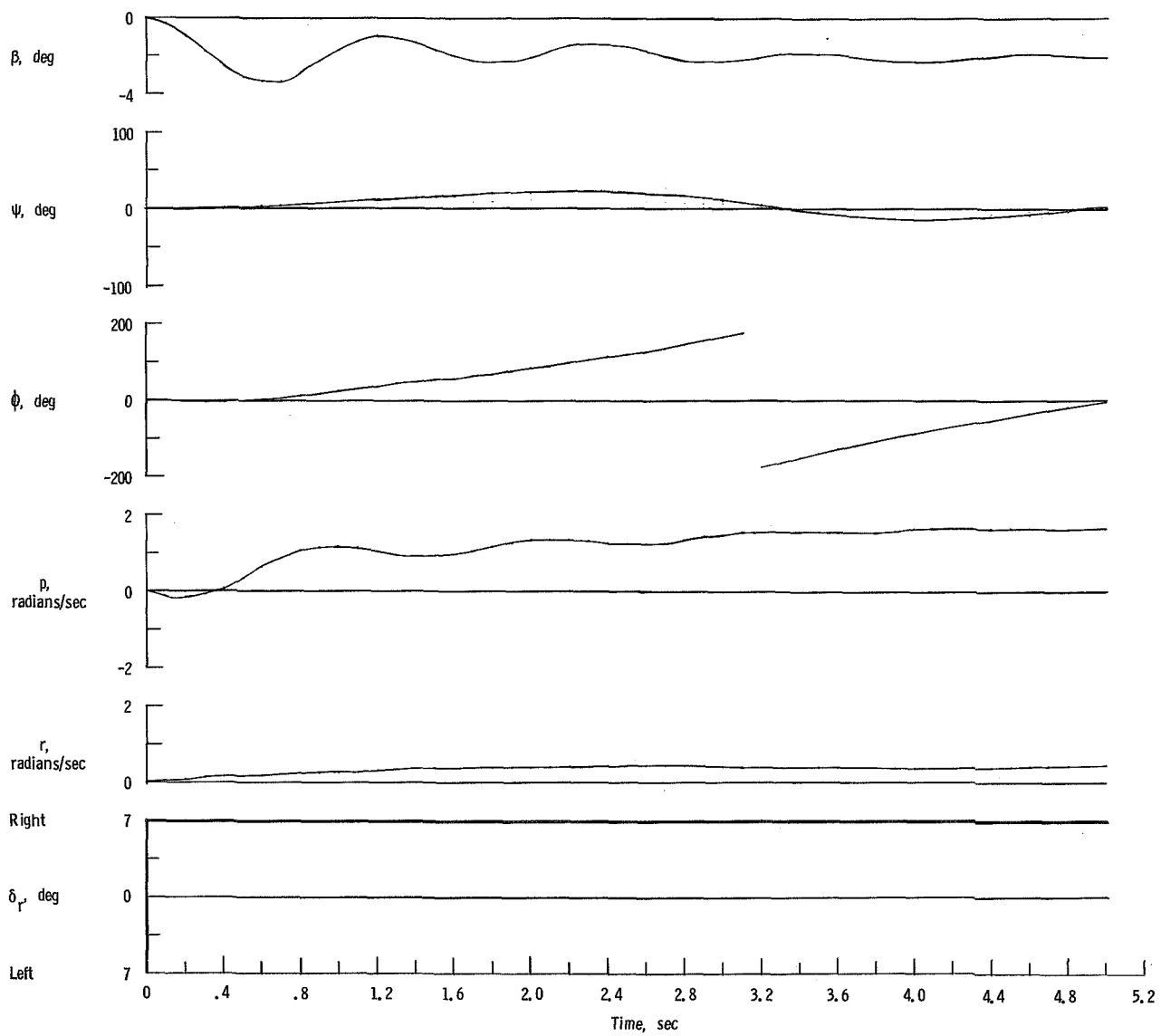
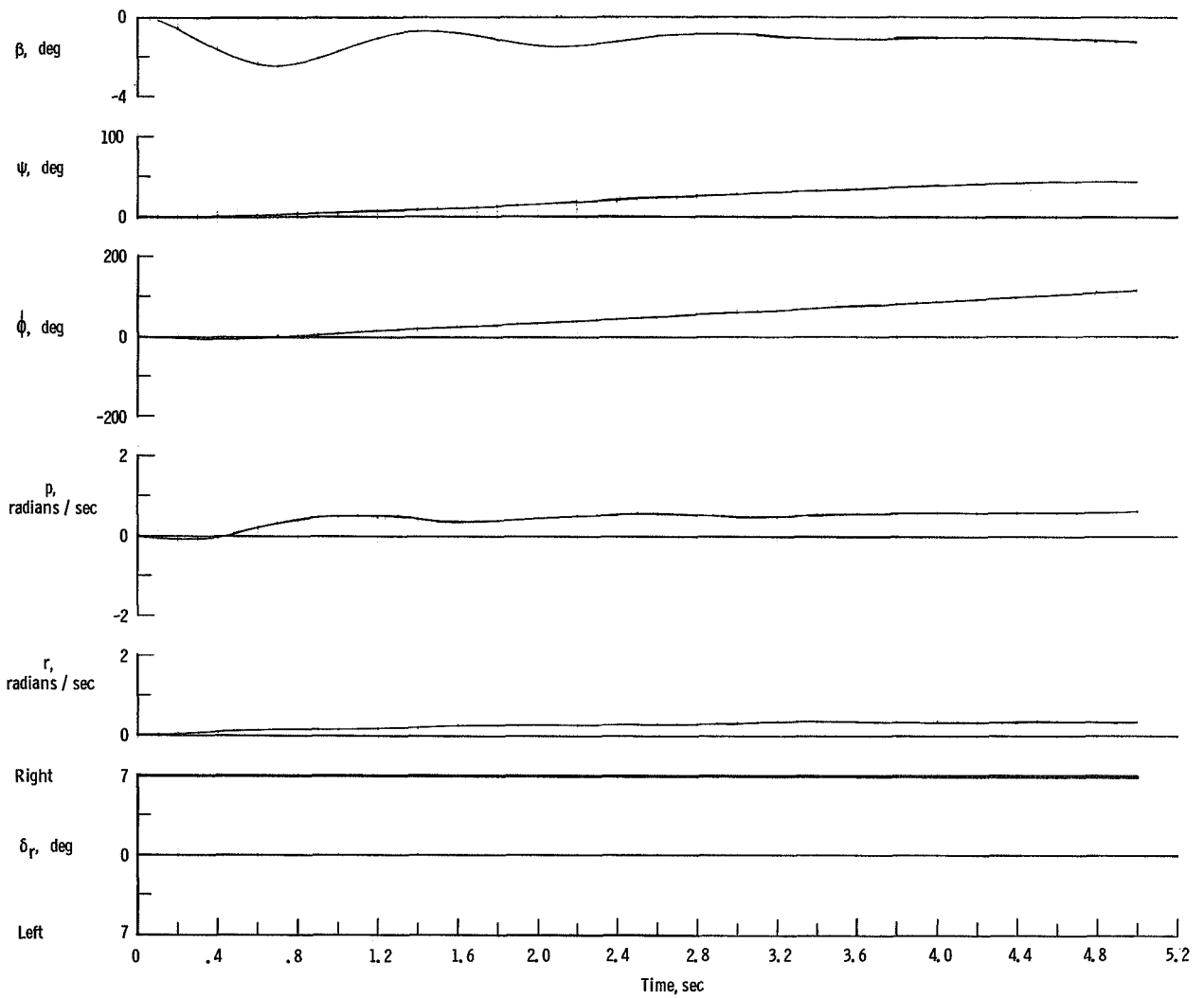


Figure 24.- Summary of roll and yaw rates and angular displacements reached in 1 second following a step aileron input. Data from figures 20 to 22.



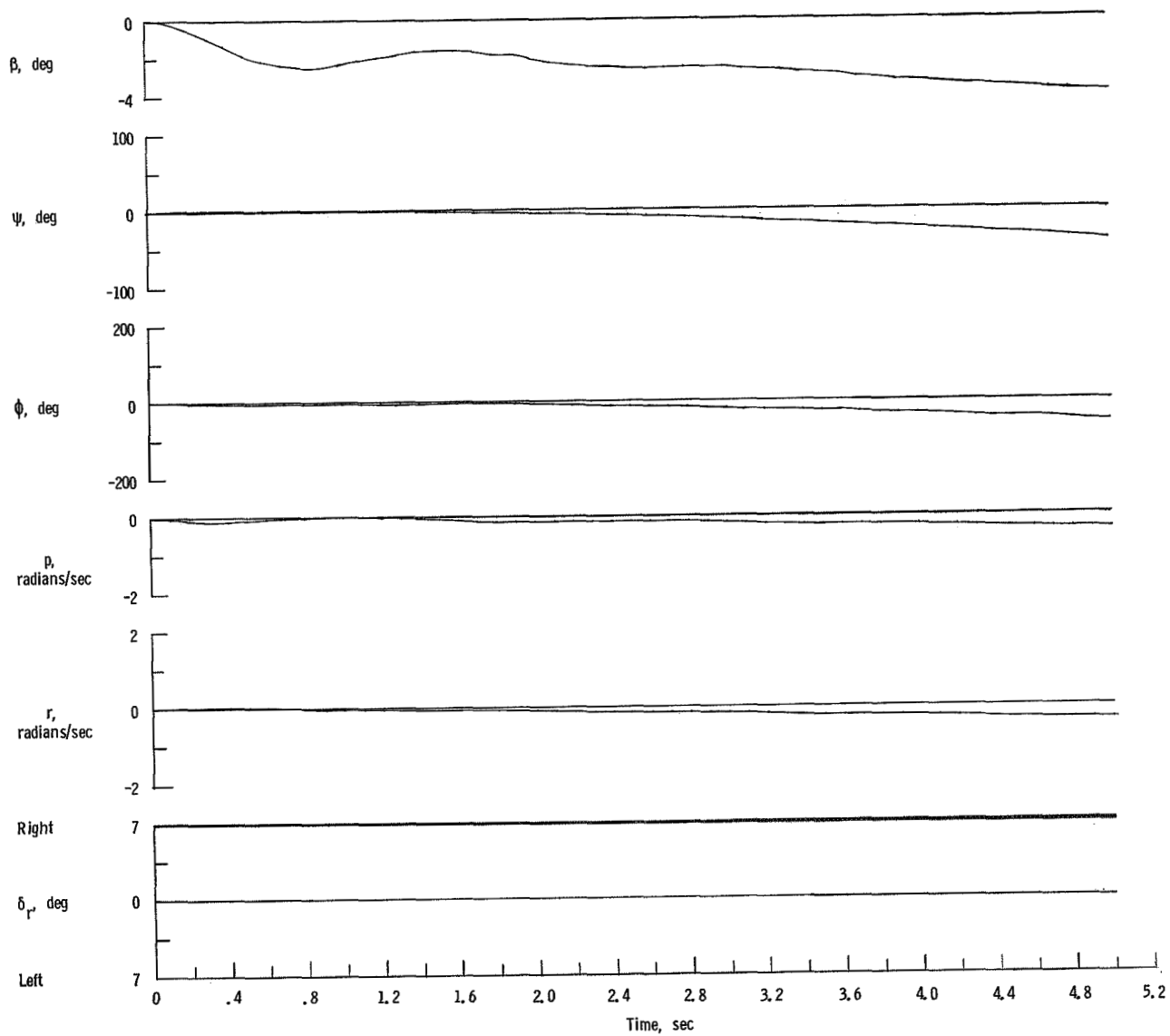
(a) $\alpha = 14^\circ$.

Figure 25.- Time histories of lateral motions following a step rudder input for HL-10 entry vehicle. W/S = 36.10; sea level.



(b) $\alpha = 21^\circ$.

Figure 25.- Continued.



(c) $\alpha = 33^\circ$.

Figure 25.- Concluded.

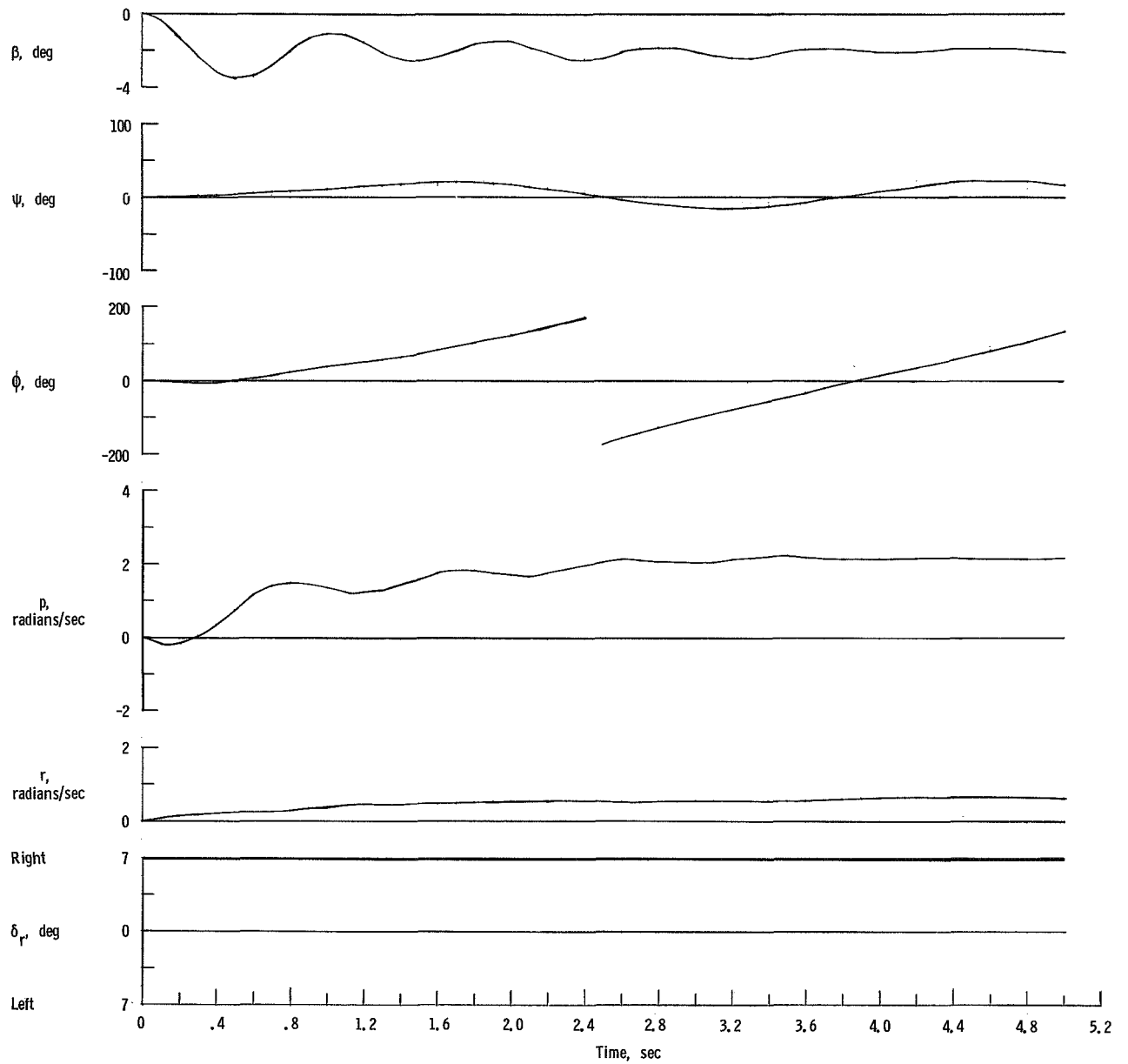
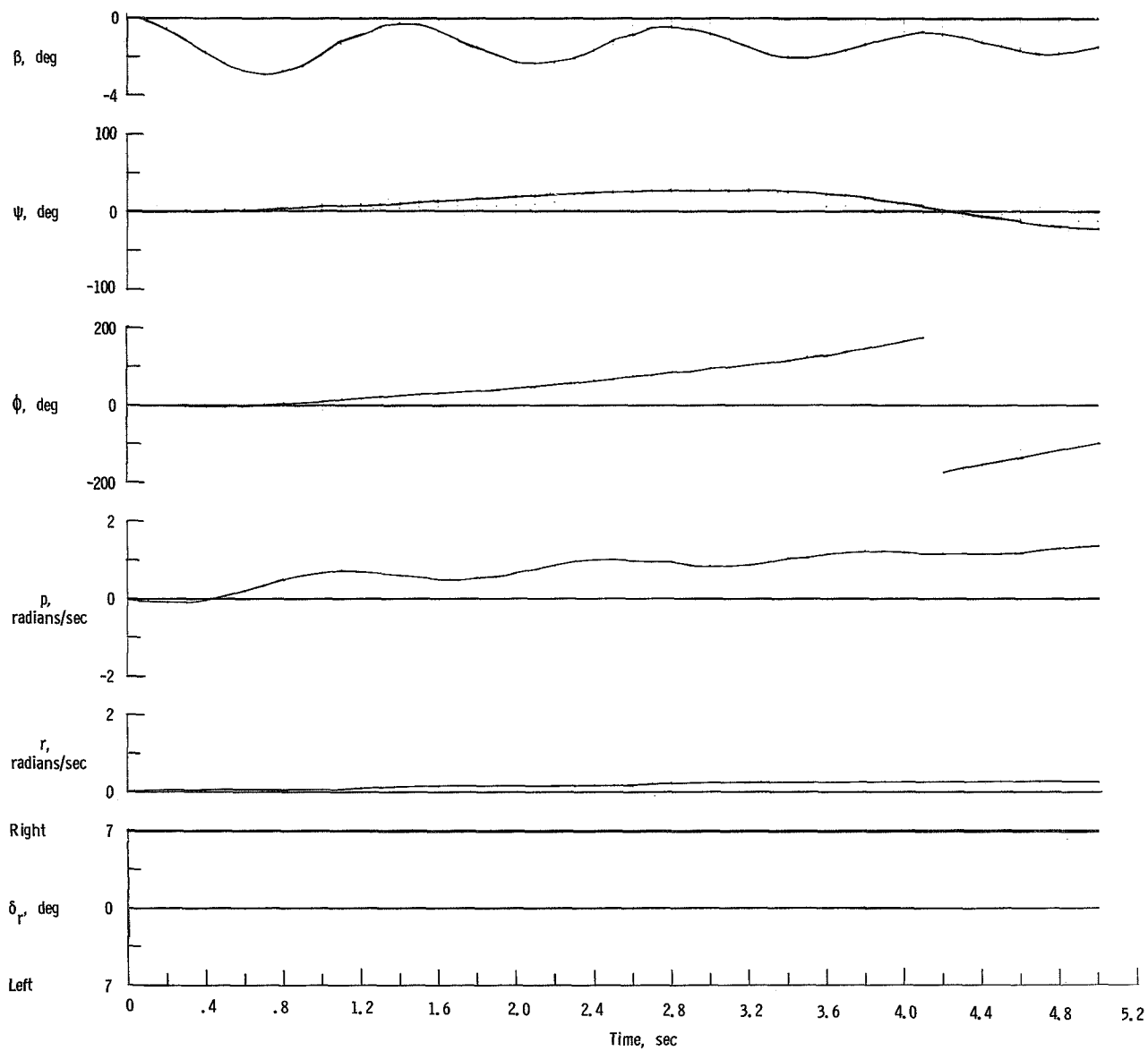
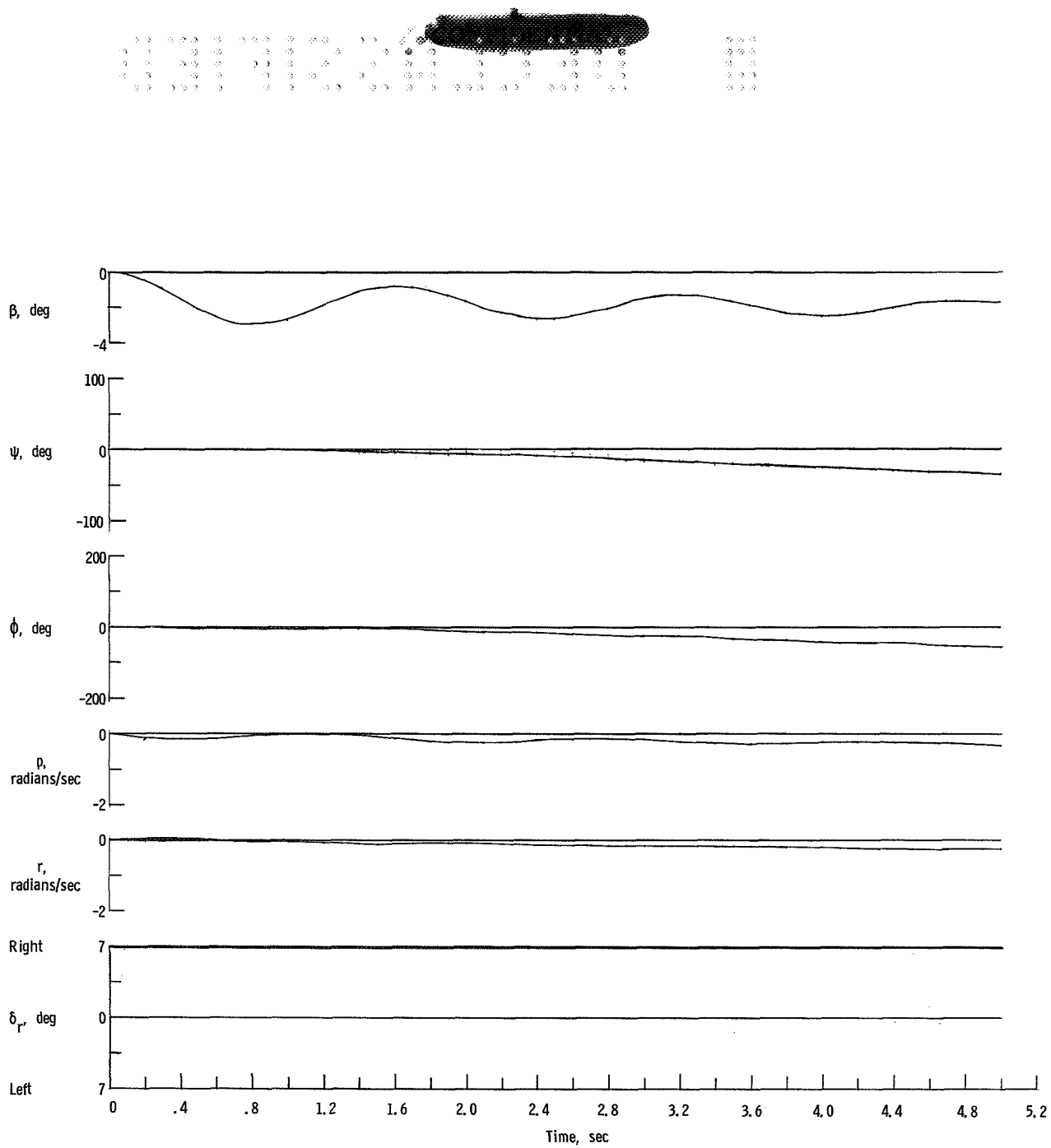


Figure 26.- Time histories of lateral motions following a step rudder input for HL-10 entry vehicle. $W/S = 58.44$; sea level; $\alpha = 14^\circ$.



(a) $\alpha = 21^\circ$.

Figure 27.- Time histories of lateral motions following a step rudder input for HL-10 entry vehicle. $W/S = 36.10$; Altitude = 55 000 ft (16.8 km).



(b) $\alpha = 33^\circ$.

Figure 27.- Concluded.

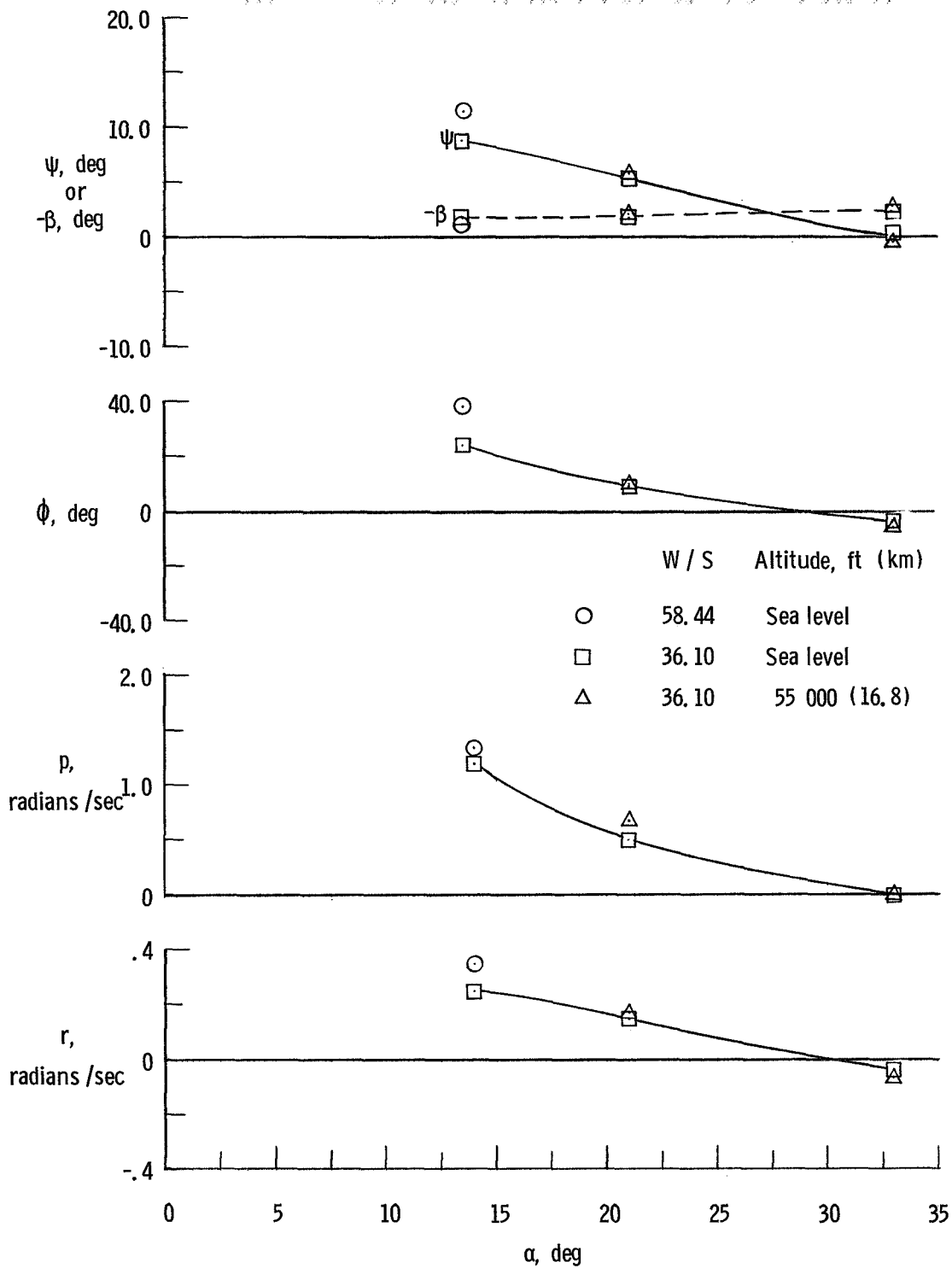


Figure 28.- Summary of yaw and roll rates and angular displacements reached in 1 second following a step rudder input. Data from figures 25 to 27.

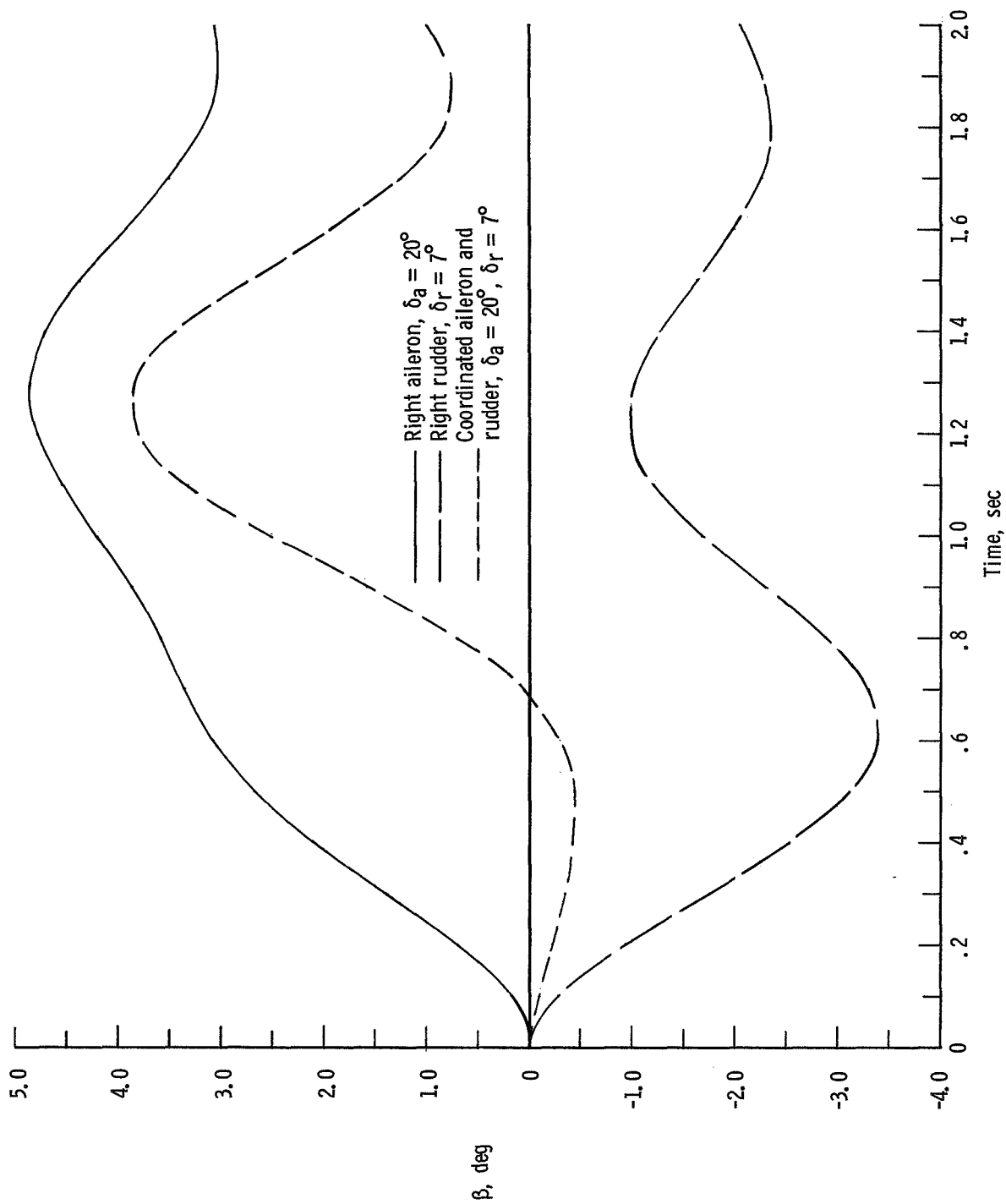


Figure 29.- Time history of sideslip angle produced by step aileron and rudder inputs. $W/S = 36.10$; sea level; $\alpha = 14^\circ$.

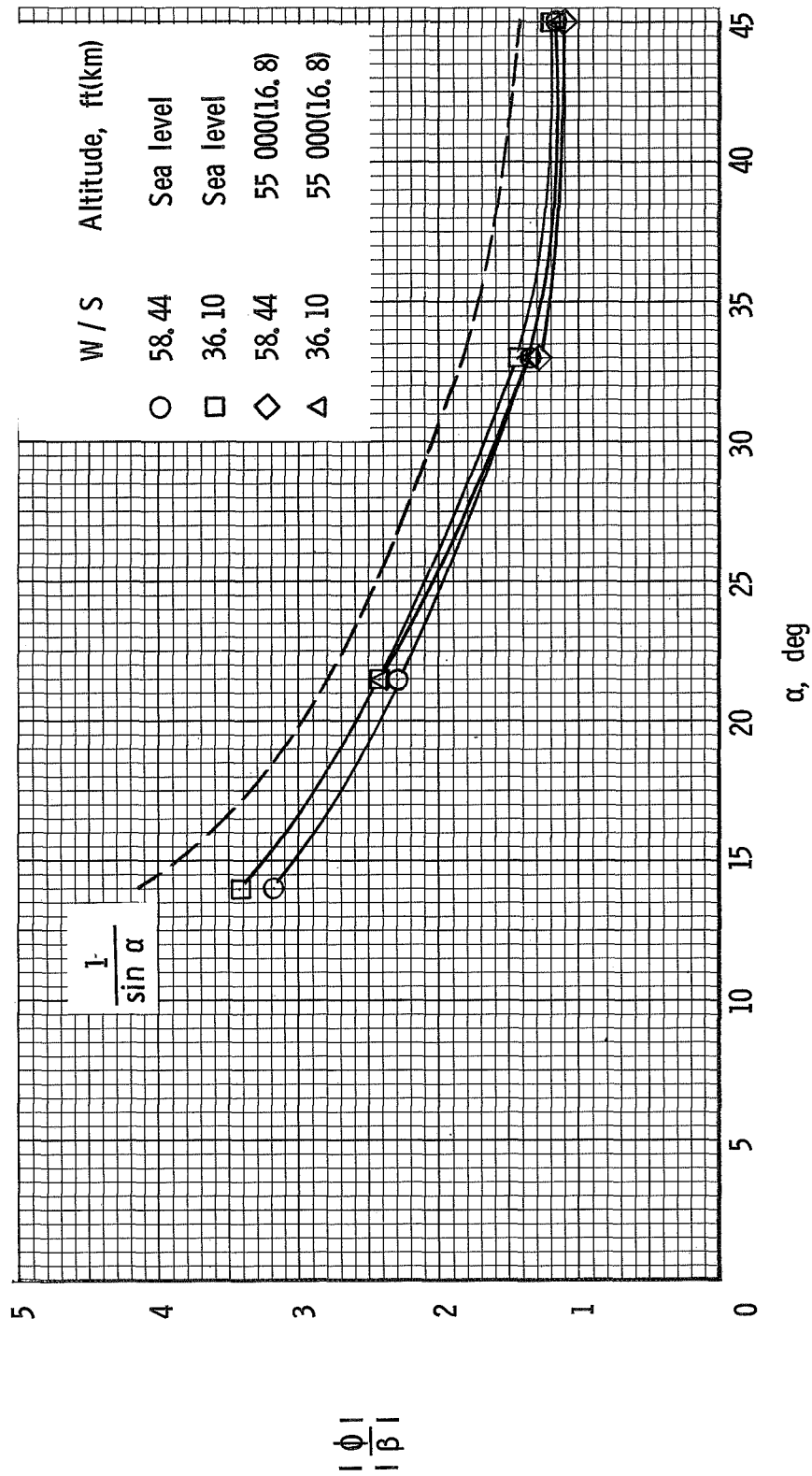


Figure 30.- Variation of roll-sideslip ratio with angle of attack for HL-10 entry vehicle.

3 2 1 0 1 2 3 4 5 6 7 8 9 10 11 12 13 14 15 16 17 18 19 20 21 22 23 24 25 26 27 28 29 30 31 32 33 34 35 36 37 38 39 40 41 42 43 44 45 46 47 48 49 50 51 52 53 54 55 56 57 58 59 60 61 62 63 64 65 66 67 68 69 70 71 72 73 74 75 76 77 78 79 80 81 82 83 84 85 86 87 88 89 90 91 92 93 94 95 96 97 98 99 100 101 102 103 104 105 106 107 108 109 110 111 112 113 114 115 116 117 118 119 120 121 122 123 124 125 126 127 128 129 130 131 132 133 134 135 136 137 138 139 140 141 142 143 144 145 146 147 148 149 150 151 152 153 154 155 156 157 158 159 160 161 162 163 164 165 166 167 168 169 170 171 172 173 174 175 176 177 178 179 180 181 182 183 184 185 186 187 188 189 190 191 192 193 194 195 196 197 198 199 200 201 202 203 204 205 206 207 208 209 210 211 212 213 214 215 216 217 218 219 220 221 222 223 224 225 226 227 228 229 230 231 232 233 234 235 236 237 238 239 240 241 242 243 244 245 246 247 248 249 250 251 252 253 254 255 256 257 258 259 260 261 262 263 264 265 266 267 268 269 270 271 272 273 274 275 276 277 278 279 280 281 282 283 284 285 286 287 288 289 290 291 292 293 294 295 296 297 298 299 300 301 302 303 304 305 306 307 308 309 310 311 312 313 314 315 316 317 318 319 320 321 322 323 324 325 326 327 328 329 330 331 332 333 334 335 336 337 338 339 340 341 342 343 344 345 346 347 348 349 350 351 352 353 354 355 356 357 358 359 360 361 362 363 364 365 366 367 368 369 370 371 372 373 374 375 376 377 378 379 380 381 382 383 384 385 386 387 388 389 390 391 392 393 394 395 396 397 398 399 400 401 402 403 404 405 406 407 408 409 410 411 412 413 414 415 416 417 418 419 420 421 422 423 424 425 426 427 428 429 430 431 432 433 434 435 436 437 438 439 440 441 442 443 444 445 446 447 448 449 450 451 452 453 454 455 456 457 458 459 460 461 462 463 464 465 466 467 468 469 470 471 472 473 474 475 476 477 478 479 480 481 482 483 484 485 486 487 488 489 490 491 492 493 494 495 496 497 498 499 500 501 502 503 504 505 506 507 508 509 510 511 512 513 514 515 516 517 518 519 520 521 522 523 524 525 526 527 528 529 530 531 532 533 534 535 536 537 538 539 540 541 542 543 544 545 546 547 548 549 550 551 552 553 554 555 556 557 558 559 560 561 562 563 564 565 566 567 568 569 570 571 572 573 574 575 576 577 578 579 580 581 582 583 584 585 586 587 588 589 590 591 592 593 594 595 596 597 598 599 600 601 602 603 604 605 606 607 608 609 610 611 612 613 614 615 616 617 618 619 620 621 622 623 624 625 626 627 628 629 630 631 632 633 634 635 636 637 638 639 640 641 642 643 644 645 646 647 648 649 650 651 652 653 654 655 656 657 658 659 660 661 662 663 664 665 666 667 668 669 670 671 672 673 674 675 676 677 678 679 680 681 682 683 684 685 686 687 688 689 690 691 692 693 694 695 696 697 698 699 700 701 702 703 704 705 706 707 708 709 710 711 712 713 714 715 716 717 718 719 720 721 722 723 724 725 726 727 728 729 730 731 732 733 734 735 736 737 738 739 740 741 742 743 744 745 746 747 748 749 750 751 752 753 754 755 756 757 758 759 760 761 762 763 764 765 766 767 768 769 770 771 772 773 774 775 776 777 778 779 780 781 782 783 784 785 786 787 788 789 790 791 792 793 794 795 796 797 798 799 800 801 802 803 804 805 806 807 808 809 810 811 812 813 814 815 816 817 818 819 820 821 822 823 824 825 826 827 828 829 830 831 832 833 834 835 836 837 838 839 840 841 842 843 844 845 846 847 848 849 850 851 852 853 854 855 856 857 858 859 860 861 862 863 864 865 866 867 868 869 870 871 872 873 874 875 876 877 878 879 880 881 882 883 884 885 886 887 888 889 890 891 892 893 894 895 896 897 898 899 900 901 902 903 904 905 906 907 908 909 910 911 912 913 914 915 916 917 918 919 920 921 922 923 924 925 926 927 928 929 930 931 932 933 934 935 936 937 938 939 940 941 942 943 944 945 946 947 948 949 950 951 952 953 954 955 956 957 958 959 960 961 962 963 964 965 966 967 968 969 970 971 972 973 974 975 976 977 978 979 980 981 982 983 984 985 986 987 988 989 990 991 992 993 994 995 996 997 998 999 1000

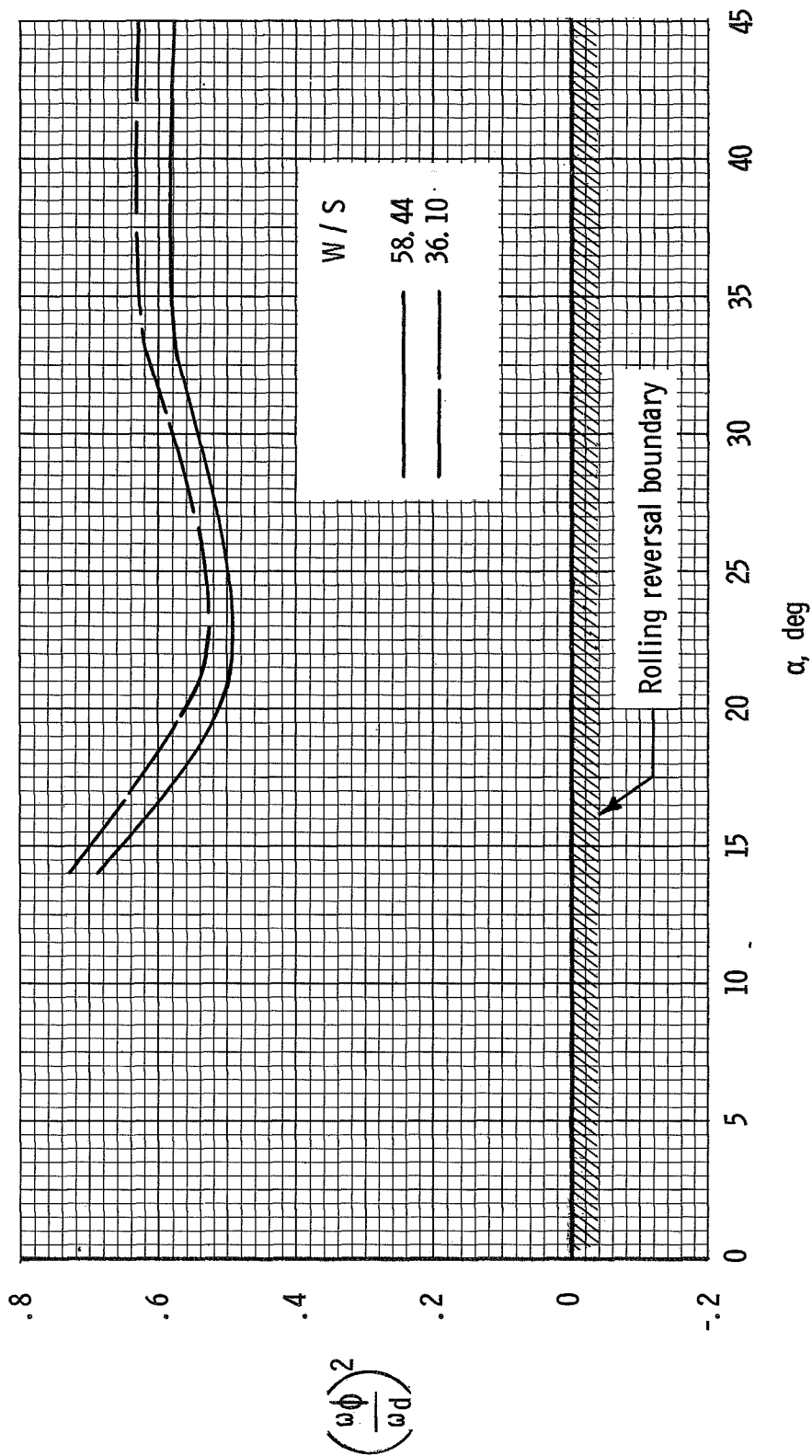


Figure 31.- Variation of rolling effectiveness parameter with angle of attack for HL-10 entry vehicle. Sea level.

0371241030

"The aeronautical and space activities of the United States shall be conducted so as to contribute . . . to the expansion of human knowledge of phenomena in the atmosphere and space. The Administration shall provide for the widest practicable and appropriate dissemination of information concerning its activities and the results thereof."

—NATIONAL AERONAUTICS AND SPACE ACT OF 1958

NASA SCIENTIFIC AND TECHNICAL PUBLICATIONS

TECHNICAL REPORTS: Scientific and technical information considered important, complete, and a lasting contribution to existing knowledge.

TECHNICAL NOTES: Information less broad in scope but nevertheless of importance as a contribution to existing knowledge.

TECHNICAL MEMORANDUMS: Information receiving limited distribution because of preliminary data, security classification, or other reasons.

CONTRACTOR REPORTS: Technical information generated in connection with a NASA contract or grant and released under NASA auspices.

TECHNICAL TRANSLATIONS: Information published in a foreign language considered to merit NASA distribution in English.

TECHNICAL REPRINTS: Information derived from NASA activities and initially published in the form of journal articles.

SPECIAL PUBLICATIONS: Information derived from or of value to NASA activities but not necessarily reporting the results of individual NASA-programmed scientific efforts. Publications include conference proceedings, monographs, data compilations, handbooks, sourcebooks, and special bibliographies.

Details on the availability of these publications may be obtained from:

SCIENTIFIC AND TECHNICAL INFORMATION DIVISION
NATIONAL AERONAUTICS AND SPACE ADMINISTRATION

Washington, D.C. 20546